Slow Modulation of Cochlear Response by the Olivocochlear Efferent System Elicited by Sustained Noise or Threshold Elevation in the Contralateral Ear

by

Erik Larsen

M.Sc. Applied Physics
Technische Universiteit Delft, 1998

SUBMITTED TO
THE HARVARD-MIT DIVISION OF HEALTH SCIENCES AND TECHNOLOGY
IN PARTIAL FULFILLMENT OF THE REQUIREMENTS FOR THE DEGREE OF

DOCTOR OF PHILOSOPHY IN
BIOMEDICAL ENGINEERING
AT THE
MASSACHUSETTS INSTITUTE OF TECHNOLOGY

SEPTEMBER 2008

Signature of author: _____
Harvard-MIT Division of Health Sciences and Technology
August 19, 2008

Certified by: _____
M. Charles Liberman
Harold Schuknecht Professor of Otology and Laryngology, Harvard Medical School
Director of the Eaton-Peabody Laboratory, Mass. Eye & Ear Infirmary
Thesis Supervisor

Accepted by: _____
Martha L. Gray
Edward Hood Taplin Professor of Medical & Electrical Engineering
Director of the Harvard-MIT Division of Health Sciences and Technology

Slow Modulation of Cochlear Response by the Olivocochlear Efferent System Elicited by Sustained Noise or Threshold Elevation in the Contralateral Ear

by

Erik Larsen

Submitted to the Harvard-MIT Division of Health Sciences and Technology
On September, 2008 in partial fulfillment of the
Requirements for the Degree of Doctor of Philosophy in
Biomedical Engineering

ABSTRACT

This thesis describes results from two projects related to the efferent innervation of the cochlea. First, we investigated peripheral olivocochlear effects of sustained contralateral broadband noise in anesthetized guinea pig. We found evidence of medial olivocochlear (MOC) effects on two timescales: the classic MOC 'fast effect', followed by a gradually increasing suppression, which we call the MOC 'delayed effect'. Delayed suppression typically takes 2-3 minutes to build up, occurs at all frequencies of guinea pig hearing, and suppresses distortion product otoacoustic emissions (DPOAEs), compound action potentials (CAPs), and round window noise. In contrast to the MOC slow effect, which has been reported for sustained shock-evoked MOC activity, MOC delayed suppression does not build up in the outer hair cells but is due to a central modulation (enhancement) of MOC responsiveness and can thus be viewed as a gradual increase in the strength of the MOC fast effect. We found that, on average, the magnitude of the delayed suppression is comparable to that of the MOC fast effect, but that there is an overall negative correlation between fast and delayed effect magnitudes. Thus, it may have significant implications for the functional roles of the MOC system, such as protection against acoustic trauma, anti-masking, and dynamic range extension.

Second, we investigated the LOC bilateral balancing model, which proposes that the LOC system acts to balance long-term average neural output from both cochleae, which would be important for binaural processing of sounds. For this, we tested various cohorts of mice by repeatedly measuring bilateral auditory brainstem responses (ABR) and DPOAE growth functions across a wide range of frequencies and levels for periods of about 1-2 months. About halfway through the period, a unilateral reduction in neural output was created, either by acoustic overexposure or conductive impairment. Although the LOC balancing model predicts that the unilateral reduction in neural output should be matched contralaterally, we found no evidence for short-term or long-term efferent-induced contralateral response changes in any of the cohorts, either for DPOAE or ABR metrics. In view of these results, a revision of the LOC bilateral balancing model is called for.

Thesis Supervisor: M. Charles Liberman
Title: Harold Schuknecht Professor of Otology and Laryngology

TABLE OF CONTENTS

I General review of olivocochlear anatomy and physiology

The cochlea, as a sensory organ, has an afferent innervation, which transmits information about the sounds impinging on the ear canals to the central nervous system. The cochlea also receives an efferent component, the olivocochlear (OC) system, originating in the superior olivary complex (SOC) of the brainstem, which innervates cochlear sensory cells and afferent neurons. Considering the flow of neural information, the OC system forms a feedback loop, which may have any of the traditional functions of feedback systems, such as output stabilization, guaranteed performance, and tolerance to design variations (Oppenheim and Willsky 1997) and perhaps other functions specifically related to the inner ear such as anti-masking, protection from acoustic overexposure, or developmental roles; for recent reviews, see (Guinan 2006; 1996; Liberman and Guinan 1998).

This efferent component can be subdivided in two groups, which are distinct in locations of their cell bodies and projections, their neurotransmitter systems, and physiological effects. The better understood of these is the medial olivocochlear (MOC) system, originating in the medial part of the SOC, which sends its axons to the basolateral membranes of outer hair cells (OHCs). Less well understood is the lateral olivocochlear (LOC) system, originating in the lateral part of the SOC, which sends its axons to the dendrites of type I afferent neurons and basolateral membranes of inner hair cells (IHCs). Much that is known regarding effects of OC activation stems from electrical stimulation of the OC axons at the floor of the IVth ventricle. However, due to differences in anatomy and axonal pathways, such stimulation exclusively activates MOC fibers. Consequently, there is now a reasonably good understanding of MOC effects on cochlear physiology, while much less is known for the LOC system.

The principal effect of MOC activation is a sustained reduction in cochlear amplification, which is measurable as a reduction in basilar membrane vibration, IHC receptor potential, and afferent neural discharge. This reduction occurs on a relatively fast timescale of about 100 ms; more recently, it has been discovered that prolonged stimulation leads to a further decrease in amplification, on a time scale of about 30 – 60 s.

LOC effects have been measured only indirectly, via stimulation of the inferior colliculus (which has efferent projections to the SOC), and appear to modulate cochlear output, either up or down, as measured via compound action potential (CAP), on time scales of about 30 – 60 s (Groff and Liberman 2003). The functional role of the LOC system is less clear; recently, there is evidence that it may play a role in balancing cochlear afferent output bilaterally (Darrow et al. 2006a), which would be important for binaural aspects of hearing such as sound localization in the azimuthal plane and hearing in noise. There is also evidence that it protects afferent neurons from acoustic injury (Darrow et al. 2007). It is not known whether, and if so, how, LOC neurons respond to sound, although results on slow suppression of round window noise by contralateral sound in awake guinea pigs (Lima da Costa et al. 1997a), can be interpreted as arising from LOC activity, especially when viewed in relation to electrically evoked slow suppression that has different pharmacological properties and is of MOC origin (Yoshida et al. 1999).

The aim of this thesis project is to gain more understanding of the potential roles and response properties of the LOC and MOC systems by conducting two experiments. First, we are specifically interested in sound-evoked slow effects, which have thus far received very little

attention. Given that most animals, especially humans, are often surrounded by sustained moderate-to-high levels of background noise, gaining more understanding of the OC system in these situations is highly relevant. Also, MOC-mediated slow effects correlate better with protection against temporary acoustic trauma then MOC fast effects (Reiter and Liberman 1995), yet very little is known about sound-evoked slow effects. Furthermore, electrically evoked MOC slow effects have been found only at higher frequencies (Sridhar et al. 1995), yet in awake animals the OC system offers protection from permanent acoustic trauma at low frequencies also (Kujawa and Liberman 1997). As sound-evoked slow effects have only been studied by their effects on round window noise (which offers no insight into frequency dependence), we may be able to resolve this paradox by studying slow effects on tonal stimuli covering a wide frequency range, pursued under project 1 of this thesis (Chapter 2). Second, we are interested in further evaluating the bilateral balancing model. We aim to find direct evidence for this by showing the predicted modulatory effects of the LOC system in real-time in response to acute, unilateral manipulations that affect cochlear afferent output, pursued under project 2 of this thesis (Chapter 3).

I.A Anatomy of the olivocochlear system

The olivocochlear (OC) system forms the efferent innervation of the cochlea, originating in various nuclei of the superior olivary complex (SOC), which is located in the brainstem. It is comprised of two subsystems, a medial and lateral part, each with distinct locations of their cell bodies, axonal projections to the cochlea (and cochlear nucleus for the medial part), and neurotransmitter systems. The medial olivocochlear (MOC) system receives afferent input from the cochlear nuclei by which it forms a sound-evoked feedback loop, the principle action of which is to reduce cochlear amplification of sound. Although sound-induced activity and cochlear effects of the lateral olivocochlear (LOC) system have not been shown directly, it seems likely that it also forms a feedback loop, probably with a different functional role than the MOC system. Both OC systems also receive efferent input from other parts of the central nervous system, including the cortex, which may allow non-sound induced modulation of cochlear processing to occur, e.g. attentional modulation. The goal of studying the OC system is to gain insight into how, and under what circumstances, it modulates sound transmission. In this section we briefly review what is known regarding the anatomy, physiology, and functional roles of the OC system in mammals; more extensive reviews are available (Eybalin 1993; Guinan 2006; 1996; Irvine 1992; Schwartz 1992).

The superior olivary complex contains two principle nuclei, the medial and lateral superior olive (MSO and LSO), and several others collectively called the periolivary nuclei (Guinan et al. 1972b; Schwartz 1992). Both MSO and LSO are relatively well studied, important nuclei of the ascending auditory pathway. They represent the first level at which considerable binaural processing takes place, and a variety of response types have been recorded (Guinan et al. 1972a; Irvine 1992). The MSO receives input from spherical bushy cells in both anteroventral cochlear nuclei (AVCN), and its principal cells are highly sensitive to the relative timing of sound in both ears. The LSO receives input from the spherical bushy cells of the ipsilateral AVCN, and from the principal cells of the medial nucleus of the trapezoid body (MNTB), which in turn receive their input from the globular bushy cells of the contralateral AVCN. The MNTB cells are glycinergic, such that LSO principal cells receive an IE input (contra: Inhibitory, ipsi: Excitatory) and are thus sensitive to the *relative* level of sound in both ears. Both humans and other animals are known to have perceptual sensitivity to interaural disparities in timing and

level and can localize sounds on the basis of these cues (for a review of human psychophysics, see Blauert 1997). The neurophysiological basis for this sensitivity begins in the SOC.

The OC neurons are located close to, or within, both MSO and LSO, cf. Figure 1. Most MOC neurons are located ventral to the MSO, in the ventral nucleus of the trapezoid body (VNTB). Sound-evoked responses are mediated by cells from the contralateral posteroventral cochlear nucleus (PVCN), most likely stellate cells, which correspond to chopper units (Brown et al. 2003; De Venecia et al. 2005). Because their sound-evoked responses can be facilitated by sound from the ipsilateral PVCN, there must be an ipsilateral innervation as well; however, it is not known which cell types are involved. A majority of MOC neurons send their myelinated axons back across the midline, superficially under the floor of the IVth ventricle, via the crossed olivocochlear bundle (COCB), to the contralateral cochlea; the remainder does not cross but travels via the uncrossed olivocochlear bundle (UOCB) to the ipsilateral cochlea. In most species the ratio of contra vs. ipsi projections is about 2/3 vs. 1/3. The superficial location of the axons in the COCB makes lesions as well as electrical stimulation at the floor of the IVth ventricle very convenient.

As indicated in Figure 1, the LOC neurons are located within and around the LSO. The cells lie within two subgroups, called 'intrinsic' and 'shell' neurons, respectively, which are distinct in several aspects that we will describe later. Although their inputs are not known with certainty, the proximity to the LSO principal cells suggests that they may receive similar IE-type inputs via cochlear nucleus and MNTB. The vast majority (90-99% depending on species) of LOC cells sends their axons to the ipsilateral cochlea via the UOCB; in contrast to MOC axons, they are not superficial, making lesions more difficult (the remainder crosses the midline with the COCB, similar to MOC axons, and innervates the contralateral cochlea). The deeper location of the axons and the fact that they are unmyelinated makes direct electrical stimulation difficult, considerably complicating the study of their physiological effects in the cochlea.

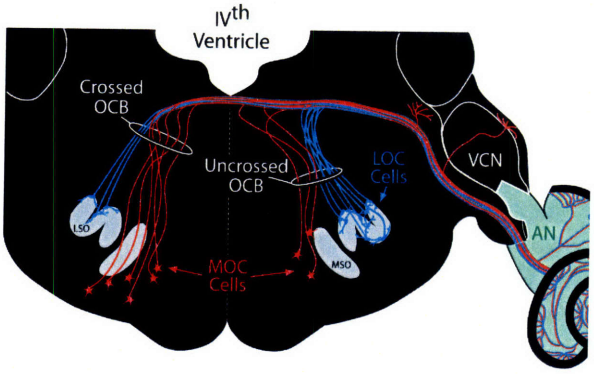

Figure 1. Schematized transverse section of the brainstem, showing locations of MOC and LOC cells, and the locations of their axons projecting into the cochlea via the COCB and UOCB. Note that the innervation for one side only is shown.

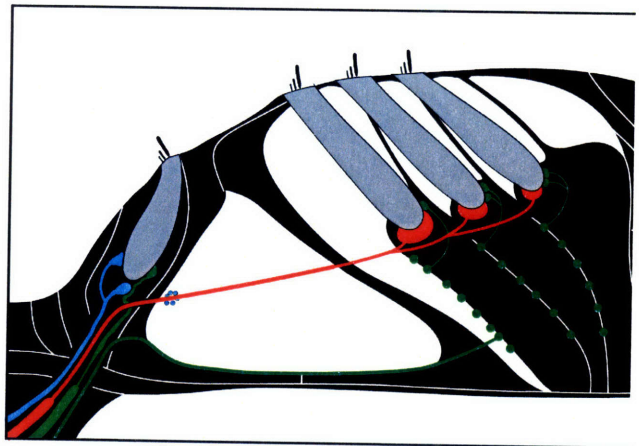

Figure 2. Schematized section of the organ of Corti showing afferent (green) and efferent (blue/red) innervation of hair cells and neurons. LOC neurons (blue) project to type I afferent neurons and IHCs, while MOC neurons (red) project to OHCs.

When reaching the organ of Corti through the habenula perforata, the MOC axons cross the tunnel of Corti to reach the outer hair cell (OHC) area, as shown in Figure 2. Each axon branches

and makes synaptic contact with the basolateral membranes of many OHCs; thus each MOC cell may be in contact with dozens of OHCs in total (up to 50 in guinea pig, Brown 1989; up to 80 in cat, Liberman and Brown 1986). This projection is towards similar characteristic frequencies (CFs) relative to the site from where it receives its dominant afferent input (Liberman and Brown 1986). The density of MOC innervation is not constant; it is relatively sparse in the apex, reaches a peak in the basal half of the cochlea, and then slightly tapers off in the extreme base (Liberman and Brown 1986).

The neurotransmitter released at the MOC/OHC synapses is acetylcholine (ACh), and the OHC receptors are cholinergic α9/α10. These are non-specific cation channels; when open the resulting Ca^{2+}-influx leads to activation of nearby Ca^{2+}-activated K^+ channels (SK2), ultimately leading to K^+ outflow and hyperpolarization of the OHC (Guinan 2006). MOC terminals also contain γ-amino decarboxylase (GAD), a marker for GABA (Eybalin 1993; Maison et al. 2003a), and accordingly a variety of GABA receptors have been shown in the cochlea and spiral ganglion (Yamamoto et al. 2002). Not much is known about the role of GABA *in vivo*, but it does not appear to have a direct modulatory role on either cochlear mechanics (as measured by DPOAEs) or afferent transmission (as measured via ABR); rather it appears to be important for long-term maintenance of hair cells and neurons (Maison et al. 2006). Finally, in mouse, VAT and GAD co-localize with calcitonin gene-related peptide (CGRP) throughout the OHC area (Maison et al. 2003a), although the functional role of CGRP is unclear.

As shown in Figure 2, LOC axons remain within the inner hair cell (IHC) area and do not cross the tunnel of Corti (Liberman 1980; Maison et al. 2003a). They branch and innervate an extended region of the cochlear spiral, synapsing mostly on dendrites of afferent type I neurons, and to a lesser extent on IHCs directly. LOC innervation density is fairly uniform throughout the entire cochlea. Some LOC axons branch in both directions and innervate a very large region along the cochlea, while the other group only spirals in one direction, and not quite as far (Brown 1987). In mouse, the bidirectional axons localize tyrosine hydroxylase (TH), a precursor to dopamine synthesis, which is consistent with the TH staining of shell neurons of the LOC, whereas the unidirectional neurons stain for both vesicular acetylcholine transporter (VAT) and GAD, which are markers for ACh and GABA, respectively, consistent with the staining of intrinsic LOC neurons for these markers (Darrow et al. 2006b). Thus, at least in this species, the two LOC neuron groups appear to differ in the location of cell bodies, axonal branching pattern in the cochlea, as well as neurotransmitter systems. There is further histochemical evidence for peptidergic neurotransmitters of the LOC system, such as CGRP and urocortin (Eybalin 1993; Maison et al. 2003a; Vetter et al. 2002), but it is not known how these localize with respect to the two LOC subsystems. CGRP appears to play a role in controlling afferent discharge rate (Maison et al. 2003b), while urocortin seems to be involved with establishing normal thresholds, perhaps via a developmental role (Vetter et al. 2002). The pharmacology of the LOC system is not well understood beyond what is known about their putative neurotransmitters in general: that dopamine and GABA are presumably inhibitory, while ACh and CGRP are excitatory, although ACh is inhibitory to OHCs (via coupling to SK2 channels). What seems clear is that the LOC system is pharmacologically more diverse and functionally perhaps more complicated than the MOC system.

I.B Physiology of the medial olivocochlear system

I.B.1 Responses of MOC neurons

Recordings of MOC cells from cats and guinea pigs indicate that several of their response properties are similar to those of type I afferents in the auditory nerve. However, there are some important differences, mainly (Brown et al. 1998a; Brown et al. 1998b; Liberman 1988b; Warren and Liberman 1989b):

- Main ear: when recording MOC responses from their central axons, most fibers respond to sound in the ipsilateral ear only (~ 2/3), but some only to sound in the contralateral ear (~ ¼). The remainder (~ 1/12) responds to sound in either ear, and these units are aptly called 'either-ear' units. Over a population of fibers, contra vs. ipsi units are equally sensitive, but in 'either-ear' units one ear is always more sensitive.
- Response properties: although MOC fibers are sharply tuned, their spontaneous rates are much lower than can be found in type I afferents, at least in anesthetized preparations. In contrast to the afferents, dynamic range is much larger, showing little saturation even at high stimulus levels. Interspike-intervals are much more regular than for the afferents, leading to a 'chopping' peri-stimulus time histogram.
- Facilitation: MOC cells increase their discharge rate (spontaneous and driven) to sound in the preferred ear when presented simultaneously with sound in the non-preferred ear (defined as that ear in which sound does not lead to a response when presented in isolation). Facilitation is stronger for continuous broadband noise vs. continuous tones or pulsed noise; it also lowers MOC thresholds. Facilitation is strongest for fibers that have a lower response rate to preferred-ear stimuli alone. Finally, facilitation has been shown to outlast the facilitating stimulus by at least several minutes; on even longer time scales, by exposure to conditioning noise over a period of several days, the effect of facilitation is further increased.

I.B.2 Response variability

A confounding factor in studying the MOC system is that driven and spontaneous discharge is reduced by drugs commonly used to induce anesthesia. To reduce variability associated with anesthetic state, the MOC system is often stimulated electrically at the floor of the IVth ventricle when studying its peripheral effects. Potential drawbacks are that this stimulates a fixed portion or possibly the entire COCB and probably leads to an unnatural spiking pattern. Boyev et al. (2002) found that MOC-mediated DPOAE adaptation was reduced by about 50% in barbiturate-anesthetized guinea pigs relative to awake guinea pigs, while fentanyl and droperidol did not affect the adaptation magnitude. On the other hand, Lima da Costa et al. (1997b) found no difference in (putatively) MOC-based suppression of round window noise in response to contralateral sound in awake vs. xylazine-anesthetized guinea pigs, while a combination of ketamine and xylazine reduced suppression by roughly 30%.

In addition to the variability introduced by anesthesia, MOC neurons appear to have some intrinsic variability between animals, as measured by thresholds and maximum rate (Liberman 1988a). This is likely the cause of the variability that is observed in the MOC reflex strength over a population of animals (Maison and Liberman 2000). Additionally, variation in MOC

responsiveness, as assessed by contralateral sound-induced CAP suppression, has been shown within the same animal over a period of about one day (Liberman 1989).

I.B.3 Peripheral effects of MOC activation. I. 'Fast effect'

As described above, activation of MOC axons leads to ACh release at the synapse with OHCs, ultimately leading to K^+ efflux through SK2 channels, which should hyperpolarize the OHCs. Hyperpolarization would shift the set point of electromechanical transduction to a less sensitive region, thereby reducing OHC electromotility (for recent reviews, see He et al. 2006; Santos-Sacchi 2003). The opening of SK2 channels also lowers the resistance of the basolateral membrane, reducing receptor potential, which also reduces electromotility. Although these mechanisms are postulates and not based on experimental evidence, they seem plausible and are consistent with the observation that MOC activation leads to reductions in cochlear gain. This gain reduction affects basilar membrane motion (Murugasu and Russell 1996), and subsequently all 'downstream' responses, notably IHC receptor potential (Brown and Nuttal 1983; Brown et al. 1983), afferent response rate (Guinan and Gifford 1988b; Warren and Liberman 1989a; Wiederhold and Kiang 1970), and CAP amplitude (Liberman 1989; Puria et al. 1996) are also reduced. In contrast, cochlear microphonic (CM) increases, presumably because the opening of SK2 channels increases the conductance of OHCs and leads to larger transmembrane currents (Mountain et al. 1980). Importantly, due to response adaptation in afferent transmission, MOC activation can *increase* the afferent response to transient signals presented in a continuous background noise, which has been called 'anti-masking' or 'unmasking' (Kawase et al. 1993; Kawase and Liberman 1993). Consistent with the peak of the innervation density of MOC fibers in the basal half of the cochlea, MOC effects are largest at mid- to high-frequency regions (Guinan et al. 1983; Liberman 1988b). When measured in terms of suppression magnitude, MOC effects decline with increasing stimulus levels, at least for shock-evoked suppression (which is typically fixed, independent of stimulus level). However, when suppression is converted to equivalent attenuation (the increase in input required to reach the same response during MOC activation), MOC effects are typically largest at medium levels, and are substantial at high levels also (Guinan and Stankovic 1996). All of the mentioned peripheral MOC effects can be elicited by electrical stimulation and contralateral- or ipsilateral sound, although these methods vary in elicited reflex strength.

MOC-induced cochlear suppression has a time constant on the order 100 ms, and is similar in various species of animals as well as humans (Backus and Guinan 2006; Kim et al. 2001; Kujawa and Liberman 2001; Liberman et al. 1996). Although slow compared to many cochlear processes, this is termed the 'fast' effect. The build-up of the MOC effect occurs peripherally (likely the OHC soma and/or the presynaptic terminal), not in the MOC cell bodies, because these are fully activated with considerably smaller delays (Liberman 1988b), and is also consistent with the 100 ms buildup as seen with shock-evoked activity. Presumably, repeated ACh release at the OHC synapse leads to increasing intracellular Ca^{2+} concentration, which is further facilitated by the sub-synaptic cistern, preventing Ca^{2+} from diffusing away from the synapse (for a review, see Fuchs 1996). Ultimately, this opens up increasing numbers of Ca^{2+}-activated SK2 channels. When MOC activity stops, the peripheral effects decay with a similar time constant.

In addition to the suppression of driven responses, MOC activation also appears to be able to suppress AN spontaneous activity. Reductions in auditory nerve spontaneous rate of up to about 35% (about 4 dB) have been reported in sensitive fibers (the average suppression was much

smaller) when electrically shocking the OC bundle in cat (Guinan and Gifford 1988a), while similar suppression has been found in round window noise in awake guinea pig in response to contralateral broadband noise (Lima da Costa et al. 1997a). It is assumed that neural spontaneous activity can be reduced because endocochlear potential decreases upon MOC activation (Mountain et al. 1980), and reduction in endocochlear potential has been shown to reduce auditory nerve spontaneous rates (Sewell 1984).

I.B.4 Peripheral effects of MOC activation. II. 'Slow effect'

Sustained shock-evoked MOC activation in guinea pig leads to a slow suppression of CAP responses beyond those induced via the MOC fast effect (Sridhar et al. 1995); slow suppression can also be seen in mouse, although it is often obscured by slow enhancement (described below) (Maison et al. 2007b). Slow suppression of CAP responses occur with a time constant of about 30 s; after reaching a maximum at about 2 minutes, the effect adapts with a similar time constant. An important difference with respect to the fast effect is its frequency distribution; slow suppression occurs only above 10 kHz in guinea pig. Thus, the ratio of slow to fast suppression magnitude increases with frequency, but remains < 1. The MOC "slow effect" pathway involves the same receptor as MOC fast effect pathway (Sridhar et al. 1995), and appears to involve calcium-induced calcium-release, which activates distant SK2 channels on the outer hair cell membrane (Sridhar et al. 1997). Consistent with the MOC fast effect, slow suppression is abolished by low doses of systemic gentamicin (Yoshida et al. 1999). MOC slow effects are also seen in basilar membrane motion, and this data suggests that different mechanical processes underlie the fast and slow effect (Cooper and Guinan 2003).

Persistent (non-adapting) suppression of round window noise in awake guinea pigs on two time scales (fast and slow) has also been demonstrated (Lima da Costa et al. 1997a). Interestingly, in this case, the slow component of the suppression was more resistant to gentamicin than the fast component. Lima da Costa et al. argued that the slow suppression was due to the MOC slow effect described by Sridhar et al. (1995), although they did not provide direct evidence to rule out a central origin (MOC response modulation) of their slow component. Such a central origin would imply that MOC neurons are capable of increasing their response rate during sustained monaural sound stimulation, which would be an interesting property. Also, because they only measured RW noise, it is somewhat ambiguous whether it was a strictly neural or outer hair cell effect, or a change in blood flow to the cochlea via sympathetic innervation. A strictly neural effect could be of LOC origin, and if true, would be the first evidence of sound-evoked LOC activity and a possible indication for a role of this system. The goal of the project described in Chapter 2 of this thesis is to resolve the ambiguities concerning the responsible neural pathway(s) and extensively characterize suppressive effects on the cochlea during sustained contralateral sound stimulation.

Recently, another type of MOC effect has been identified in mouse during sustained shock-evoked stimulation, which manifests as a slow (peaking after about 5 s) *enhancement* of DPOAE, and which does not depend on the nAChR (as verified by strychnine blockade and α9-null mice), apparently constituting a separate mechanism of the MOC system to interact with cochlear physiology (Maison et al. 2007b).

I.C Physiology of the lateral olivocochlear system

Because LOC fibers are thin and unmyelinated, they are not amenable to single-fiber recording nor to direct electrical stimulation (Guinan 1996). Therefore, there is no direct

evidence whether they respond to sound; however, given the proximity of LOC cells to LSO principal cells, which have well-characterized IE-type responses to sound (for a review, see Irvine 1992), it is plausible that LOC cells also receive IE-type binaural inputs, although their response dynamics may be different from the LSO principal cells. Indirect activation of LOC cells via electrical stimulation of the inferior colliculus leads to slow (~30 – 60 s) suppression or enhancement of CAPs, without affecting OHC-based measures (Groff and Liberman 2003). However, another experiment with gentamicin (a blocker of the MOC system) abolished both inhibitory and excitatory cochlear effects of inferior colliculus stimulation (Mulders and Robertson 2006), although the stimulation sites could have been different than those used by Groff and Liberman.

There is no direct evidence that positively identifies any substance as an LOC-neurotransmitter according to the usual criteria (pre-synaptic presence, depolarization- and Ca^{2+}-dependent release, post-synaptic receptors). However, several putative neurotransmitters have been identified: acetylcholine (ACh), γ-amino butyric acid (GABA), dopamine, urocortin, calcitonin gene-related peptide (CGRP), enkephalin, dynorphin, and opioids (for a review, see Eybalin 1993). In most cases this is based on histochemical evidence for the presence of key enzymes in the biosynthetic pathway of the transmitter and/or presence of specific postsynaptic receptors; Ca^{2+}-dependent release of these putative neurotransmitters upon depolarization of the terminal is very hard to demonstrate convincingly given the difficulty in recording from/stimulating these neurons. In the following, we briefly review studies involving some of these putative neurotransmitters.

Presence of acetylcholine (ACh) is usually indicated by immunostaining for vesicular acetylcholine transporter (VAT). In mouse, VAT immunoreactivity is seen throughout the IHC area and also in cells of the LSO region, and colocalizes with GAD and CGRP, but not with TH (Darrow et al. 2006b; Maison et al. 2003a).

GABA is present in both IHC and OHC areas in mouse and guinea pig (Fex et al. 1986; Maison et al. 2003a). Relatively little is known about the functional roles of this putative inhibitory neurotransmitter. Genetic manipulations that removed specific GABA receptor subtypes showed no specific changes in afferent transmission (Maison et al. 2006). The latter study did report progressive hearing loss in mice lacking specific GABA receptor subtypes, which may indicate a role in long-term maintenance of cochlear health.

Inner and tunnel spiral bundles, as well as cells in the LSO region of the brainstem, are immunoreactive to the key enzyme of catecholamine synthesis, tyrosine hydroxylase (TH), but not to dopamine-β-hydroxylase (DBH) and phenylethanolamine-N-methyl transferase (Eybalin 1993; Jones et al. 1987); this implies that dopamine is synthesized in these locations, but not further converted to epinephrine or norepinephrine. There is physiological evidence for dopamine receptors in the IHC area of guinea pig (d'Aldin et al. 1995). In mouse, TH-positive LOC cells do not co-localize with VAT-positive cells in the brainstem, nor do their terminals in the cochlea (Darrow et al. 2006b); TH immunoreactivity is fairly constant from base to apex. This finding of separate cytochemical subgroups may correspond to the different functional subgroups of LOC cells that have been reported in guinea pig (Groff and Liberman 2003), if we assume that the dopaminergic subgroup inhibits neuronal responses while the ACh-GABAergic subgroup increases neuronal excitability. Evidence for inhibitory function of DA was shown by cochlear perfusion of DA agonists and DA transporter inhibitors, either of which depresses CAP amplitudes and round window noise in a dose-dependent reversible manner in guinea pig (d'Aldin et al. 1995; Ruel et al. 2006). Also, ABR amplitudes are enhanced ipsilateral to selective

unilateral LSO lesions, which suggests that at least a portion of the LOC system is inhibitory to the auditory nerve (Darrow et al. 2006a).

I.D Postulated functional roles of the olivocochlear system

I.D.1 Protection from acoustic trauma

The MOC system has been shown to protect against temporary as well as permanent acoustic injury (for a review, see Rajan 1991). Presumably, this is because MOC activation reduces cochlear responses (although such reductions are small at high stimulus levels), thereby decreasing mechanical, metabolic, and/or chemical stress. Consistent with this, MOC reflex strength has been shown to correlate with resistance to sound-induced trauma in guinea pig (Maison and Liberman 2000), and overexpressing α9 nAChR (a subunit of the MOC-OHC postsynaptic receptor) in mice leads to increased protection against temporary and permanent acoustic injury (Maison et al. 2002). However, the protective pathways are not entirely understood; for example, although the MOC fast effect and its associated decrease in cochlear response might be expected to be protective against overstimulation, it does not appear to be responsible (Maison et al. 2007a; Reiter and Liberman 1995), favoring a role for the MOC slow effect. It is thus paradoxical that MOC slow effects appear to exist at high frequencies only (>10 kHz in guinea pig with electrical stimulation of MOC fibers), while sound-evoked OC-mediated protection against acoustic overstimulation is effective at all frequencies of guinea pig hearing (Kujawa and Liberman 1997; Sridhar et al. 1995; Zheng et al. 1997). Although a comparison between these studies is complicated by the fact that temporary and permanent acoustic trauma probably result from at least partially different mechanisms and result in different pathologies, the discrepancies merit further research.

Given the presumed presence of inhibitory neurotransmitters in LOC terminals, in particular dopamine, it is possible that the LOC system could protect type I afferent neurons from excitotoxicity, either induced by excessive sound stimulation or ischemia. Consistent with this hypothesis, cochlear perfusion of piribedil, a dopaminergic agonist, in guinea pig reduced swelling and vacuolization of afferent terminals after intense sound exposure and ischemia, and reduced loud sound-induced CAP threshold shift (d'Aldin et al. 1995). In mouse, selective unilateral destruction of LOC cell bodies by injection of neurotoxin into the LSO leads to larger temporary threshold shifts in the ipsilateral ear relative to the control side, as measured by ABR, while DPOAE shifts are equal on both sides (Darrow et al. 2007). This implies that the protective mechanism of the LOC system act after the OHC stage, consistent with the fact that the MOC system was not compromised by the LSO lesion.

Although the protective effects of both LOC and MOC systems are robust and repeatable in various experimental conditions, it has been argued that they are an epiphenomenon, because the necessary conditions (traumatic noise levels) for the evolution of a protective system were not present until relatively recently in evolutionary history (Kirk and Smith 2003).

I.D.2 Enhanced sensory information processing

Given that MOC activity suppresses cochlear responses, this leads to reduced adaptation of the IHC-neural synapse. Adaptation occurs because the readily releasable pool of neurotransmitter vesicles becomes depleted upon prolonged activation. Synaptic adaptation leads to a reduction in auditory nerve firing rate, which seems to be a physiological correlate of psychophysical masking (Delgutte, 1990). If MOC activation leads to reduced IHC stimulation,

the synapse will be less adapted, decreasing the amount of masking. Indeed, anti-masking properties of the OC system have been shown both in terms of CAP amplitude as well as auditory nerve spike rate (Kawase et al. 1993; Kawase and Liberman 1993; Winslow and Sachs 1988). Given that it is more common to be surrounded by low- to medium-level background noise rather than complete silence, these anti-masking properties appear to be an important characteristic of the OC system. Thus, although the MOC system suppresses the mechanical response of the cochlea, it appears to increase the neural response to transient signals in the presence of background noise.

Although the anti-masking capability of the MOC system is well established, other roles in information processing have also been proposed. These are in the realm of attentional modulation of auditory processing, although these claims have mostly remained controversial, lacking clear-cut evidence and reproducibility of incidental positive results. Recently, a convincing result has been reported involving experiments in awake chinchilla, showing strong modulation of cochlear responses, consistent with MOC activation, during periods of high attentional load involving a visual discrimination task (Delano et al. 2007). If true, this implies that attentional modulation of sensory information processing, which is well established at cortical levels, begins at the most peripheral level of the auditory system.

I.D.3 Development

In cochlear development, the immature state is characterized by supernumerary branches of both radial and spiraling afferent fibers, and the lack of efferent innervation in the OHC area. In cat, the pruning of afferent branches, the arrival of the efferent innervation at the bases of OHCs, and the maturation of hearing all appear to be roughly coincident (Pujol et al. 1978), which suggests a developmental role of efferent fibers. Although differences in afferent innervation *density* in IHC or OHC areas of neonatally de-efferented cats with respects to controls were not found (Liberman et al. 2000), marked abnormalities in afferent *responses*, in particular increases in threshold at CF, decreased tuning sharpness and decreased spontaneous rates do result (Walsh et al. 1998). In contrast, in adult cats that are chronically de-efferented the only abnormality is a lowered spontaneous rate (Liberman 1990). Similar to the findings of Walsh et al., Vetter et al. (2002) found marked threshold elevations in transgenic urocortin-null mice; urocortin is a peptidergic neurotransmitter that localizes to the inner spiral bundle. Overall, these findings strongly suggest an important role for olivocochlear efferents in certain aspects of normal cochlear development, especially in the outer hair cell area.

I.D.4 Interaural balancing by the LOC system

It has been proposed that one of the roles of the LOC system is to balance the long-term average neural output from both cochleae (Guinan 1996), and recently supporting evidence has been obtained (Darrow et al. 2006a). Such a 'calibration' could be important for binaural processing tasks such as sound localization and binaural signal detection, yet has to our knowledge never been explicitly considered prior to the cited study.

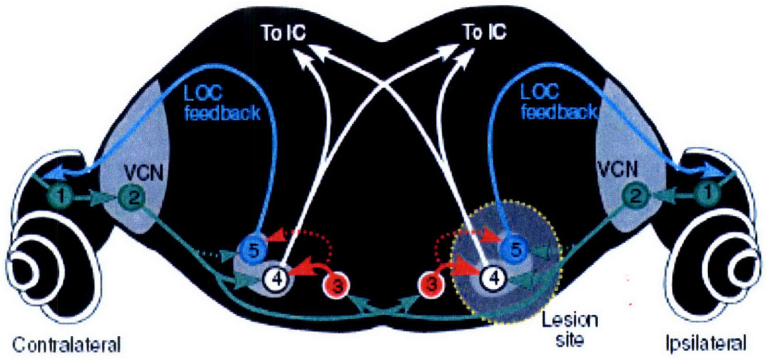

Figure 3. Hypothesized LOC feedback model (Darrow et al. 2006a). A schematized transverse section of the brainstem showing cochlear afferent output (1), projecting to the ventral cochlear nucleus (2), and ipsilaterally to LSO principal cells (4) and contralaterally to the MNTB (3) via the trapezoid body. Glycinergic MNTB cells inhibit LSO principal cells (4), giving rise to their IE-type response. LSO principal cells then project onwards to the inferior colliculus (IC) bilaterally. It is hypothesized that LOC cells (5) receive similar IE-type responses, and provide net negative feedback mainly to the ipsilateral cochlea. This circuit could act to reduce differences in long-term average output between both cochleas.

In this model, LOC inputs are assumed to be IE-type, i.e. contralateral inhibitory and ipsilateral excitatory, as they are for the LSO principal cells. It is further assumed that these IE inputs are integrated over a sufficiently long duration, such that momentary interaural level differences are not processed, but rather difference in long-term average cochlear output. By providing net negative feedback to the LSO's ipsilateral cochlea, differences in long-term average cochlear output will be reduced, as schematized in Figure 3. Because this proposed feedback loop is insensitive to momentary interaural level differences, sound localization is not affected. This LOC model makes the binaural auditory pathway a closed-loop system, with all the traditional advantages over open-loop systems such as disturbance rejection, guaranteed performance, and reduced sensitivity to design variables (Oppenheim and Willsky 1997). The only potential disadvantage is that net cochlear output in terms of spike count is reduced relative to 'open-loop' performance, although it is not trivial to assess the functional implications thereof. Given that the LOC system appears to consist of at least two subdivisions with multiple neurotransmitter systems, this model is clearly an oversimplification. However, it can explain some experimental data (Darrow et al. 2006a), and offers a framework that can be used for further experiments to probe the LOC system, such as those described in Chapter 3 of this thesis.

I.E Summary

The olivocochlear efferent system comprises a large number of neurons that innervate sensory cells and afferent neurons in the cochlea. Current knowledge is limited mostly to the MOC system, which acts to reduce cochlear gain, providing protection against acoustic injury and enhanced detection of transient signals in noise. Recent advances in our understanding of the OC system point towards slow effects that act on a timescale of minutes, including suppressive effects of the MOC system, as well as suppressive and enhancing effects of the LOC system. These LOC effects were among the first published results that indicated a role for the LOC system, although they were obtained with indirect electrical stimulation in the inferior colliculus. The binaural balancing model provided further insight into the possible functional significance of

the suppressive/enhancing effects of the LOC system by showing that this system may play a role in regulating cochlear afferent output to improve binaural signal processing.

Further experiments, described in Chapter 2, investigating OC slow effects with sound stimulation (instead of electrical shocks) will lead to new insights into the properties of these effects and their neural origin(s), with implications for their role in hearing in noise and protection against acoustic overexposure – the protective role of the MOC system has not been well explained by the known properties of electrically evoked slow effects. In addition, obtaining direct evidence for the proposed bilateral balancing role of the LOC system would attach great significance to this system as it relates to binaural aspects of hearing. Such experiments are described in Chapter 3.

II Sound-evoked suppression of cochlear responses by the medial olivocochlear system: delayed suppression

II.A Introduction

Medial olivocochlear (MOC) efferent effects on cochlear processing can be substantial, and have been extensively studied (for recent reviews, see Guinan 2006; Guinan 1996). The most well-characterized effect of MOC activation (either via electrical shocks or sound stimulation) is a fast (~100 ms) reduction of cochlear responses, by hyperpolarizing the outer hair cells through Ca^{2+}-activated outward K^+ currents (involving SK2 channels), mediated via α9/α10-nicotinic acetylcholine receptors (nAChR) at the MOC/outer hair cell synapse. This suppression is called the MOC 'fast effect', and can be measured in the mechanical response of the basilar membrane (Murugasu and Russell 1996), inner hair cell receptor potential (Brown et al. 1983), and afferent response rate (Wiederhold and Kiang 1970).

It is now also well established that sustained MOC activation in guinea pig evokes an MOC 'slow effect', a progressive response suppression of compound action potential (CAP) that builds up on a timescale of about 30 s (Sridhar et al. 1995). The effect is initiated via the same α9/α10 nAChR and is thought to rely on a Ca^{2+} "wave" diffusing along the outer hair cell membrane to distant SK2 channels (Sridhar et al. 1997), of different pharmacological profile than the SK2 channels mediating the fast effect (Yoshida et al. 2001). Basilar membrane data indicates that the slow effect may additionally induce a decrease in outer hair cell mechanical stiffness (Cooper and Guinan 2003). Further, protection from temporary threshold shift following intense noise exposure is better explained by the properties of the slow effect than the fast effect (Reiter and Liberman 1995). Similarly, mice with overexpression of SK2 channels have enhanced MOC fast effects yet are not more protected from acoustic injury relative to wildtype controls (Maison et al. 2007a), yet overexpression of the α9 nAChR does lead to enhanced protection (Maison et al. 2002), implying that other downstream effects, possibly the MOC slow effect, are responsible for protection. However, MOC slow effects are measurable at high frequencies only (>10 kHz, Sridhar et al. 1995), yet guinea pigs with an intact OC bundle suffer less permanent acoustic injury at both high *and* low frequencies following intense noise exposure vs. animals that are surgically de-efferented (Kujawa and Liberman 1997; Zheng et al. 1997).

Slow effects on round window (RW) noise can be induced via contralateral sound in awake guinea pig (Lima da Costa et al. 1997a). The sound-evoked slow effects resemble the shock-evoked MOC slow effect in terms of suppression magnitude and time course, and are sensitive to gentamicin (a blocker of MOC effects on the cochlea), although a higher dose is required than for the fast effect (250 vs. 150 mg/kg, Lima da Costa et al. 1997a). Although the properties and pharmacological profile of the shock-evoked slow effect clearly implicate the MOC system, no such direct evidence exists for the sound-evoked slow effects. In particular, the differential sensitivity to gentamicin of sound-evoked fast and slow effects found by Lima da Costa et al. is difficult to reconcile with the fact that shock-evoked MOC fast and slow effects have identical sensitivity to gentamicin (Yoshida et al. 1999).

We consider another possibility, namely that sound-evoked slow effects are mediated by the lateral OC (LOC) system. In cat and mouse, LOC axons synapse exclusively in the inner hair cell

area (Liberman 1980; Maison et al. 2003a), primarily on the dendrites of the afferent neurons, and there is some evidence (in guinea pig) that they are able to suppress or enhance afferent neural responses on a timescale of minutes, without affecting outer hair cells as measured via distortion-product otoacoustic emission (DPOAE) and cochlear microphonic (CM) (Groff and Liberman 2003). Thus, suppression of RW noise would be possible through the action of the LOC system alone, and if this component is more resistant to gentamicin than the MOC system, it could explain the differential sensitivity observed in the sound-evoked experiments (Lima da Costa et al. 1997a). If true, such sound-evoked slow effects should not alter outer hair cell response such as DPOAEs.

Finally, sound-evoked cochlear suppression on a slow timescale could also be due to a central modulation of the MOC system, rather than a peripheral effect occurring in the outer hair cells. Modulation of MOC responsiveness has been reported in several different kinds of situations. First, it is firmly established that MOC cells can be facilitated, i.e. increase their response rate, by sound delivered from the non-preferred ear, which does not evoke a response when presented in isolation, and this effect can outlast the facilitating stimulus by at least several minutes (Brown et al. 1998a; Liberman 1988b). Efferent thresholds relative to afferent thresholds are quite variable between animals (Liberman 1988a), which could reflect permanent between-animal differences in the efferent reflex, but may also indicate variability over time in the same animal. Such temporal variability in one animal can be observed over a period of one day (Liberman 1989). Finally, daily noise conditioning for more than one week leads to modest, yet statistically significant, increased effects of facilitation with respect to controls (Brown et al. 1998b). Thus, to postulate that MOC responses and its cochlear effects can increase over time during sustained monaural sound stimulation seems a plausible possibility.

The goal of our experiments was to extensively characterize sound-evoked cochlear suppression mediated via the OC system during sustained contralateral noise, not only in terms of its effects on spontaneous potentials (RW noise), but also in terms of sound-evoked neural (CAP) and outer hair cell based responses (DPOAE and CM). Through this we aim to definitively resolve whether such effects arise via the LOC or the MOC system, and in case of the latter, whether through a central modulation of the MOC system or through the peripheral MOC slow effect. The basic characterization of these sound-evoked efferent effects will be supplemented with pharmacological and lesion experiments; in particular, sensitivity to gentamicin will be used to probe the role of the MOC system, and lesions of the crossed portion only, as well as the entire OC bundle, will be used to assess contra- vs. ipsilateral reflex pathways. Lesions made during contralateral noise will be used to differentiate between central vs. peripheral origins of the slow effects. Finally, by characterizing sound-evoked suppression on long time scales, we may shed more light on OC-mediated protection against acoustic overexposure, which appears to rely on the MOC slow effect, the properties of which are not entirely consistent with established protective capabilities of the OC system (Kujawa and Liberman 1997; Reiter and Liberman 1995; Zheng et al. 1997).

A preliminary version of this work has been presented (Larsen and Liberman 2008).

II.B Methods

II.B.1 Animal preparation

Results from 24 female albino guinea pigs (*Cavia Porcellus*, Hartley strain, Charles River Labs), weighing 350-800 g, are reported. Surgical and experimental procedures were approved by the Animal Care Committees of both the Massachusetts Eye & Ear Infirmary and MIT. Animals were anesthetized with sodium pentobarbital (Nembutal, 25 mg/kg i.p.), Fentanyl (0.20 mg/kg i.m.) and Droperidol (10 mg/kg i.m.), with boosters given as needed to maintain an areflexive state. Bullas were exposed bilaterally via a dorsal approach and opened to allow access to the round window of the cochlea. After positioning of the electrodes, the hole in the bulla was covered with fine cotton lightly soaked in petroleum jelly, to impede convective air flow that might cool the cochlea. The ear canals were severed close to the tympanic ring to allow positioning of a custom-built acoustic assembly. In experiments requiring access to the IV^{th} ventricle, a posterior craniotomy was performed, and the medial portion of the cerebellum was aspirated. Lesions to the OCB were made with a microknife, guided by landmarks on the dorsal surface of the brainstem. Animals were tracheotomized and artificially respirated (only if necessary; Harvard Rodent Ventilator, Model 683; tidal volume 3.5 ml, rate 50 min^{-1}). General physiological state was monitored by EKG (normal rate 280-350 bpm) and rectal temperature (maintained at 37-38 C by heating the experimental chamber and using a heating pad, if necessary). Experiments were continued either until sufficient data were collected, or DPOAE/CAP thresholds has deteriorated significantly (>10 dB) at two or more frequencies. Typically, baseline thresholds could be maintained for the entire duration of the experiment (approximately 10 hours).

II.B.2 Stimuli

All cochlear potentials were measured from a Teflon-coated silver-wire electrode terminating in an uncoated ball, placed on the round window, referenced to an electrode in the neck muscles. The differential voltage was filtered (300-3000 Hz) and amplified 10,000x (Grass P5 series). Gross neural activity was measured from compound action potentials (CAP) in response to 5 ms tone pips (0.5 ms rise/fall time). Tone pips were presented in alternate-polarity pairs and averaged to obtain CAPs, or subtracted and divided by 2 to obtain cochlear microphonic (CM). CAP amplitude was calculated as the peak-to-peak voltage of the CAP waveform, and usually converted to dB re 15 μV (the criterion for CAP threshold). CM response was obtained as the magnitude of the Fourier transform component at the stimulus frequency of the CM waveform, expressed as dB re 1 μV. Round window (RW) noise, a measure of auditory nerve spontaneous activity (Dolan et al. 1990), was measured during 128 ms of silence. Its value was calculated as the integral of the power spectrum of the electrode signal between 683 and 917 Hz (30 samples of the FFT centered on 800 Hz, the maximum of the RW noise spectrum), expressed as dB re 1 μV^2.

Distortion-product otoacoustic emissions (DPOAEs) were measured in the ear canal in response to two concurrent 40 ms primary tones (f_1 and f_2), presented in a frequency ratio f_2/f_1=1.22 and level ratio $f_1=f_2+10$ dB. Tones were passed through custom-built precision attenuators, drivers (TDT ED-1), and electrostatic loudspeakers (TDT EC-1). The cubic DPOAE at $2f_1-f_2$ was extracted from the microphone signal (Etymotics Research ER-10C, low-noise pre-amplification of 40 dB) by Fourier transform. The microphone was occasionally calibrated using

a calibrated pistonphone (Bruel & Kjaer 4228) and a dedicated calibration microphone (Bruel & Kjaer 4132); the earphones are calibrated at the start and routinely during the experiment.

All signal generation and online analysis was performed by custom Labview software and a data acquisition I/O card (National Instruments PCI-6052E) interfaced with a BNC terminal block (National Instruments BNC-2090).

II.B.3 Electrophysiological procedures

Experiments were conducted in a sound-proof and electrically shielded room, heated to 30-35 C. Background noise levels varied between 0 and -20 dB SPL depending on frequency and signal averaging. At the start of the experiment, baseline measures of hearing were acquired as follows. DPOAE input-output (I/O) functions were measured, typically using f_2 frequencies of 4, 5.6, 8, 11.3, 16, 22.6, and 32 kHz; at each frequency f_2 level varied from 20 to 80 dB SPL in steps of 5 dB. At each level, 4 spectra were averaged to extract the DPOAE; each spectrum was the average of 25 40-ms waveforms (no gaps between successive waveforms) measured near the tympanic membrane. DPOAE thresholds at each frequency were interpolated as the f_2 level required to obtain a $2f_1$-f_2 level of 0 dB SPL. CAP I/O functions were acquired at the same frequencies from 10-80 dB SPL in 10 dB steps; at each level, 128 tone pip (5 ms with 0.5 ms raised cosine on- and offset) pairs were averaged. Additionally, CAP thresholds from 2-30 kHz were obtained with an automated tracking algorithm, using a criterion level of 15 μV. DPOAE and CAP I/O functions, and CAP thresholds, were measured several times in both ears during the course of the experiment. CAP thresholds were also obtained by interpolating I/O functions a 15 μV criterion level. After establishing baseline CAP and DPOAE metrics, slow suppression effects were characterized as outlined in .

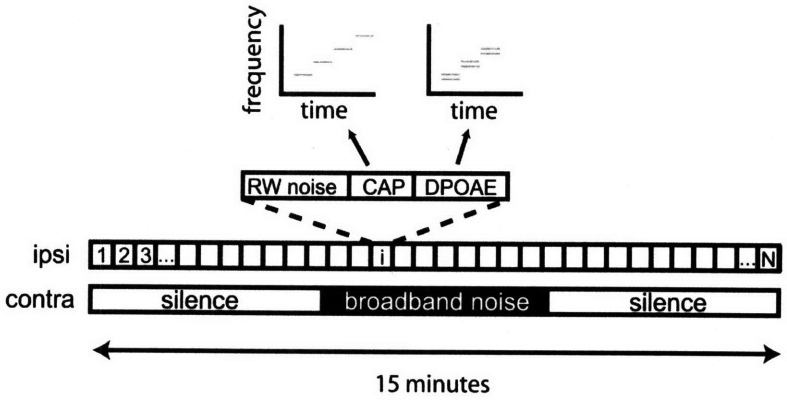

Figure 4. Ipsilateral and contralateral stimulus presentation for one measurement *trial*, typically lasting 900 s (15 min). In the ipsilateral ear, RW noise, CAP (2-6 frequency/level combinations), and DPOAE (1-3 frequency/level combinations) responses were sequentially obtained in interleaved fashion, where a complete measurement of all metrics (a *block*) required about 10 s. Blocks were repeated until the trial was complete. The contralateral stimulus consisted of an epoch of broadband noise (300 s), flanked by silent intervals (typically 300 s each).

Ispilateral responses were measured in continuously interleaved fashion for 900 s (15 min), constituting one measurement *trial*. A complete set of ipsilateral responses typically took about 10 s to measure, and is defined as a *block*. Blocks were acquired until the end of the trial, typically yielding about 90 blocks per trial. Each block consisted of RW noise, measured during

128 ms of silence, followed by CAPs at 2-6 frequency/level combinations (8 averages each), followed by 1-3 DPOAE frequency/level combinations (4 waveform averages per spectrum, 2 spectral averages each). CAP tone pip levels were typically 30-40 dB SPL and produced CAPs of 50-100 μV; DPOAE primaries were typically 25-40 dB SPL and produced $2f_1$-f_2 distortions of 10-15 dB re noise floor (absolute levels: 0-10 dB SPL). All metrics included 'artefact reject' controls, which caused a repeat of the same measurement if a criterion level was exceeded; this level was set differently for each experiment, but at roughly -10 dB for RW noise, 125 μV for CAP, and -5 dB SPL for DPOAE noise level at the $2f_1$-f_2 frequency band. Because of the artifact reject feature, blocks vary in duration, and the sample periods for the metrics are not fixed (although approximately 10 s).

The contralateral ear was stimulated with broadband noise at about 75 dB SPL during the middle 300 s (5 min) of the trial; thus, the first and last 300 s of the trial were silent at the contralateral side. Depending on suppression magnitude and signal-to-noise ratio, typically 3-6 averages of such 900-s trials with fixed stimulus parameters were obtained.

II.B.4 Data analysis

II.B.4.a Quantification of suppression magnitude

All offline analysis was done with custom software in MatLab. CAP, CM, DPOAE and RW noise metrics were all processed in similar fashion, as follows. The entire 900-s time window was subdivided in 10-sec bins, and for each individual metric, data from all available trials was averaged in the appropriate bin. All metrics were expressed in a dB scale, and the initial 300-s measurements (silence in contralateral ear) were averaged to obtain a baseline response measure, normalized to 0 dB. Data from the remaining 600 s was adjusted according to the same normalization. Slow suppression was characterized by averaging each metric's response in a specific time window (reported where appropriate) during contralateral noise. Statistical significance was assessed by two-tailed two-sample *t*-test, at the 5% significance level ($p < 0.05$).

Quantitative comparison of pooled (over animals) suppression magnitudes between various metrics (CAP, DPOAE, RW noise) or different time windows within the same metric made use of the Kendall tau rank correlation coefficient (Kendall 1938). We use this correlation coefficient instead of the usual Pearson correlation coefficient, because the latter assumes a linear relationship between variables and normally distributed errors, while the Kendall τ is a non-parametric test on the variable rankings, which is more appropriate for assessing the degree of correspondence between two variables that have an unknown monotonic relationship. It is calculated as

$$\tau = \frac{4P}{n(n-1)} - 1,$$

where P is the number of concordant pairs and n is the number of items. We used a built-in MatLab function (`corr`) to calculate τ; its value has a straightforward interpretation: the odds ratio of the concordant to discordant sets of observations is $(1+\tau)/(1-\tau)$. Significance of the correlation is computed by the `corr` function and will be assessed at the 5% level ($p < 0.05$).

II.B.4.b Conversion of suppression magnitude to equivalent attenuation

To facilitate comparison of OC-mediated effects on CAP and DPOAE responses, suppression magnitude was converted to 'equivalent attenuation' (Gifford and Guinan 1987; Guinan and Stankovic 1996), although with a subtle difference from the method in the cited studies. We define equivalent attenuation as the *decrease* in input sound pressure level that would yield an identical response change as observed during contralateral sound, and requires the input/output (I/O) function of CAP (or DPOAE) in quiet only, as illustrated in Figure 5 and explained below. Guinan's approach for computing equivalent attenuation is to compare I/O functions measured with and without efferent stimulation, and to find the *increase* in sound level required for obtaining the same response with efferent stimulation vs. no efferent stimulation. Effectively, our approach uses an iso-response criterion on the suppressed response, while the conventional approach uses an iso-response criterion on the unsuppressed response. Our paradigm required deviating from the conventional approach because the nature of the experiment did not permit a reliable measurement of I/O functions during sustained contralateral noise; we could make use of the I/O function measured in quiet only.

Equivalent attenuation was computed using the I/O function measured closest in time to the data being processed (i.e., we did not use a mean I/O function). We used a piecewise cubic Hermite interpolating polynomial (PCHIP, using `interp1` in MATLAB; Fritsch and Carlson 1980) on the I/O functions to convert suppression values into equivalent attenuations; see Figure 5 for examples. First, from the interpolated I/O function, we computed the baseline response level given the stimulus level (blue dots), and subtracted the suppression magnitude to find the suppressed response (red dots). Using an iterative zero-finding algorithm (`fzero` in MATLAB), we then numerically solved for the shifted input level required to produce the suppressed response (green dots). The equivalent attenuation is then equal to the shifted input level minus the original input level.

The relationship between suppression magnitude and equivalent attenuation depends on the local slope of the I/O function. If the slope is <1, equivalent attenuation will be larger than suppression magnitude; if the slope is >1, the opposite is true.

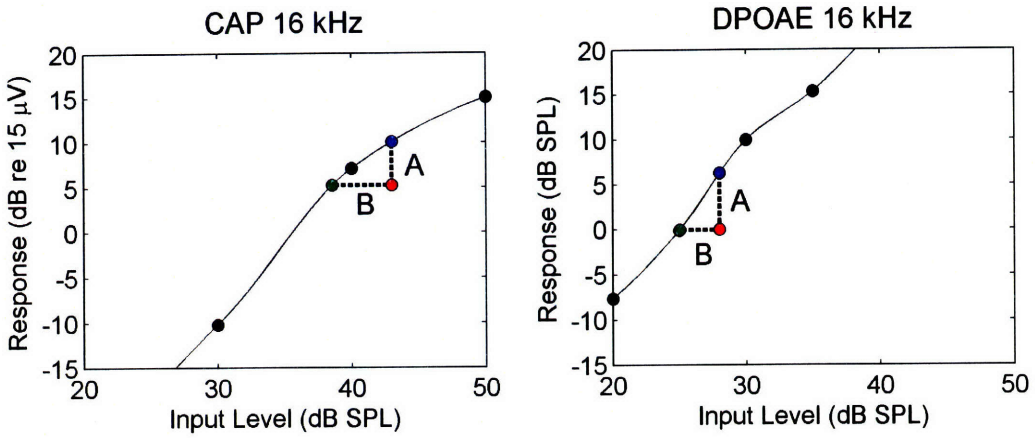

Figure 5. Response reduction, i.e. suppression (A), is converted to 'equivalent attenuation' (B) by PCHIP interpolation (solid black line) of sampled I/O functions (measurements taken at black dots). In this example, CAP response to 16 kHz 43 dB SPL tone pips (blue) was suppressed by 4 dB (red) during contralateral noise; DPOAE response to f_2 of 16 kHz 28 dB SPL (blue) was suppressed by 5.9 dB (red). Expressed as equivalent attenuation, the CAP shift was 3.9 dB and the DPOAE shift 2.7 dB (both green). Data from EL140.

II.B.5 Paralysis of middle ear muscles

Contralateral sound may evoke the middle-ear muscle (MEM) reflex, which could suppress some ipsilateral responses (Borg 1968). To assess the effect of the MEM reflex, control experiments were conducted with paralyzed animals, using a non-depolarizing muscle relaxant (curare, 3 mg/kg i.p.). Although complete paralysis is difficult to ascertain in anesthetized animals, prior experiments involving shocks to the floor of the IVth ventricle (which activate the middle ear muscles) have shown that a dose of 1.25 mg/kg curare abolishes MEM contractions, see Figure 6 (figure from Groff 2003). Shown are primary levels of f_1 and f_2 as would be used when evoking DPOAE responses measured before, during (gray shading), and after shocks to the 4th ventricle. Primary levels are strongly suppressed during shocks (left), but not after injection of curare (right). 'Noise' in the primary tone levels around the shocks epoch before curare reflects spontaneous middle ear muscle contractions, which also disappear after curare. Suppression of primaries is due to a change in the impedance of the middle ear during MEM contractions (Borg 1972); thus, absence of changes in primary levels indicates absence of MEM contractions. Furthermore, the MEM reflex appears to be relatively weak even in awake guinea pigs (Avan et al. 1992), and given the known effective dose of curare we can be confident that 3 mg/kg will abolish the sound-driven MEM reflex in anesthetized guinea pig.

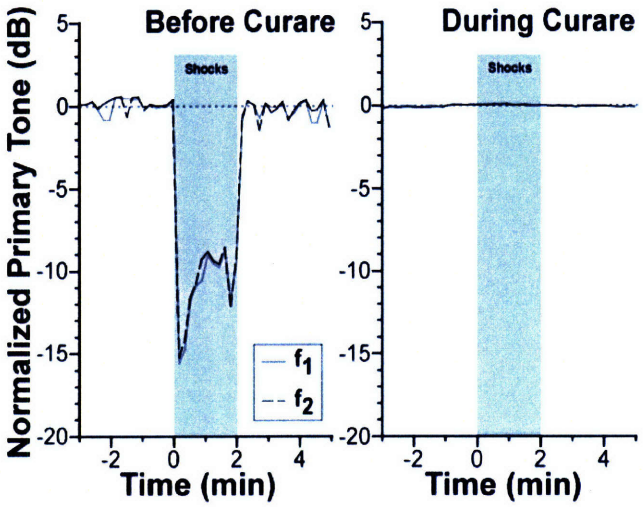

Figure 6. Curare abolishes middle-ear muscle (MEM) contractions during electrical stimulation of the MOC system, from (Groff 2003). MEM contractions are assayed by monitoring primary levels of a DPOAE stimulus before (left) and during (right) systemic curare (1.25 kg/mg, i.m.); absence of changes in primary levels during curare indicates absence of MEM contractions.

II.B.6 Histology

In experiments where data was collected after brainstem lesions, histology was performed to verify location of the lesion, using an acetylcholinesterase (AChE) staining method to mark cholinergic cell bodies and axons (which includes MOC and LOC systems). For this, at the end of the experiment, animals were perfused intracardially with 4% paraformaldehyde, and brains were stored in the same fixative overnight. Pons and medulla were dissected from the brain and cryoprotected in 30% sucrose in 0.1 M phosphate buffer overnight, after which 80 μm sections were cut in the transverse plane on a freezing microtome and stored in 0.1 M phosphate buffer. Staining for AChE was done by incubating at room temperature for 1 hour in a solution

containing 0.0072% ethopropazine, 0.1156% acetylthiocholine iodide, 0.075% glycine, 0.05% copper sulfate, 0.68% sodium acetate (solution titrated to a pH of 5.0 using glacial acetic acid), followed by 1 minute in a solution of 4.0% sodium sulfide (titrated to a pH of 7.8 using hydrochloride), and finally 1 minute in a solution of 1.0% silver nitrate. Sections were washed 6 times in double-distilled water between solutions. Sections are finally placed on gel-subbed slides, air-dried overnight, dehydrated in 100% ethanol, and coverslipped with Permount dissolved in xylene. An example of an intact AChE-stained brainstem section is shown in Figure 7

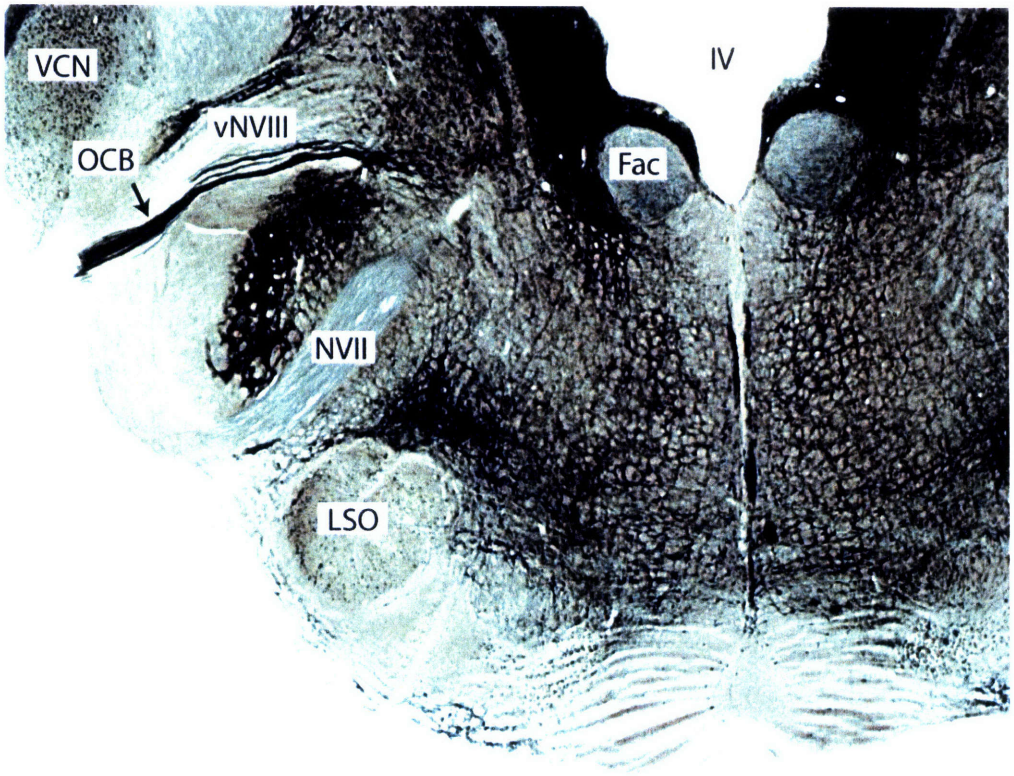

Figure 7. AChE stain of an intact guinea pig brainstem, with relevant structures indicated (VCN: ventral cochlear nucleus, OCB: olivocochlear bundle, vNVIII: vestibular portion of the 8th cranial nerve (vestibule-cochlear), NVII: 7th cranial nerve (facial), LSO: lateral superior olive, Fac: facial genu, IV: IVth ventricle). The OCB as shown here contains axons of both crossed and uncrossed MOC components, as well as the LOC axons. Lesions to the OCB are made by cutting ventrolaterally from the exposed IVth ventricle, ideally sparing the facial nerve. Compare to schematized brainstem section of Figure 3.

II.C Results

We present data from 24 guinea pigs, which all had normal hearing and were free from obvious middle ear infections. Although there was considerable variability in sound-induced suppression between animals, there were no obvious subgroups with distinct responses, so summary data includes all animals as one group, unless otherwise specified. Much of the data will be presented as acquired at low ipsilateral stimulus levels, pooled across 22 of 24 animals; the other 2 animals were measured at a range of levels to assess the effect of ipsilateral stimulus level on suppression characteristics, and are presented separately. Out of the pool of animals, some were also used for special experiments after obtaining baseline data, such as drug injections or brainstem lesions: these results are presented separately.

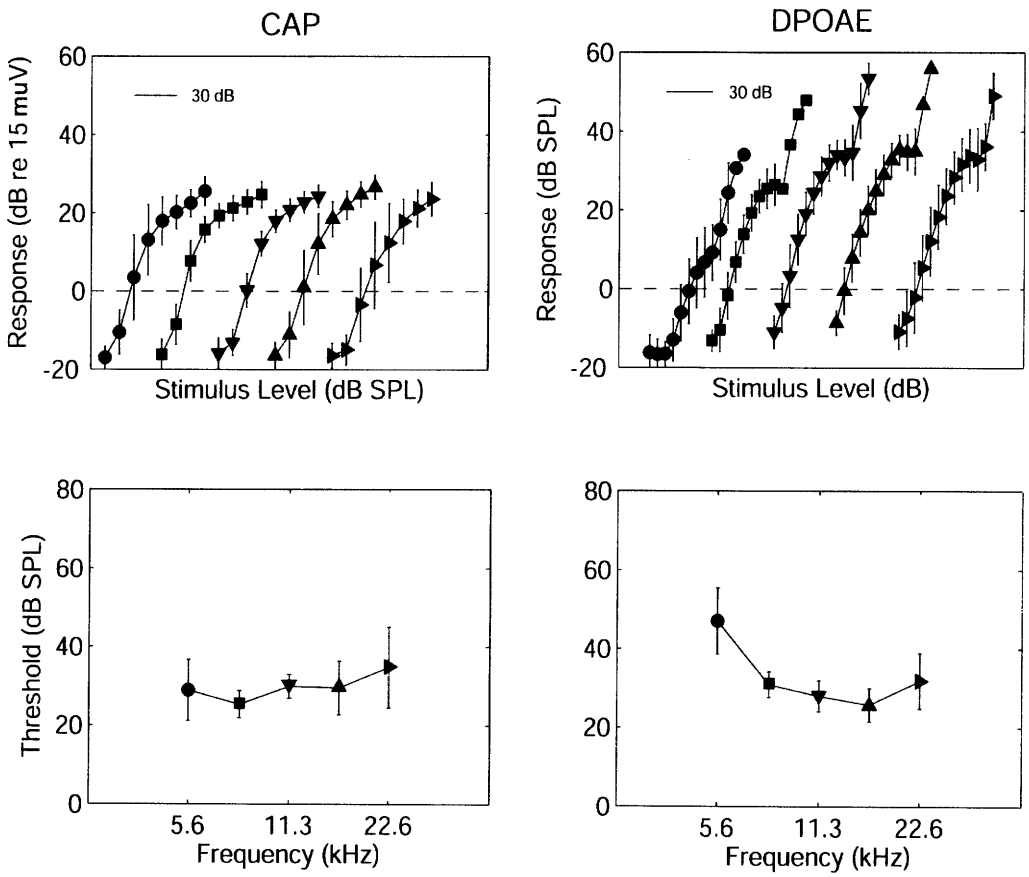

Figure 8. Mean (± standard deviation) DPOAE (right, n=23) and CAP (left, n=18) I/O functions (top) and thresholds (bottom) for all animals, at 5 frequencies (symbols code for frequency, as shown in both lower panels). I/O functions are offset horizontally for clarity. Each CAP I/O function is measured from 10 to 80 dB SPL in 10 dB steps (scale bar indicates 30 dB); each DPOAE I/O function is measured from 20 to 80 dB SPL in 5 dB steps (scale bar indicates 30 dB). Both CAP and DPOAE thresholds derived from interpolated I/O functions. DPOAE threshold criterion is $2f_1$-f_2 of 0 dB SPL; CAP threshold criterion is peak-to-peak voltage of 15 μV.

Summary input/output (I/O) functions (top) and thresholds (bottom) for CAP (left) and DPOAE (right) are shown in Figure 8 (here we use standard deviation instead of standard error

to indicate the range of responses that is representative of our sample of guinea pigs). Data shown here were measured at the beginning of each experiment, although it was routinely measured once or twice additionally throughout the duration of each experiment. As we did not obtain CAP I/O functions for all animals, the CAP data shown in Figure 8 includes only 19 of 24 animals.

II.C.1 Response characteristics to sustained contralateral noise

II.C.1.a Representative slow suppression examples

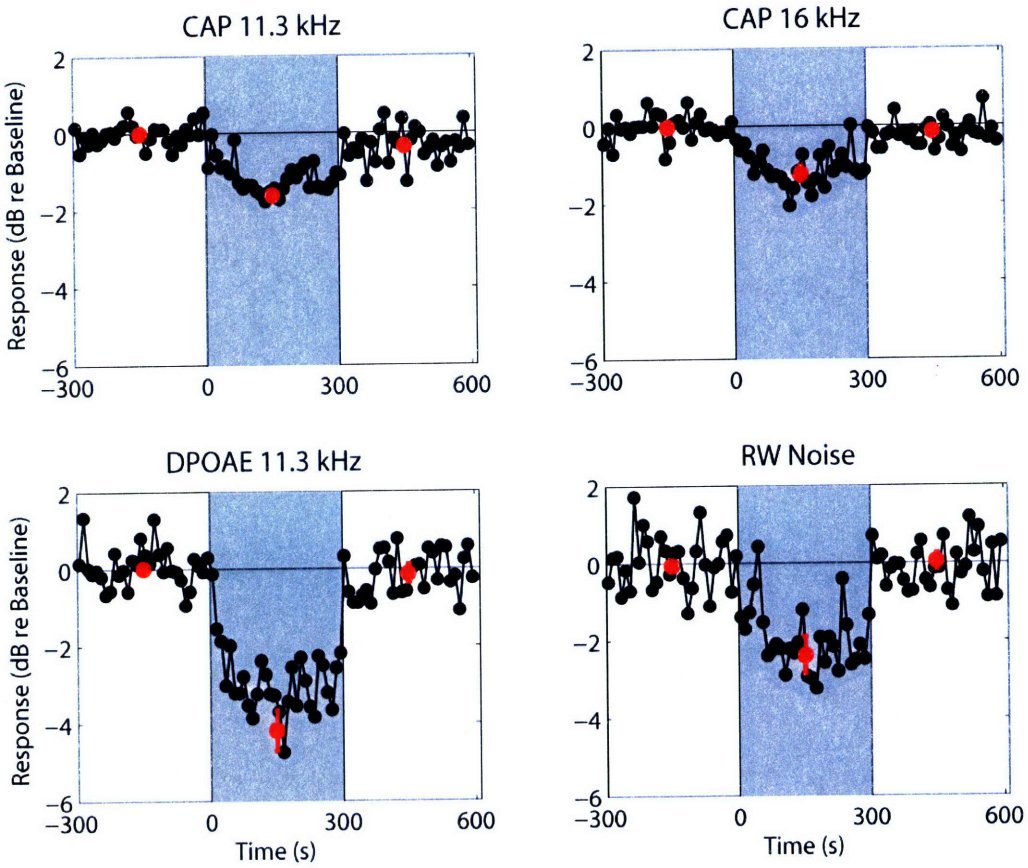

Figure 9. Examples of slow suppression of ipsilateral responses during a 300-s epoch of contralateral noise (shaded area); responses recover after noise terminates (data from EL45, mean of 7 trials). Suppression magnitudes are 1.6 and 1.4 dB for CAP at 11.3 and 16 kHz, respectively; 3.4 dB for DPOAE at 11.3 kHz; 2.1 dB for RW noise. Baseline (defined as 0 dB) was the mean of all samples <0 s; the during-noise mean utilized samples halfway through the noise epoch (130-170 s); the post-noise mean utilized the final portion (>500 s); all means (± s.e.) indicated with red symbols. Trial-to-trial variability shown in Figure 10.

Sound-evoked slow suppression had previously been documented in awake guinea pigs (Lima da Costa et al. 1997a), but we found similar effects in anesthetized guinea pigs. Representative examples of ispilateral suppression during contralateral noise are shown in Figure 9, for CAP (top), DPOAE (bottom left), and RW noise (bottom right). The contralateral noise level was 74 dB SPL in the band 1-30 kHz, and the ipsilateral stimuli were tone pips at 11.3 kHz (37 dB SPL), 16 kHz (33 dB SPL), and DPOAE primaries with f_2 at 11.3 kHz and 23 dB SPL. The CAP responses were suppressed by 1.6 and 1.4 dB, respectively; the DPOAE by 3.4 dB, and the RW noise by 2.1 dB, all relative to pre-noise baseline measures. To facilitate comparison of tone-evoked suppressions, changes are expressed as equivalent attenuation (see *Methods*), in which case the CAP effects are 2.0 and 2.1 dB, respectively, and the DPOAE effect is 1.2 dB.

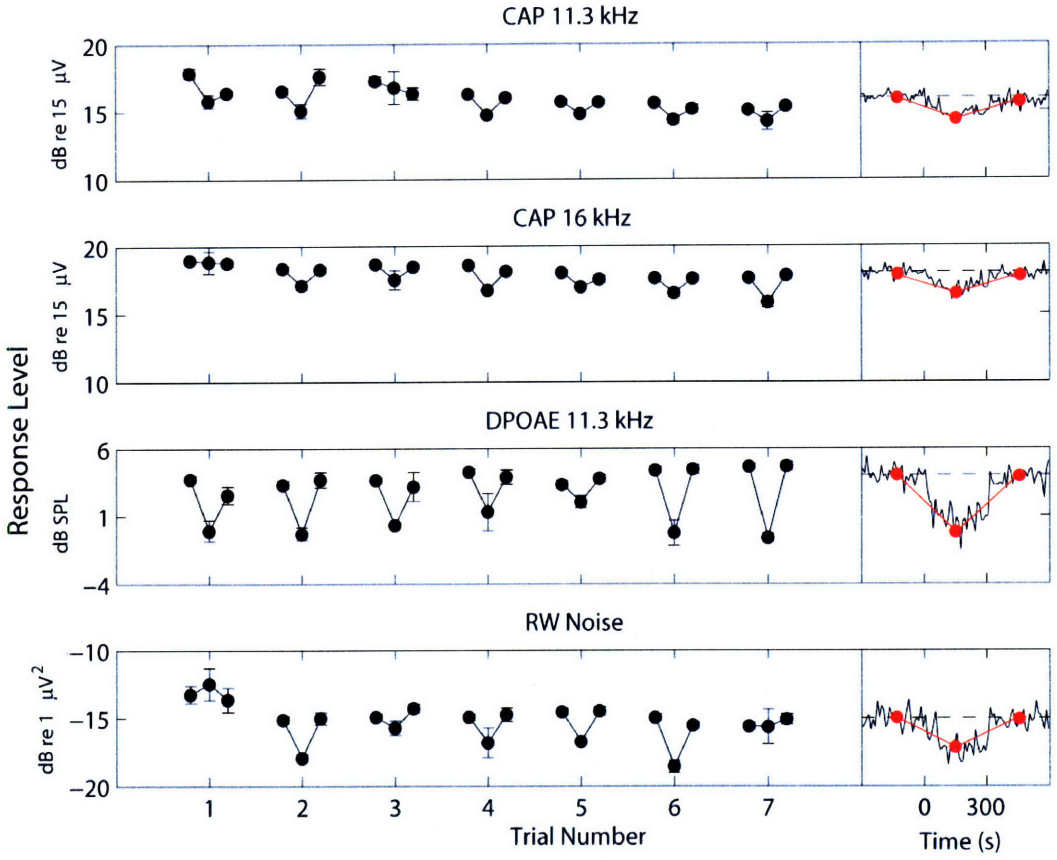

Figure 10. Data from the same case as in Figure 9, but shown by individual trials, and not normalized. Each trial is represented by three data points (mean ± s.e.) indicating baseline, suppression, and recovered response (see Figure 9 caption for details) – these are analogous to the three means for each metric shown with red symbols in Figure 9. The right-hand side of each panel reproduces the mean (over trials) response for each metric, using the same scale with respect to the individual trials (contralateral noise: 0 – 300 s).

There is no immediate ipsilateral suppression at the onset of the contralateral noise; rather, suppression builds up very slowly, at least until half-way through the noise epoch (150 s, 2.5 minutes). After reaching maximum suppression, the responses appear to stabilize, or, in case of the CAP response at 16 kHz, suppression appears to adapt and responses start returning to baseline values. DPOAE and RW noise responses appear to return to baseline immediately when

contra-noise terminates, while for the CAP responses this is more difficult to ascertain. Summary statistics for suppression magnitude, equivalent attenuation, and time course of the suppression are reported in a later section.

The data in Figure 9 were computed as the mean of responses recorded in 7 consecutive trials, using identical stimulus parameters. The stability of suppression characteristics in this experiment can be appreciated from Figure 10, showing mean (± s.e.) absolute response levels for CAP, DPOAE, and RW noise measures before, during, and after contralateral noise, for each 900-s measurement trial; the right-hand side of each panel reproduces the across-trials mean response of each metric. These 7 trials were measured over a time span of about 2 hours, during which some variability is evident; however, suppression is clearly not a transient phenomenon, but can be evoked repeatedly. We computed standard deviations of the suppression magnitudes, resulting in 0.5 and 0.6 dB for the CAP suppression at 11.3 and 16 kHz, respectively; 1.3 dB for the DPOAE suppression at 11.3 kHz; 1.6 dB for the RW noise. Expressed as coefficient of variation (CV), we have 0.3 and 0.4 for the CAP suppression, 0.4 for the DPOAE suppression, and 0.8 for the RW noise.

Finally, suppression of DPOAE responses indicates that this effect, if of OC origin, cannot be solely attributed to the LOC system, but must involve the MOC system acting on the outer hair cells.

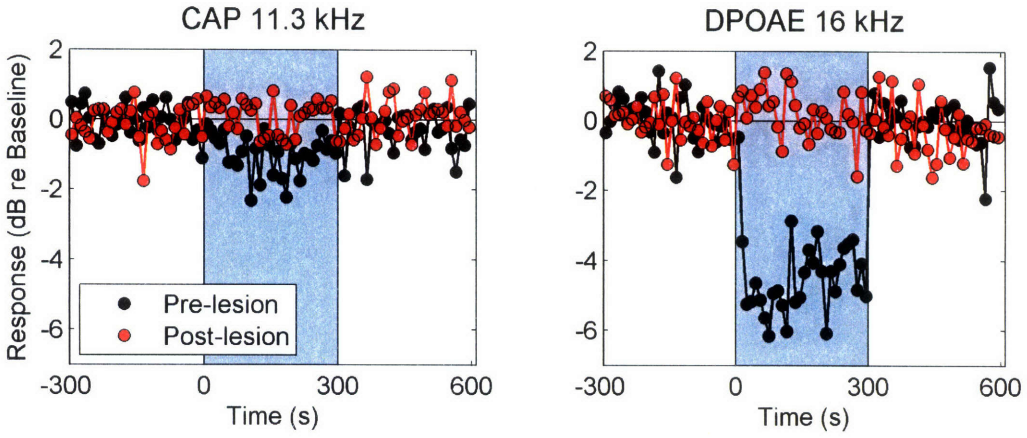

Figure 11. CAP and DPOAE responses before (black, mean of 4 trials) and after (red, mean of 3 trials) contralateral cochlear destruction with a probe. RW noise suppression was also abolished (not shown). These results indicate the ipsilateral suppression is not due to acoustic crosstalk (data from EL141).

II.C.1.b Acoustic crosstalk

The data just shown indicate robust suppression of cochlear responses during sustained contralateral noise. Beside affecting the ipsilateral cochlea via the olivocochlear system, direct transmission from the contralateral acoustic system to the ipsilateral ear canal is possible (i.e., crosstalk), and may directly affect ipsilateral responses. However, contralateral-noise induced suppression is abolished after contralateral cochlear destruction (Figure 11). CAP (left) and DPOAE (right) responses (RW noise responses were also suppressed, data not shown) were obtained to characterize suppression characteristics (black); afterwards, the contralateral cochlea was mechanically lesioned by breaking the cochlear capsule with a fine probe penetrating the round window (accessed via the opened bulla). Such a lesion should have minimal effect on the possible pathways for direct acoustic transmission to the ipsilateral ear, yet responses acquired

after the lesion (red) indicate that suppression was abolished completely (also at frequencies not shown in Figure 11, as well as for RW noise). The CAP suppression magnitude (mean ± s.e., computed half-way through the noise epoch) went from 1.1 ± 0.4 dB (pre-lesion) to 0.2 ± 0.3 dB (post-lesion). For DPOAE suppression magnitude, the change was from 5.0 ± 0.3 dB to 0.0 ± 0.5 dB. This pattern of results (abolishment of suppression post-lesion) was obtained in 3 other experiments also. Altogether, this data provides strong evidence that suppression is not mediated by acoustic crosstalk, but involves a neural pathway that originates in the contralateral cochlea.

II.C.1.c Cochlear microphonic

MOC activity leads to increases in cochlear microphonic (CM), the magnitude of which is correlated with CAP suppression, at least for electrical stimulation of the COCB in cat (Gifford and Guinan 1987). This relationship, when expressed as dB increase in CM per dB shift of CAP (equivalent attenuation), is about 0.10-0.15, independent of shock rate. Although Gifford and Guinan used moderate-level clicks and electrical stimulation, we have no a priori reason to expect this ratio to change dramatically for tonal signals and sound-induced MOC activation. Accordingly, we measured low-frequency CM responses in several animals to investigate the relationship with CAP suppression. However, given that equivalent attenuation of CAP is on the order of 1.5 dB on average, we should not expect more than 0.15-0.25 dB of increase in CM, which will be hard to detect given the relatively low signal-to-noise ratio of the CM data at low levels. The predicted relationship between CAP and CM effects is confirmed by data shown in Figure 12, indicating CM (left) and CAP (right). The CM response was measured using 4 kHz 75 dB SPL tone pips, and we used the CAP at 5.6 kHz (45 dB SPL) as this was most sensitive frequency (lowest CAP threshold). The CM was increased relative to baseline, halfway through the contralateral noise, by 0.37 ± 0.08 dB. The CAP suppression magnitude was 2.5 ± 0.2 dB, which was 2.7 ± 0.3 dB expressed as equivalent attenuation. The ratio of CAP equivalent attenuation to CM enhancement, 0.37/2.7 = 0.14, is in the same range as reported above. Furthermore, we overlaid the CAP response (inverted, scaled by 0.125) on the CM response (red) as a 'predicted CM'; the correspondence with the measured CM is good. Overall, the CM data are consistent with an MOC origin of suppression during sustained contralateral noise, not with an LOC origin. CM responses from three other experiments were not conclusive, either because the CM responses were measured at lower stimulus level, resulting in poorer signal-to-noise ratio, or because those animals had weaker CAP suppression effects.

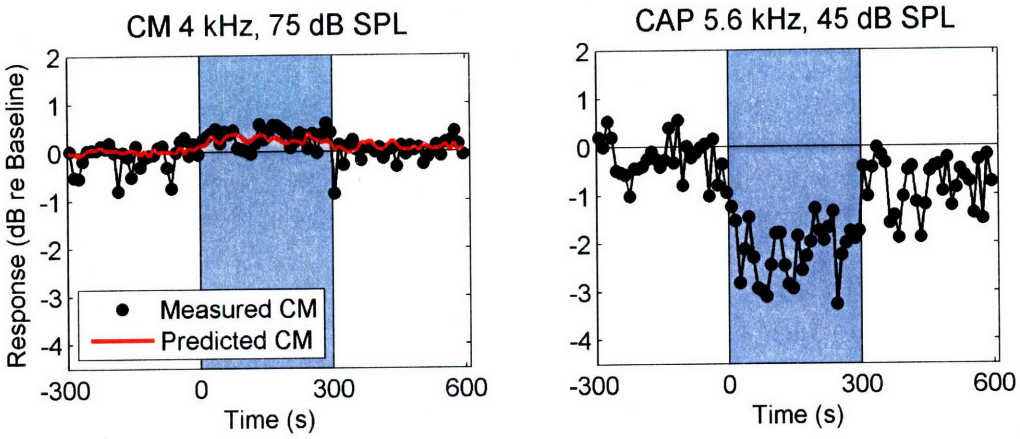

Figure 12. CM at 4 kHz (left, mean of 3 trials) and CAP response at 5.6 kHz, the most sensitive frequency (right, mean of 3 trials). The CAP suppression magnitude is 2.5 dB; in terms of equivalent suppression this is 2.7 dB. This CAP equivalent attenuation predicts a CM *increase* during contralateral noise of 0.3-0.45 dB. The measured CM increase halfway though the contralateral noise is 0.37 dB. For comparison purposes, the CAP response (inverted and scaled by 0.125) has been overlayed in the CM plot as a 'predicted' CM (data from EL144).

II.C.2 Frequency and level dependence of suppression

II.C.2.a Frequency dependence

II.C.2.a.i Suppression magnitude

We pooled data on suppression magnitude from all experiments and divided these into non-overlapping half-octave bins using the ipsilateral stimulus frequencies; for DPOAEs, f_2 frequency was used. Suppression magnitude was computed with respect to baseline for onset suppression, delayed suppression, and total suppression and is shown as a function of frequency for CAP (left) and DPOAE (right) in Figure 13 (see caption for calculation of onset, delayed, and total suppression). Delayed suppression is defined as the additional suppression obtained after the onset suppression; it is calculated as total-onset suppression.

Onset suppression magnitude (white circles) shows mild frequency dependence with a broad maximum at mid-frequencies, gently tapering off at low and high frequencies, for both CAP and DPOAE. RW noise onset suppression is not statistically different from zero ($p = 0.47$). The total suppression magnitude (black circles) has very little variation across frequency for CAP, but more for DPOAE. RW noise total suppression is somewhat smaller than CAP suppression, but is statistically different from 0 ($p = 0.004$). Finally, the delayed suppression component (onset-total, gray circles) is robust at all frequencies for CAP and DPOAE. The mean suppression magnitudes for RW noise, CAP, and DPOAE (all frequency-averaged) are indicated in Table 1, decomposed into onset, delayed, and total components. This shows that all components of DPOAE suppression are larger than the CAP counterparts, which in turn are larger than the RW noise suppression (although the difference between RW noise and CAP do not reach 5% significance level for any component).

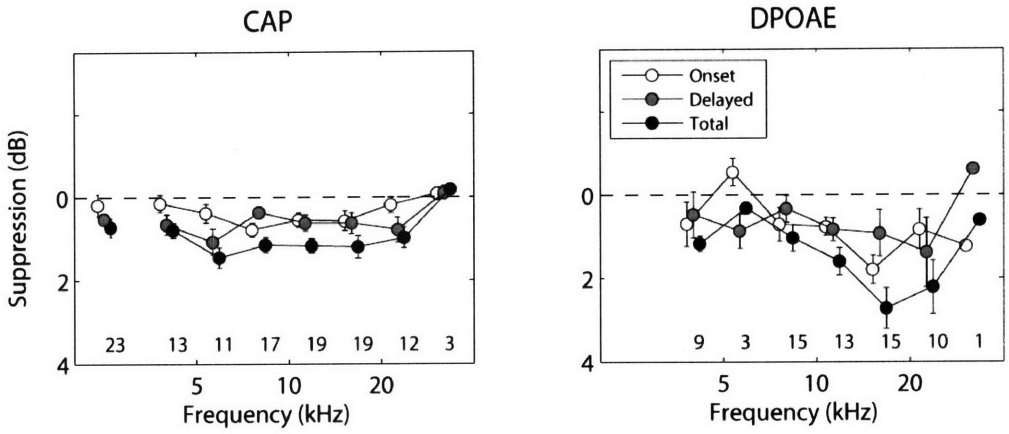

Figure 13. Mean (± s.e.) CAP and RW noise (left) and DPOAE (right) suppression magnitude as a function of ipsilateral stimulus frequency, decomposed into onset (mean of 0-10 s), delayed (total-onset), and total components (mean of 130-170 s). RW noise is not associated with a stimulus frequency, but is indicated at left in the panel for the CAP data. The number of data points per half-octave bin is indicated at the bottom of each panel. Mean suppression data is reported in Table 1.

The broadband nature and large magnitude of DPOAE suppression confirms the single case shown in Figure 9, which led to the conclusion that the observed suppression must involve the MOC system. Given that neural suppression (CAP, RW noise) is relatively smaller in magnitude, this also confirms that any role for the LOC system is probably minor.

Table 1. Frequency-averaged mean (± s.e. of the mean) suppression magnitudes in dB for RW noise, CAP, and DPOAE. Suppression is decomposed into onset, delayed, and total components, as in Figure 13. Data from 21 animals.

	RW noise	CAP	DPOAE
Onset	-0.19 (0.26)	-0.47 (0.08)	-0.93 (0.17)
Delayed	-0.53 (0.24)	-0.66 (0.10)	-0.78 (0.21)
Total	-0.72 (0.23)	-1.13 (0.09)	-1.71 (0.20)

II.C.2.a.ii Equivalent attenuation

We converted CAP and DPOAE suppression magnitude to 'equivalent attenuation' using I/O functions (see *Methods*), so that the effects on each metrics are compared in terms of the same quantity (change in input level) rather than on (different) output variables. Representative I/O functions for CAP and DPOAE at various frequencies are shown in Figure 14. CAP I/O functions are moderately steep at low stimulus levels, but typically saturate at moderate stimulus levels. In contrast, DPOAE I/O functions can be very steep at low stimulus levels (up to 3 dB/dB in some cases), and generally have a larger response range such that their slope can remain > 1 at moderately high stimulus levels. During measurement trials, we typically obtained CAP responses of 10-15 dB re 15 μV, where the I/O slope is approximately 0.5-1 dB/dB. DPOAE responses were in the range of 0-5 dB SPL, where the slope is typically 1-2 dB/dB. This implies that for CAP, equivalent attenuation should typically be larger than suppression magnitude, while the opposite should be true for DPOAE.

Figure 15, together with frequency-averaged data reported in Table 2, confirms that mean CAP equivalent attenuation is larger than CAP suppression magnitude, while the opposite is true

for DPOAE equivalent attenuation (there are fewer data points for CAP equivalent attenuation than for suppression magnitude, because we did not obtain CAP I/O functions in all experiments). RW noise suppression magnitude cannot be converted to equivalent attenuation, because it is measured in silence. Also, CAP equivalent attenuation is larger than that of DPOAE, for both total and delayed components; the early components are of equal size. The relative sizes of onset, delayed, and total components are roughly equal for equivalent attenuation as for suppression magnitude. This is to be expected as the slope of the CAP and DPOAE I/O functions change gradually with increasing stimulus level.

As described in *Methods*, to compute equivalent attenuation, we used an iso-response criterion at the suppressed response level, while the conventional approach is to use as iso-response the unsuppressed level. There is little published data on tone-evoked CAP I/O functions with and without MOC activation, besides a few graphs from shock-evoked MOC activation in cat (Gifford and Guinan 1987; Wiederhold and Kiang 1970; Wiederhold and Peake 1966). From this, it does not appear that using unsuppressed vs. suppressed iso-response criteria makes a substantial numerical difference in resulting equivalent attenuation; if at all, using the suppressed criterion may lead to 15-20% smaller values than the unsuppressed criterion.

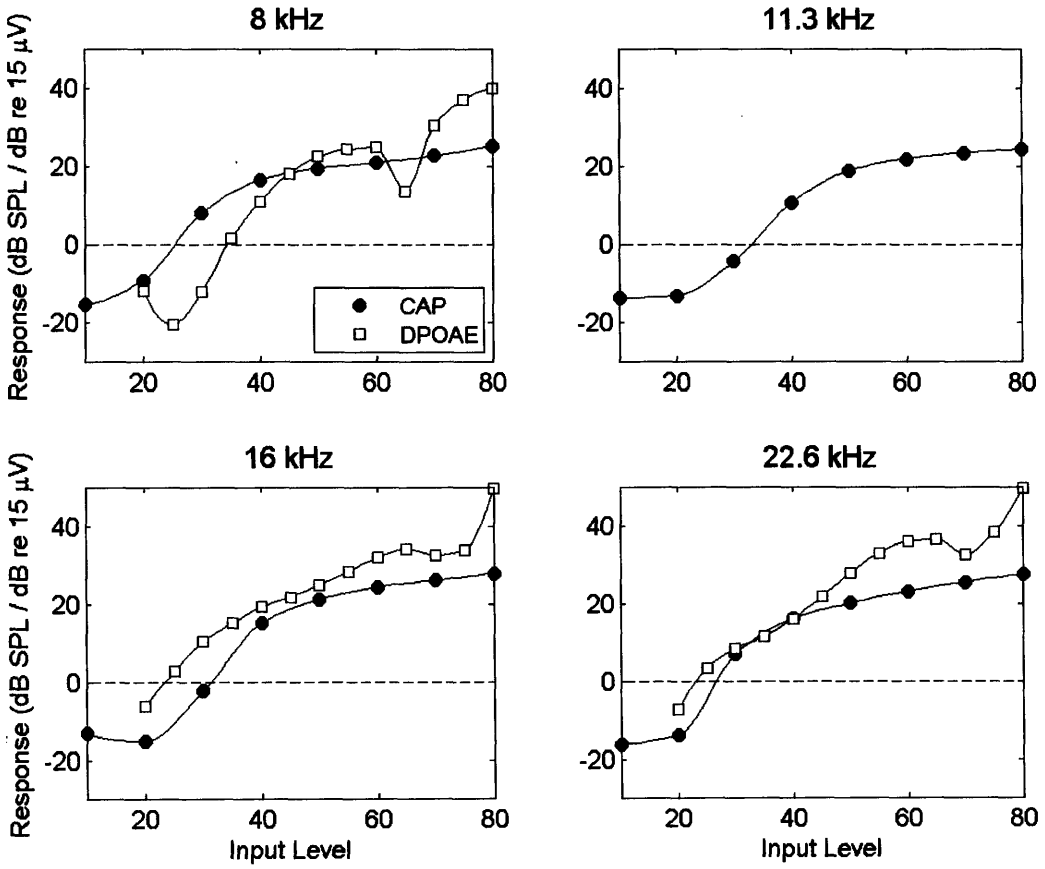

Figure 14. Representative CAP (filled dots, expressed as dB re 15 µV) and DPOAE (open squares) I/O functions (data from EL141); solid black line is a PCHIP interpolation. At stimulus levels used in the experiments, I/O slope is generally greater for DPOAE than CAP, such that for a given amount of suppression, equivalent attenuation will be larger for CAP than DPOAE.

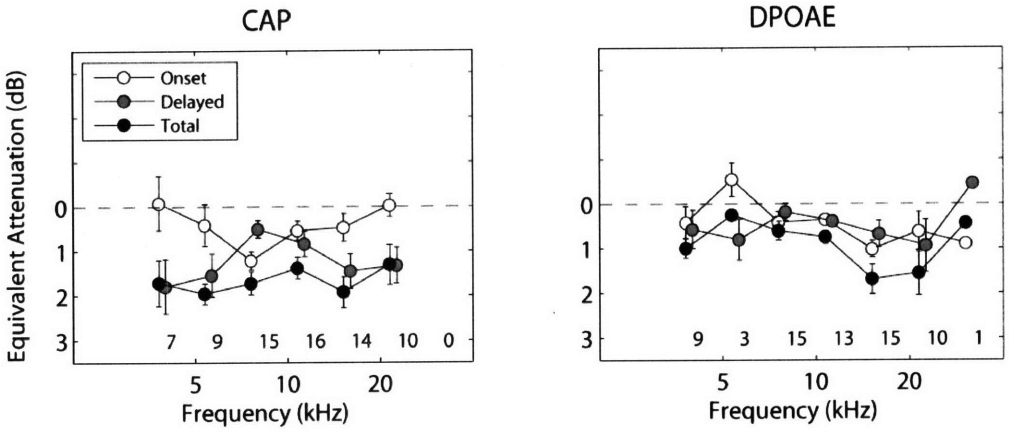

Figure 15. Mean (± s.e.) CAP (left) and DPOAE (right) equivalent attenuation as a function of ipsilateral stimulus frequency, decomposed into onset, delayed, and total components. The number of data points per half-octave bin is indicated at the bottom of each panel. Equivalent attenuation was computed using suppression magnitude and the I/O function. Compare to suppression magnitude in Figure 13. Mean equivalent attenuation data is reported in Table 2.

Table 2. Frequency-averaged (mean ± s.e.) equivalent attenuation in dB for CAP and DPOAE. Attenuation is decomposed into early, delayed, and total components, as in Figure 15. Compare to suppression magnitude data in Table 1.

	CAP	DPOAE
Onset	-0.51 (0.13)	-0.53 (0.12)
Delayed	-1.14 (0.15)	-0.54 (0.14)
Total	-1.66 (0.13)	-1.08 (0.13)

II.C.2.b Ipsilateral stimulus level dependence

Suppression magnitude associated with the MOC fast effect generally decreases with increasing ipsilateral stimulus level for both neural and OHC-based metrics, although DPOAE suppression can be large near non-monotonicities in the I/O function (Kujawa and Liberman 2001). In four animals we investigated the dependence of suppression magnitude on ipsilateral stimulus level, at constant frequency. Figure 16 shows mean (± s.e.) results for CAP (left) and DPOAE (right) total suppression magnitude (top) and equivalent attenuation (bottom), computed halfway through the contralateral noise (130-170 s). One of the animals (EL30, squares) had very small suppression, so there is little level dependence. The other three cases indicate that suppression magnitude decreases strongly with increasing stimulus level, for both CAP and DPOAE. One animal shows significant *enhancement* of DPOAE response at high levels (top right, triangles). At this stimulus level, the DPOAE function at 4 kHz showed a notch (similar to the 8 kHz DPOAE function from another animal, shown in Figure 14), locally reversing the slope of the I/O function, which explains the enhancement; such increases have been reported by others also (e.g., Kujawa and Liberman 2001). The onset and delayed components of the suppression magnitude show a similar decrease with increasing stimulus level, although the pattern is noisier primarily because the onset component is estimated using one sample only (data not shown). Overall, the dependence of suppression magnitude on ipsilateral stimulus level is consistent with a role for the MOC system.

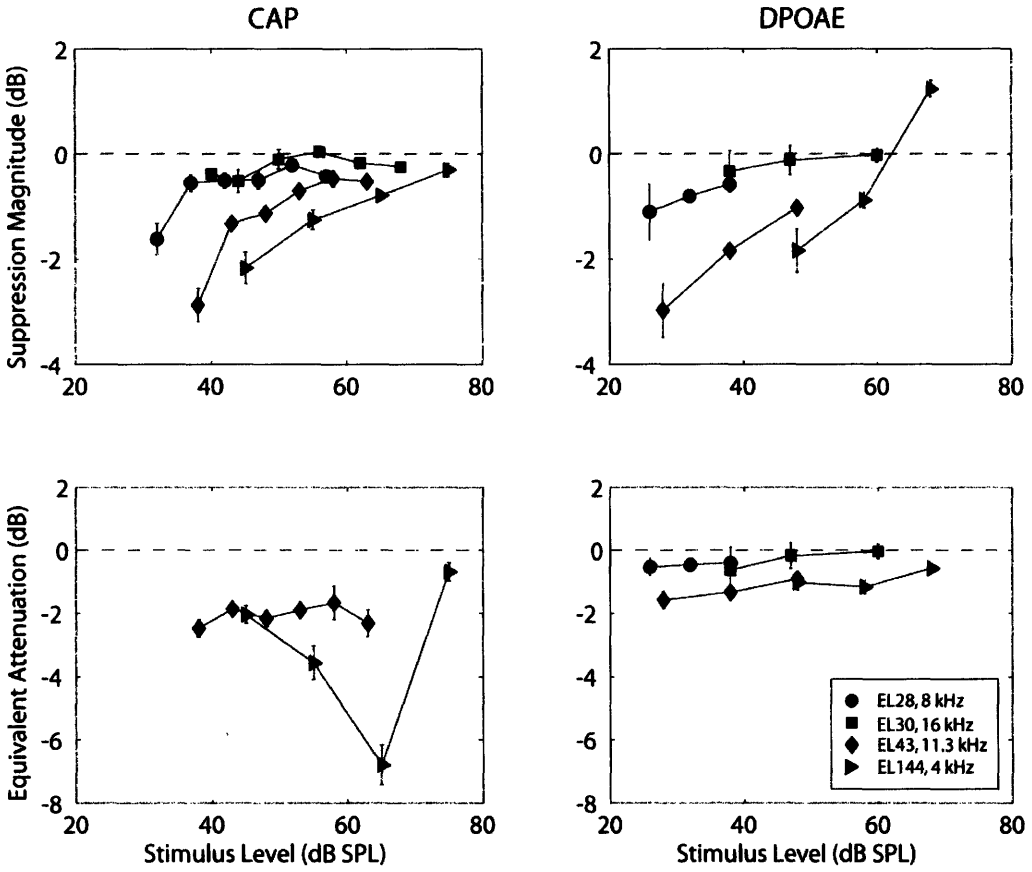

Figure 16. CAP (left) and DPOAE (right) mean (± s.e.) total suppression magnitude (top) and equivalent attenuation (bottom, converted from suppression magnitude using I/O functions) as a function of ipsilateral stimulus level, obtained in four different animals. Suppression magnitude decrease strongly with increasing stimulus level; expressed as equivalent attenuation, there is little to no systematic dependence on level.

Part of the reduction in suppression magnitude may be explained by the decreasing slope of the CAP and DPOAE I/O functions at higher stimulus levels (cf. Figure 8). As an example, for animal EL43 (diamonds in Figure 16), the CAP I/O slope decreases from 1.0 dB/dB at an input level of 38 dB SPL to 0.2 dB/dB at 63 dB SPL. Similarly, the DPOAE I/O slope decreases from 1.9 dB/dB at an input level of 28 dB SPL to 1.1 dB/dB at 48 dB SPL. To assess the effect of the change in I/O slope, we converted suppression magnitudes to equivalent attenuation and re-plotted the results, see Figure 16 (bottom). For CAP, we only measured I/O functions in two of the four animals. For those cases, the level dependence that was obvious for suppression magnitude is not apparent in terms of equivalent attenuation. However, estimates of equivalent attenuation at the highest input levels are problematic because the I/O function slope can very small in those regimes (0.10-0.20 dB/dB in some cases), and the uncertainty of equivalent attenuation estimate scales with the inverse of the I/O slope. Thus, small errors due to measurement noise or changes in the animal's hearing can strongly affect the equivalent attenuation estimates in these cases, which therefore probably have higher uncertainty than is apparent from the error bars: these are scaled from uncertainty related to estimating suppression magnitude, and do not reflect uncertainty in the I/O function. For DPOAE, a level dependence of equivalent attenuation is barely apparent. Overall, the data indicate a strong influence of

ipsilateral stimulus level on all components (onset, delayed, and total) of suppression magnitude, but at most a modest effect on equivalent attenuation.

II.C.3 Investigating sources of variability in suppression

II.C.3.a Effect of cochlear threshold on ipsilateral suppression

Because MOC activation reduces cochlear gain, in animals with sensorineural hearing loss (reduced baseline cochlear gain) MOC effects will be smaller (e.g., see Maison et al. 2007b). Thus, we investigated whether thresholds in the ipsilateral ear correlated with either suppression magnitude or equivalent attenuation. For this, we calculated mean CAP and DPOAE thresholds between 5.6 and 22.6 kHz for each animal and created subsets of the five best and five worst cases, separately for both CAP and DPOAE. Figure 17 shows equivalent attenuation (top) for CAP (left) and DPOAE (right), for subsets of best and worst thresholds as grouped according to DPOAE thresholds (i.e., 'best' and 'worst' CAP thresholds used the rank ordering obtained from DPOAE thresholds, in this case). The mean thresholds for CAP and DPOAE for the two subsets are shown in the lower panels.

The CAP results are unexpected in that, on average, animals with worse thresholds appear to have larger equivalent attenuations, at least at 11.3 and 16 kHz. At 5.6 and 8 kHz the differences are smaller, perhaps because mean thresholds for the two subsets are nearly equal at these frequencies. The DPOAE result does conform to the original expectation (at most frequencies) in that equivalent attenuation is considerably smaller for the group with worse thresholds vs. the group with best thresholds, except at 16 kHz. The difference in DPOAE thresholds for the two subsets is larger than for CAP thresholds, which may explain the larger difference in equivalent attenuation. Alternatively, DPOAE suppression may be more sensitive to cochlear condition. Grouping by CAP thresholds did not lead to more marked differences in CAP equivalent attenuation, nor for DPOAE (data not shown).

Overall, ipsilateral thresholds do not appear to be useful predictors of contralateral-sound induced suppression magnitude/equivalent attenuation. Although ipsilateral DPOAE thresholds do correlate with DPOAE equivalent attenuation, they do not predict CAP equivalent attenuation (if at all, the correlation appears negative, which seems paradoxical). Ipsilateral CAP thresholds do not predict either CAP or DPOAE equivalent suppression well. Perhaps these results are due to the relatively small differences in 'best' and 'worst' thresholds, resulting from the fact that we did not use animals with obviously elevated thresholds.

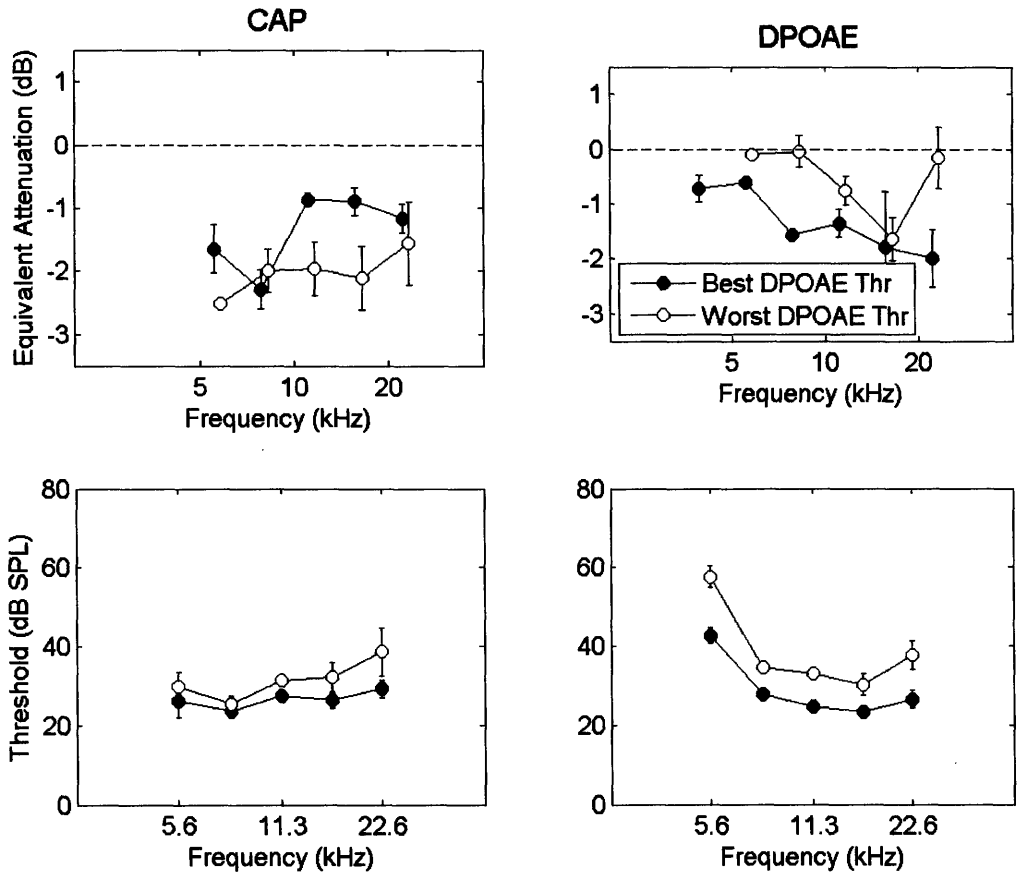

Figure 17. Comparison of equivalent attenuation (top) for CAP (left) and DPOAE (right) suppression, grouped by ipsilateral DPOAE threshold. Filled symbols indicate mean (± s.e.) of the five animals with best DPOAE thresholds, while open symbols indicate mean (± s.e.) of the five animals with worst DPOAE thresholds. The mean (± s.e.) CAP and DPOAE thresholds, grouped into five best and five worst as before, are shown at the bottom.

II.C.3.b CAP vs. DPOAE suppression magnitude in the same animal

To analyze correspondence between neural and OHC-based contralateral-sound induced effects, we paired CAP and DPOAE total suppression magnitudes measured at the same frequency (using f_2 frequency for DPOAE) in the same animal, for all animals; these pairs are shown in Figure 18 (left). There is considerable scatter in the data, and the Kendall τ rank correlation coefficient is only 0.21, although statistically significant (p = 0.016). Suppression magnitudes were converted to equivalent attenuation, also shown in Figure 18 (right). In this case, τ is even smaller at 0.12, and is non-significant in this case (p = 0.23). Apparently, the *ratio* of CAP to DPOAE suppression magnitude (and equivalent attenuation) is highly variable between animals, even though when pooled over a large number of animals, well-defined means for CAP and DPOAE suppression can be obtained (cf. Figure 13 and Figure 15).

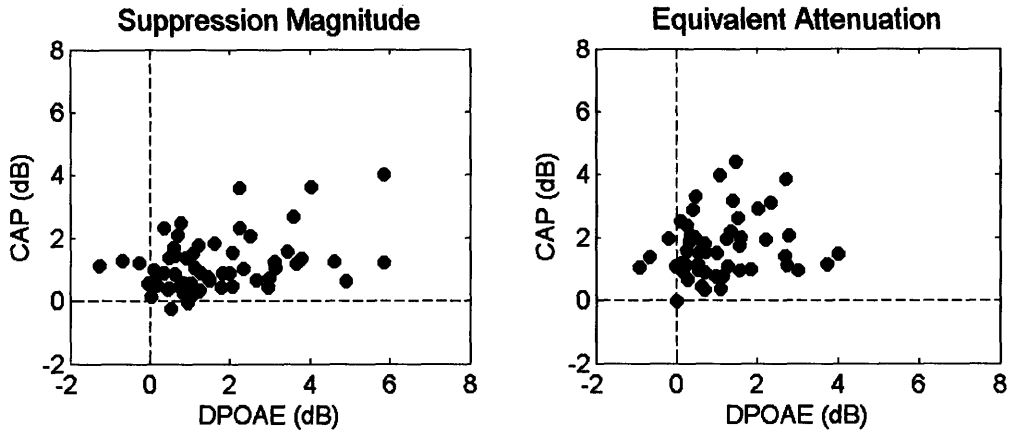

Figure 18. Comparison of DPOAE and CAP effects in the same animals at the same frequency. Comparison of suppression magnitudes (left) reveals a modest yet significant correlation (τ=0.21, p=0.016), while equivalent attenuations (right) are not significantly correlated (τ=0.12, p=0.23).

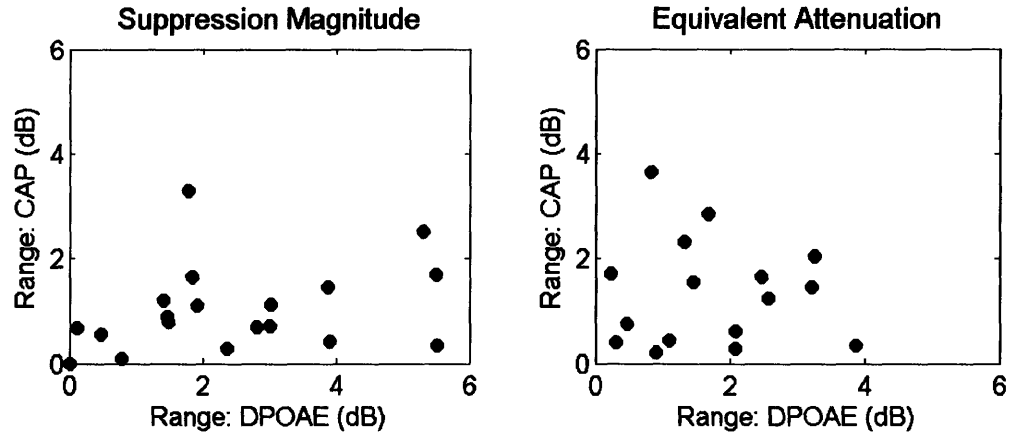

Figure 19. Range of DPOAE and CAP suppression magnitudes (left) and equivalent attenuation (right) for each animal. Each data point represents the difference in maximum and minimum suppression/equivalent attenuation across frequency in DPOAE vs. CAP in one animal. Median range of CAP suppression (0.7 dB) is considerably smaller than that of DPOAE suppression (1.9 dB), while they are more nearly equal when expressed as equivalent attenuation (1.4 vs. 1.6 dB).

By analyzing CAP and DPOAE suppression in individual animals, it appears that the largest amount of variability is associated with DPOAE suppression. Although CAP suppression magnitude varies between animals, in any one animal it is fairly consistent across frequency. However, DPOAE suppression magnitude can vary considerably across frequency, even within one animal. This is shown in Figure 19 (left), which plots the range (maximum-minimum) of DPOAE suppression vs. range of CAP suppression, for each animal. The median range for CAP is 0.7 dB, while it is 1.9 dB for DPOAE. This difference is larger than would be expected solely on the basis of the larger *average* suppression in DPOAE vs. CAP (1.5 vs. 1.1 dB), and indicates some other source of variability may act on DPOAE suppression magnitude, perhaps indicating that more than one functional pathway is involved. However, when expressed as equivalent attenuation, the range of CAP and DPOAE effects across frequency, per animal, is more nearly

equal (Figure 19, right), with medians of 1.4 vs. 1.6 dB. Thus, if equivalent attenuation is the appropriate measure to compare different variables, this finding may be consistent with all sources of suppression originating at the level of the outer hair cells, as little to no additional variability is introduced at the inner hair cell level (as evidenced by the neural metrics), such as by the LOC system.

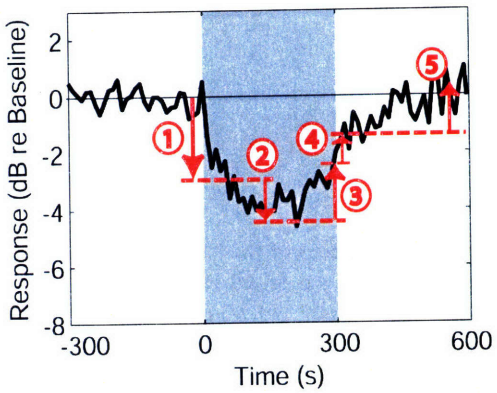

Figure 20. Illustration of components of suppression and recovery for a typical CAP time series before, during (gray bar), and after contralateral noise. 1: Onset suppression, 2: delayed suppression (1+2: total suppression), 3: adaptation, 4: offset recovery, 5: delayed recovery (4+5: total recovery). Quantities are defined as positive in the direction of the arrows. DPOAE and RW noise suppression components are defined analogously.

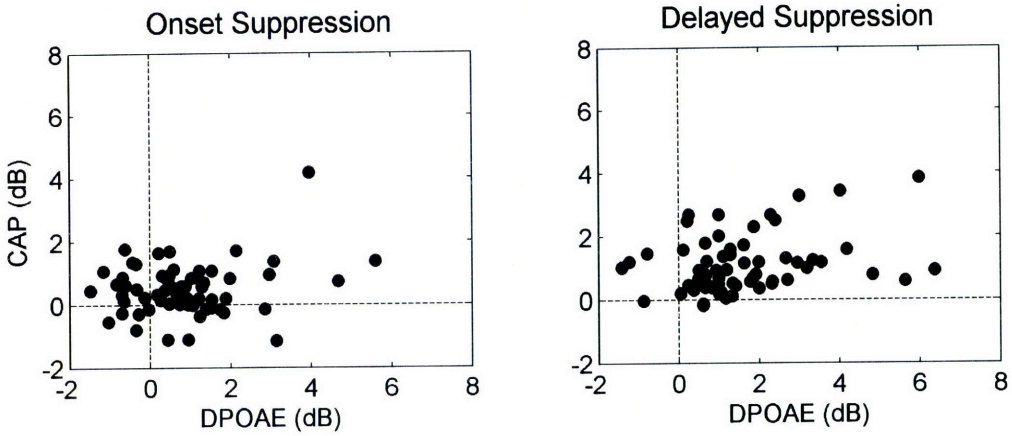

Figure 21. Onset (left) and delayed (right) DPOAE vs. CAP suppression magnitude. The onset suppression data is uncorrelated (τ=-0.04, p=0.68), while the delayed suppression shows a modest yet significant positive correlation (τ=0.19, p=0.025); compare to total suppression data in Figure 18.

II.C.3.c Onset and delayed components of the suppression

To probe potentially separate physiological mechanisms, the ipsilateral response to contralateral sound can broken down into several segments, as shown in Figure 20 for an example CAP time series – DPOAE and RW noise components are defined analogously. All pre-noise samples (-300 to 0 s) are averaged to compute the baseline of (defined as 0 dB); arrow 1 indicates the onset suppression; arrow 2 indicates delayed suppression. The other arrows indicate

adaptation and recovery, and will be addressed in the next section. Note that quantities are defined as positive in the direction of the arrows.

Figure 21 shows DPOAE vs. CAP suppression for onset (left) and delayed (right) components. Onset suppression appears to be uncorrelated between DPOAE and CAP metrics (τ = -0.04, p = 0.68), while delayed suppression shows a modest and statistically significant positive correlation (τ = 0.19, p = 0.025). As with total suppression magnitude, the components are poorly, if at all, correlated between metrics. Next we will address whether these components are correlated if compared for the same metric (RW noise, CAP, or DPOAE).

To investigate the relationship between onset, delayed and total suppression of neural and DPOAE responses, we isolated each component in each animal at available frequencies and visualized these for the pooled data, as shown in Figure 22. Relationships between CAP components are divided in onset vs. total suppression (top) and onset vs. delayed suppression (bottom); RW noise components are plotted in the inset of each panel (the RW noise axes are centered on (6, 6) and are scaled by 0.5). For CAP, the magnitude of early suppression was a poor predictor of total suppression, having a correlation of only 0.18, yet was significant (p=0.012); for RW noise, the correlation coefficient was 0.29, but not significant (p=0.61). The correlation between onset and delayed suppression was stronger and highly significant, -0.38 ($p<10^{-7}$); for RW noise, this correlation was -0.39 and significant (p=0.010). Apparently, there is a trade-off between onset and delayed suppression, such that either one or the other is large, but not both. This yields a pattern where data points are scattered around a line with negative slope.

Similar results were obtained for the DPOAE component relationships (Figure 22, right). Onset suppression was slightly better at predicting total suppression than in the neural case, with a correlation coefficient of 0.28 ($p<10^{-3}$). The relationship between DPOAE onset and delayed suppression was highly significant and had a correlation of -0.34 ($p<10^{-4}$).

The relatively small correlations between onset and total (and also onset and delayed) suppression must be due in part to the relatively low signal-to-noise ratio of our recordings. Even after averaging 3-6 experimental blocks per condition, standard deviation of the noise is typically of the same order of magnitude as onset suppression magnitude; thus, this leads to significant noise-induced scatter in all panels of Figure 22, in particular along the abscissa.

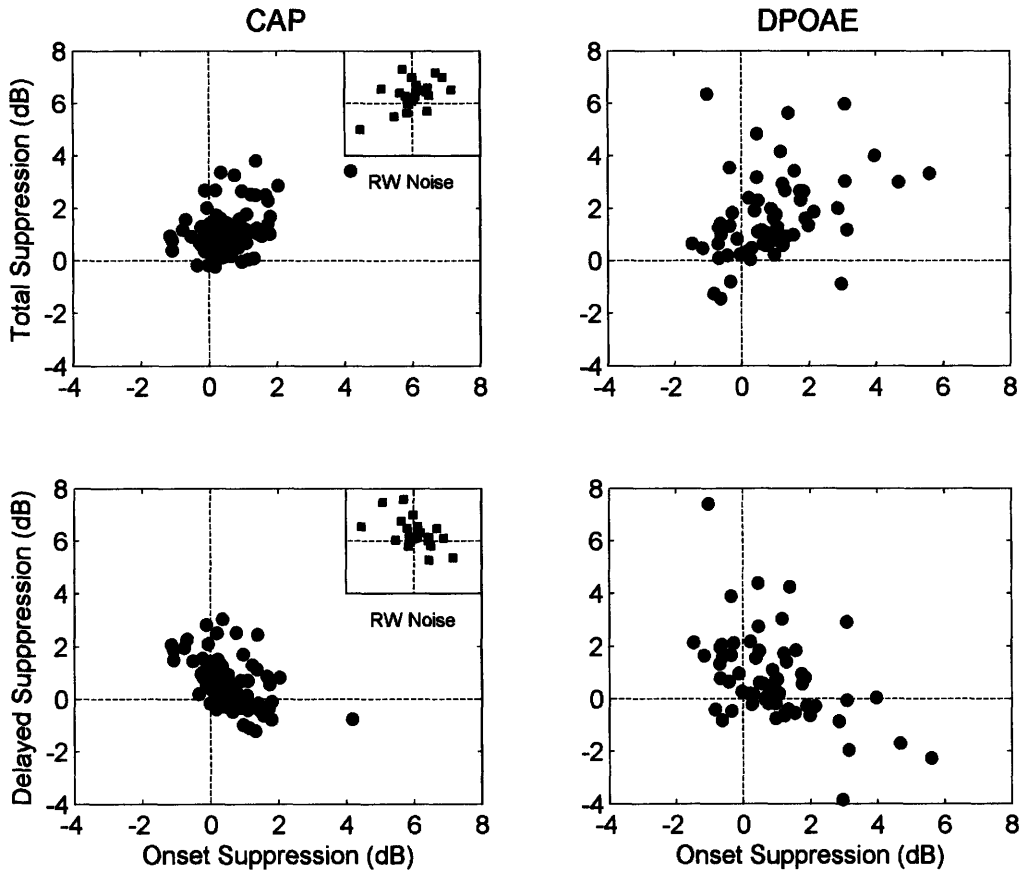

Figure 22. Components of suppression for CAP (left, circles) and RW noise (left, inset, squares) and DPOAE (right). Onset vs. total suppression (top) had a low positive correlation of about 0.2-0.3 for CAP, RW noise, and DPOAE. The negative correlation of onset vs. delayed suppression (bottom) was about -0.4 for all three variables and highly significant in all cases.

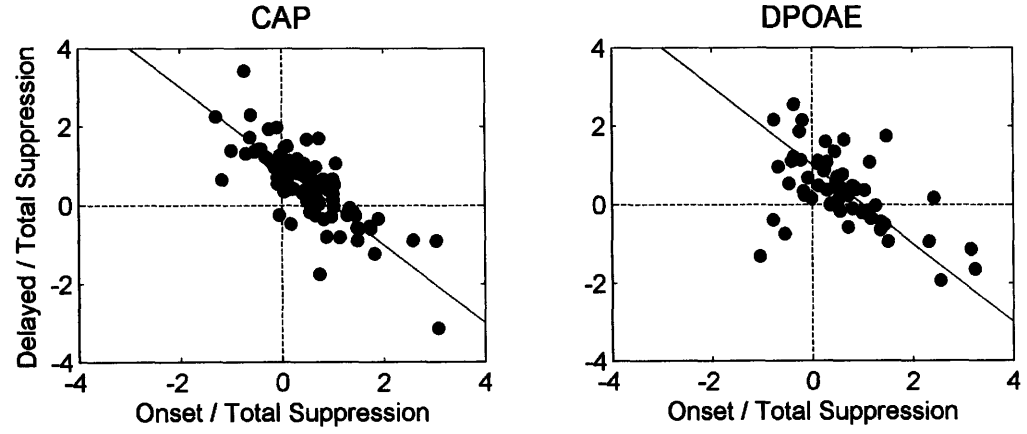

Figure 23. CAP (left) and DPOAE (right) onset vs. delayed suppression components, normalized by total suppression magnitude. Each data point represents suppression at a single frequency in one animal, while the normalization factor represents the frequency-averaged total suppression for that animal. Correlation coefficients are higher for this normalized data than for the absolute data as in Figure 22 (CAP: τ=-0.60, $p<10^{-17}$; DPOAE: τ=-0.46, $p<10^{-7}$).

Another source of variability for the onset vs. delayed suppression relationship (Figure 22, bottom) may be the variation in total suppression magnitude between animals, as this shifts the relationship a direction perpendicular to the long axis of the data distribution. To account for this, we normalized onset and delayed suppression at each frequency by the frequency-averaged total suppression magnitude, separately for each animal. Data pooled across animals is shown in Figure 23, for both CAP (left) and DPOAE (right); the solid line in each panel is a linear function with slope -1 intersecting coordinates (0, 1) and (1, 0); in the ideal case, all data points should lie on this line. The normalization does appear to produce a fairly narrow distribution of the data, and this is confirmed by the correlation coefficients, which are higher than for the onset vs. delayed suppression relationship using absolute suppression data (Figure 22). For CAP, the correlation coefficient is -0.60 ($p<10^{-17}$), and for DPOAE it is -0.46 ($p<10^{-7}$). The lower absolute correlation for the DPOAE data is likely due to the fact that DPOAE suppression magnitude variation across frequency, in a given animal, is larger than for CAP (cf. Figure 19). This normalization procedure is not meaningful for RW noise, as it would produce perfectly correlated data, given that there is only one early and late suppression component per animal.

The negative correlation between onset and delayed suppression is consistent with a 'ceiling' for the total suppression magnitude. It argues against a delayed suppression mechanism that relies on input from the onset suppression, because in that case the correlation should be positive. Given that the magnitude of the correlation is quite high, and that onset suppression reflects the MOC system (fast effect), delayed suppression is likely also mediated by the MOC system (if the LOC system was responsible, a correlation with MOC strength would not necessarily be expected).

II.C.4 Adaptation and recovery from suppression

Electrically-evoked slow suppression in the guinea pig cochlea persists only for a few minutes, after which it adapts (Sridhar et al. 1995). However, sound-evoked slow suppression in awake guinea pigs has been shown to persist for up to two hours (Lima da Costa et al. 1997a). Thus, we investigated the characteristics of suppression adaptation during contralateral noise in our data. Figure 20 defines adaptation with arrow 3: the difference between total suppression (130-170 s after noise onset) and suppression at the end of the noise epoch (260-300 s after noise onset). Adaptation is defined positive in the direction of the arrow, i.e. when suppression decreases.

Delayed suppression vs. adaptation (at the same frequency), pooled over all animals, has a moderate correlation, shown in Figure 24; both for CAP (left) and DPOAE (right). CAP delayed suppression magnitude is significantly correlated with adaptation ($\tau=0.34$, $p<10^{-6}$), and a linear regression yields a slope estimate of +0.28 dB/dB. DPOAE delayed suppression shows a similar pattern as it is significantly correlated with adaptation ($\tau=0.39$, $p<10^{-5}$), with a regression slope of +0.33 dB/dB (y-intercepts for both CAP and DPOAE regressions were within 0.01 dB of zero). Figure 24 also indicates instances of "negative adaptation", implying a further late suppression during the second half of the contralateral noise. However, in most instances, the magnitude of this effect was less than 0.5 dB.

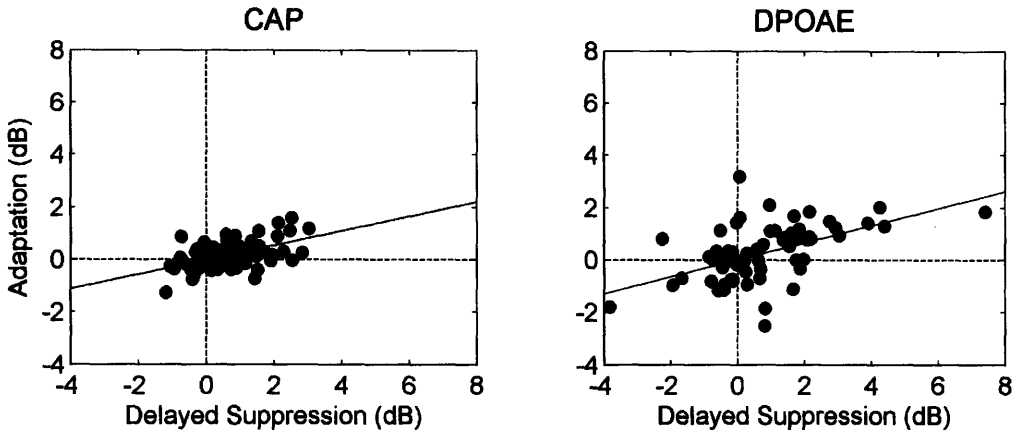

Figure 24. Delayed suppression vs. adaptation for CAP (left) and DPOAE (right) are significantly correlated (τ=0.34 and 0.39, respectively, $p<10^{-5}$) with linear regression slopes of +0.28 dB/dB and +0.33 dB/dB, respectively.

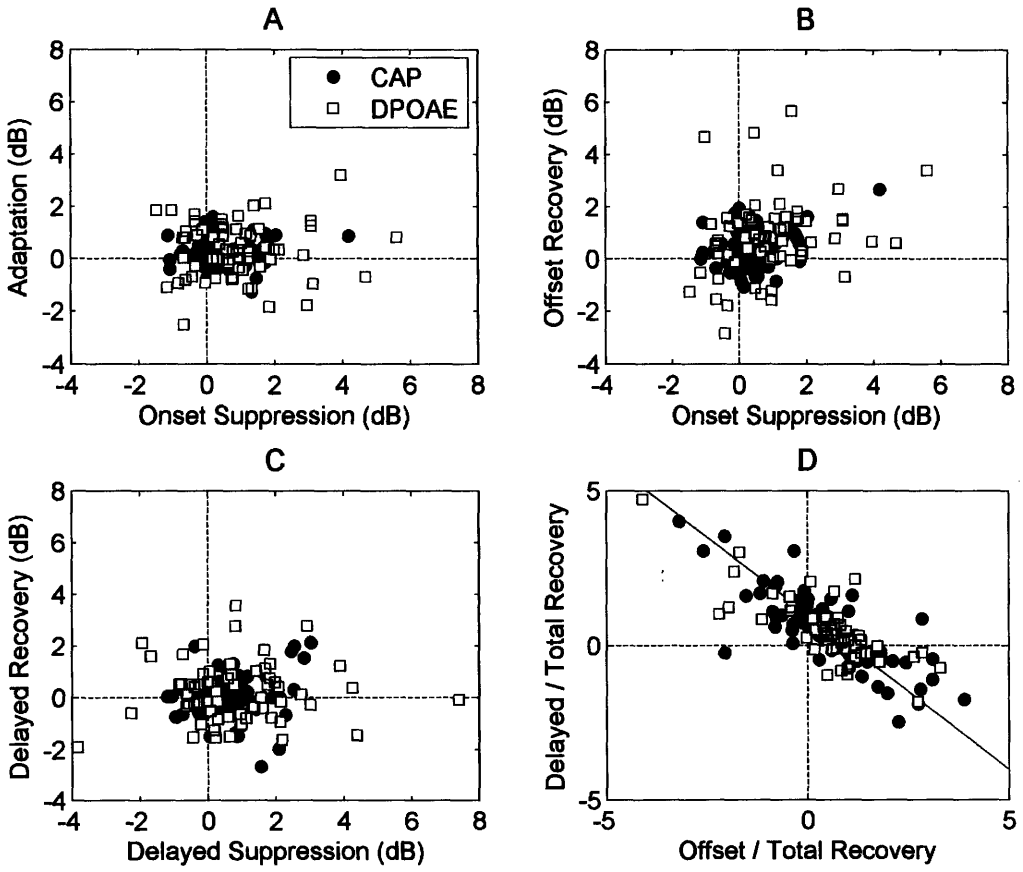

Figure 25. Onset suppression is a poor predictor of adaptation (panel A, non-significant correlation). Furthermore, onset (delayed) suppression is generally a poor predictor of offset (delayed) recovery (panels B and C), except that CAP onset suppression is moderately correlated with CAP offset recovery (τ=0.46, $p<10^{-5}$). When normalized by average total recovery magnitude per animal, the relative offset and delayed recovery are highly (CAP: -0.80, DPOAE: -0.88, $p<10^{-21}$ for both). The diagonal line in panel D is not a fit but a prediction of where the data points should lie.

For both CAP and DPOAE, onset suppression magnitude was not significantly correlated with adaptation, as shown in panel A of Figure 25. Thus, although adaptation of suppression during long-term contralateral sound does occur, it appears to be relatively modest in magnitude compared to the stronger adaptation seen in electrical stimulation experiments. Whether adaptation would be stronger during longer contralateral sound stimulation is not known, as we did not use noise bursts longer than 5 minutes.

We characterized the recovery process in two stages, consisting of an offset recovery (the difference between the first sample after contralateral noise offset and the adapted during-noise response) and a delayed recovery (the difference between mean response 200-300 s after noise offset and the offset recovery); indicated by arrows 4 and 5 in Figure 20. We found a moderate but highly significant correlation between onset suppression and offset recovery for CAP (τ=0.46, $p<10^{-5}$), both not for DPOAE (panel B of Figure 25). Neither CAP nor DPOAE delayed suppression predicted delayed recovery (non-significant correlations, panel C of Figure 25). As a check, we analyzed the relationship between the ratio of offset recovery to delayed recovery, where magnitudes were normalized by the frequency-average total recovery magnitude per animal (panel D in Figure 25; compare with similar data for the relative onset vs. delayed suppression magnitudes in Figure 23). These variables were negatively correlated (CAP: τ=-0.80, DPOAE: τ=-0.88, $p < 10^{-21}$ for both).

The fact that adaptation is correlated with delayed but not onset suppression implies that adaptation reflects a weakening of the delayed suppression component. The absence of a correlation between onset (delayed) suppression and offset (delayed) recovery is more difficult to interpret. In some cases, offset recovery is large even when onset delay is small, implying that a delayed suppression component disappears immediately when contralateral noise terminates (Figure 25 D). A possible explanation is that both onset and delayed suppression components reflect response rate of MOC neurons (without any peripheral component, as in the MOC slow effect), which can decrease abruptly when sound input to the neurons terminates.

II.C.5 Dissecting the neural pathways mediating suppression

Contralateral noise can affect ipsilateral responses through two main neural pathways: the middle ear muscle (MEM) reflex or the olivocochlear reflex. We need to rule out the MEM reflex by direct experimentation to confidently ascribe the observed suppression effects to the olivocochlear (OC) system. Also, within the OC system, there is a medial (MOC) and lateral (LOC) subsystem, and the MOC subsystem consists of a crossed and an uncrossed component. Here we describe a series of experiments to investigate the responsible pathway(s) for onset and delayed suppression in response to contralateral noise.

II.C.5.a Middle ear muscle reflex

In one animal, we tested the middle ear muscle (MEM) reflex by paralyzing the animal with curare, a non-depolarizing blocker of the neuromuscular junction. First we obtained suppression characteristics in the usual manner, after which we applied a systemic injection of curare (3 mg/kg, i.p.) while the animal was artificially respirated.

Ipsilateral response suppression magnitude pre- (black, mean of 4 trials) and post-curare (red, mean of 3 trials) for CAP (top), DPOAE (bottom left), and RW noise (bottom right) did not change by a statistically significant amount, except the CAP suppression at 8 kHz, which went from 0.9 ± 0.1 dB to 1.3 ± 0.1 dB (p = 0.015), see Figure 26. Even so, as for the other response measures, the overall response characteristic over time did not appear to change in any important

way. Given the observed variation in suppression magnitudes from trial-to-trial (cf. Figure 10), the similarity in response traces in Figure 26, using data taken several hours apart, is in fact quite good. Thus, from the available data, there is no evidence that eliminating the MEM reflex by curare-induced muscle paralysis alters contralateral-noise induced suppression of ipsilateral responses in a major way.

Another characteristic of middle ear muscle contractions is that they increase the impedance of the middle ear, as seen from the ear canal, and thereby increase reflectance of sound at the tympanic membrane (Guinan 2006). Thus, monitoring primary levels of DPOAE stimuli during contralateral noise is another indirect method of detecting the MEM reflex (Figure 6). However, in none of our experiments did we observe a consistent change in primary levels that exceed a few tenth of a dB during contralateral noise.

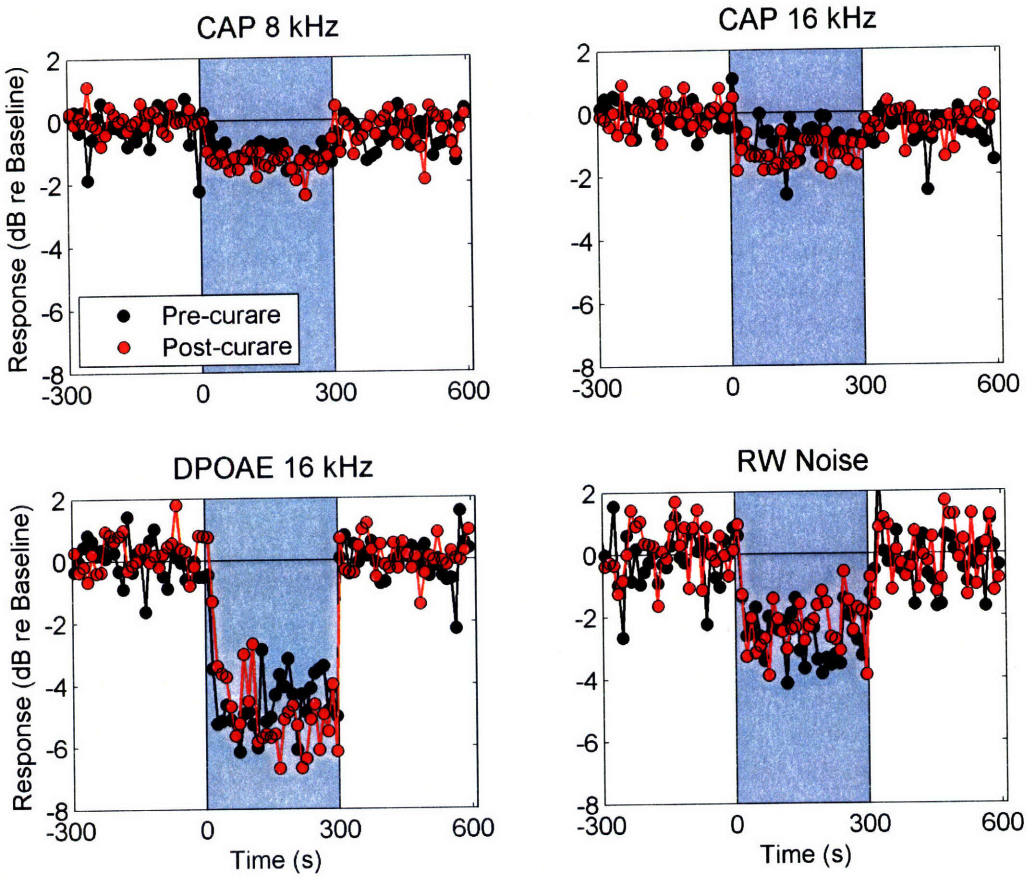

Figure 26. Pre- (black, mean of 4 trials) and post-curare (red, mean of 3 trials) normalized responses, for CAP, DPOAE, and RW noise (data from EL141). Curare at 3 mg/kg abolishes the MEM reflex – but does not affect suppression during contralateral noise.

II.C.5.b Sensitivity to gentamicin

We evaluated the sensitivity of slow suppression to systemic injection of gentamicin (150 mg/kg, i.m.), a blocker of MOC effects (Yoshida et al. 1999), in two animals. Figure 27 shows CAP (top), DPOAE (bottom left), and RW noise (bottom right) responses obtained in one of these (EL29), both before (black) and 2 hours after (red) a gentamicin injection (150 mg/kg, i.m.). In the normal state, delayed suppression in response to the contralateral noise is evident, but is completely abolished by gentamicin. Mean (± s.e.) suppression magnitudes for this and the

other animal are shown in Figure 28, for CAP (left) and DPOAE (right) before (black) and 2 hours after (red) gentamicin. This summary data confirms that suppression is, on average, strongly reduced by gentamicin, especially for DPOAE; for CAP, one animal (EL45) appears to have some residual suppression left, but reduced by at least 50%. The results are consistent with an MOC role in onset and delayed suppression, and further argue against involvement of the MEM reflex.

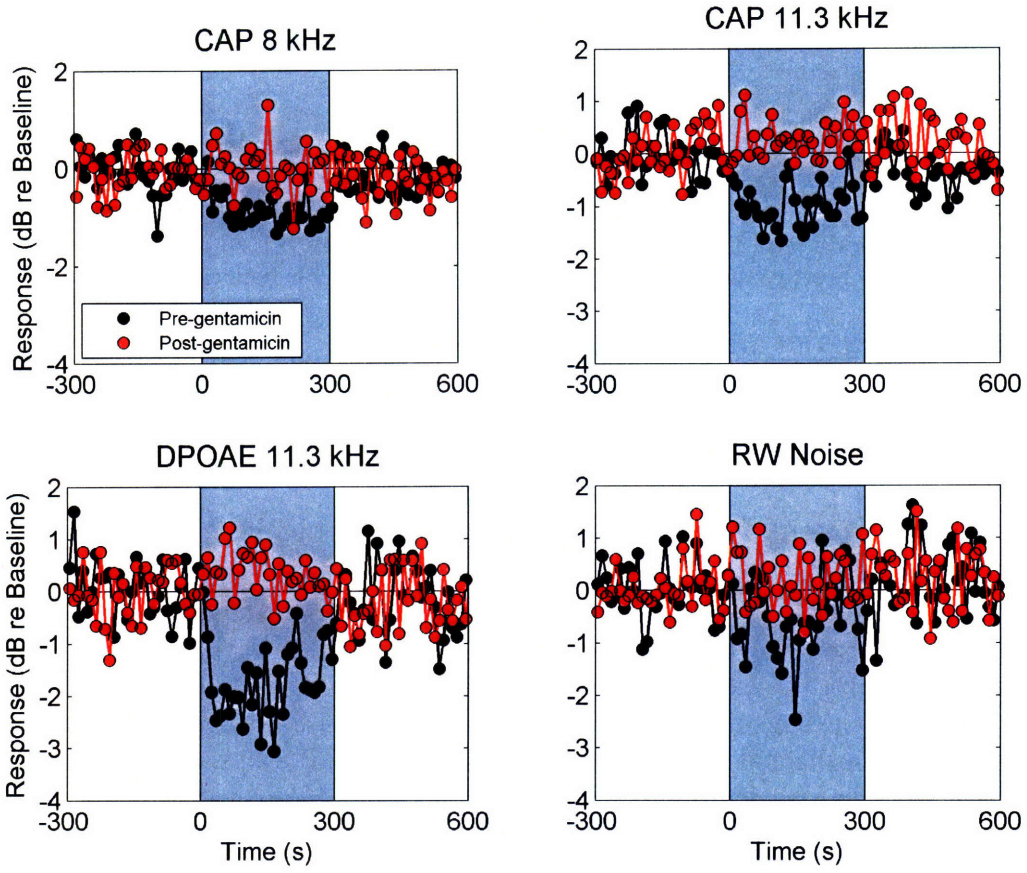

Figure 27. Normalized CAP (top), DPOAE (bottom left), and RW noise (bottom right) responses measured pre- (black, mean of 9 trials) and 2 hours post-gentamicin (red, mean of 8 trials, 150 mg/kg, i.m.). Delayed suppression, evident in the pre-gentamicin condition, is abolished in all metrics after gentamicin injection (data from EL29). Summary data on pre- and post-gentamicin suppression magnitude in Figure 28.

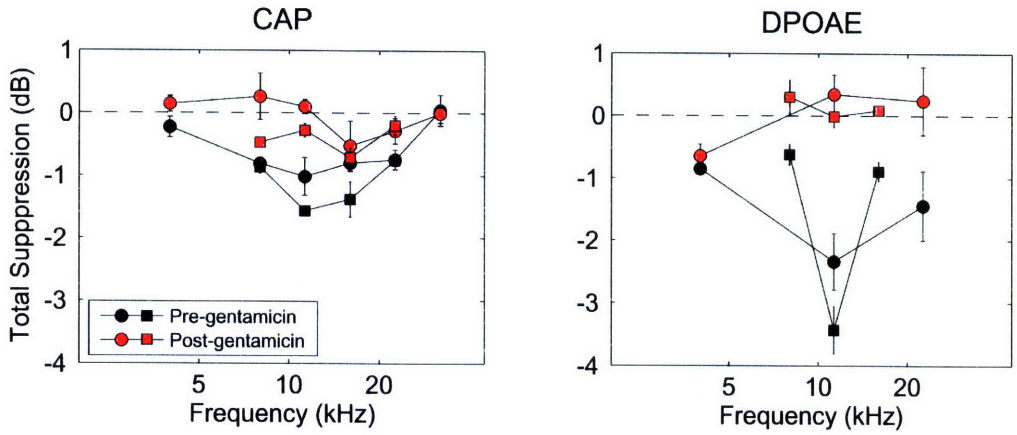

Figure 28. CAP (left) and DPOAE (right) mean (± s.e.) total suppression magnitudes pre- (black) and 2 hours post-injection of gentamicin (red, 150 mg/kg i.m.). Data from two animals (EL29: circles, EL45: squares). The gentamicin abolishes, or greatly reduces, the magnitude of the suppression in both cases.

II.C.5.c Components of the olivocochlear system

The experiments involving curare and gentamicin provide direct evidence against a role for the middle ear muscles in suppression. Thus, we now turn to dissecting the olivocochlear pathways, described below.

II.C.5.c.i Effects of interrupting the crossed olivocochlear bundle

The OC innervation of the ipsilateral ear is comprised of the crossed (COCB) as well as the uncrossed OCB (UOCB), mediating the ipsilateral and contralateral reflexes, respectively (Guinan 1996). To assess the differential contributions of both pathways, the effects of a midline (lesion to COCB only) vs. a lateral cut (lesion to both COCB and UOCB) were investigated. With our paradigm, ipsilateral effects of the contralateral noise are mediated via the UOCB, while effects of the ipsilateral tones are mediated via the COCB. Thus, a midline lesion can be used to assess whether ipsilateral MOC effects are driven by neurons responding to contralateral noise or driven by neurons responding to ipsilateral tones facilitated by contralateral noise. A lateral cut is a direct verification of whether some part of the OC system is involved in suppressive effects.

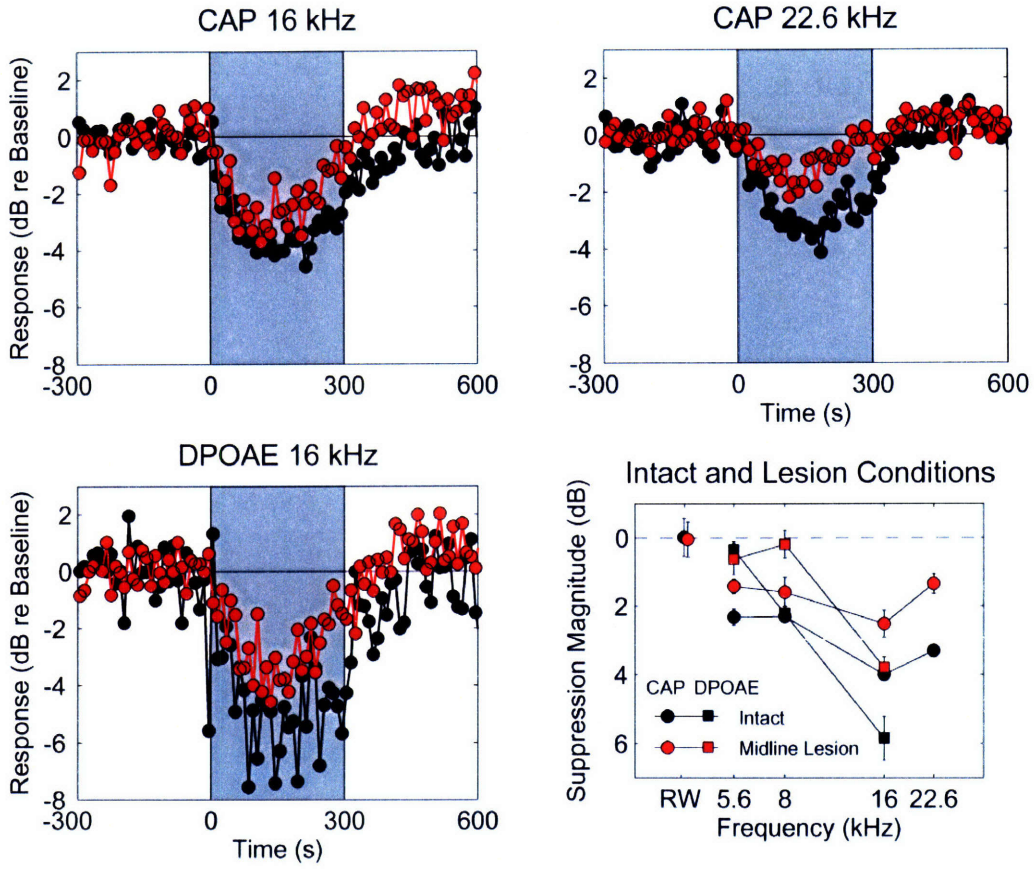

Figure 29. CAP and DPOAE responses before (black, mean of 5 trials) and after (red, mean of 4 trials) a midline cut that lesioned the COCB (verified histologically, not shown). Response traces for CAP (top) and DPOAE (bottom left) indicate that slow suppression is not abolished by the lesion, although its magnitude appears somewhat reduced; this is confounded somewhat by the upward drift visible in the post-lesion data. Mean (± s.e.) suppression magnitudes for CAP, DPOAE, and RW noise (bottom right) confirm that slow suppression remains, although with reduced magnitude. Data from EL140.

shows CAP (top) and DPOAE (bottom left) responses to contralateral noise before (black) and after (red) a midline cut that successfully lesioned the COCB (verified histologically); mean (± s.e.) suppression magnitude for CAP and DPOAE at all stimulus frequencies, as well as RW noise, are also indicated (bottom right). The overall shape of the responses with and without an intact COCB is similar, except for an apparent slight upward drift throughout the entire measurement period in some of the responses, as well as a somewhat reduced suppression during contralateral noise. The reduced suppression magnitude is confirmed by the estimated suppression magnitudes (bottom right panel), and is apparent in both CAP and DPOAE (RW noise was not suppressed in the intact condition, and was unaffected by the lesion). The baseline drift complicates estimation of suppression magnitude, and probably yields underestimates. On the other hand, the CAP response at 22.6 kHz (top right) shows no appreciable baseline drift yet a clear difference in suppression. This may be caused by variability of suppression magnitude over time (cf. Figure 10), but may be genuine result of the midline lesion. Whether or not a midline lesion at the IVth ventricle affects suppression, the main observation is that such lesions do not substantially diminish delayed suppression during contralateral noise, ruling out a large role for contralateral MOC cells that innervate the ipsilateral cochlea via the COCB.

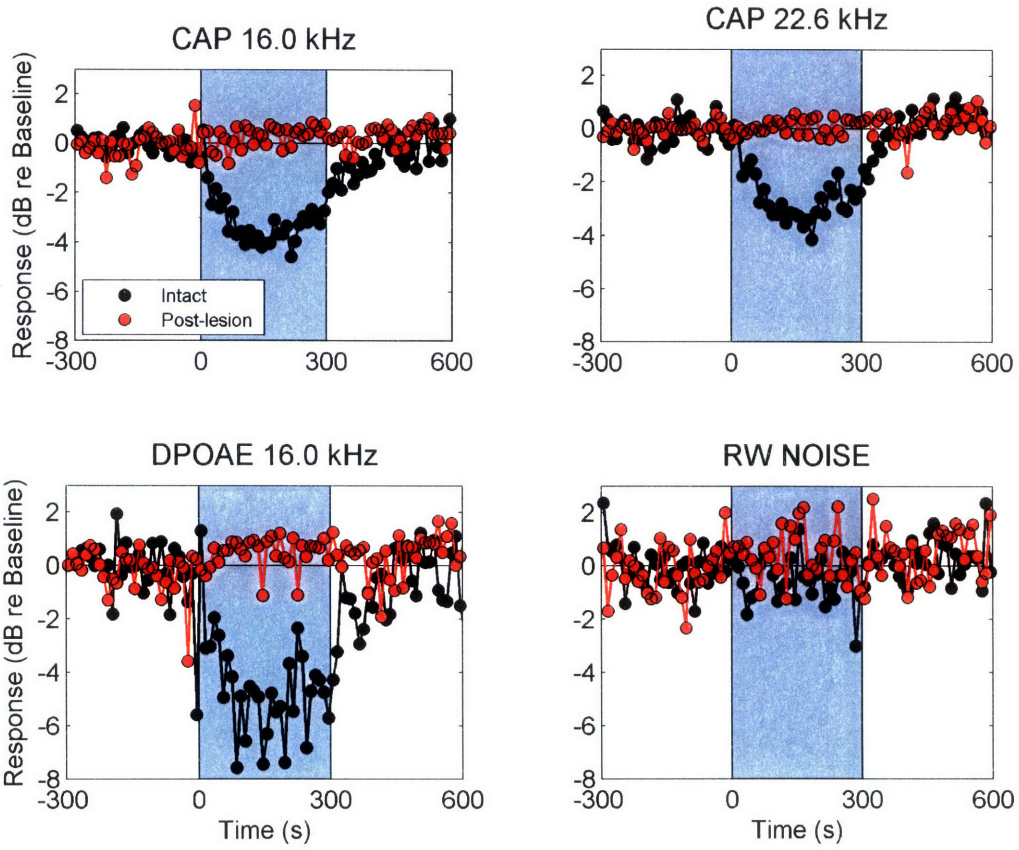

Figure 30. Baseline (black) and post-lesion (red) normalized responses, for CAP, DPOAE, and RW noise (data from EL140). The lesion was a lateral cut in the brainstem that completely severed the OCB to the ipsilateral ear (verified histologically).

II.C.5.c.ii Effects of complete ipsilateral de-efferentation

Subsequent to the midline cut, a lateral cut was made that lesioned the entire OCB (COCB and UOCB) innervation of the ipsilateral cochlea, effectively de-efferenting this side. CAP (top), DPOAE (bottom left), and RW noise (bottom right) responses in the intact (black, mean of 5 trials) and OCB-lesioned case (red, mean of 3 trials) are shown in Figure 30. Suppression is completely abolished for both CAP and DPOAE, also at the stimulus frequencies not shown in the figure. RW noise suppression was not apparent in the intact case, and RW noise responses appeared unaffected by the lesion. Note that slight enhancement of DPOAE at 16 kHz is visible; this was paired with a few tenths of a dB reduction in primary levels. This may represent a small residual middle-ear muscle effect that is revealed after the much larger OC effect has been abolished. We conducted 4 additional experiments with lateral cuts that lesioned the OCB; in all cases, slow suppression was abolished (data not shown). We also conducted 4 experiments where we attempted to lesion the OCB by a lateral cut, but where the cut was placed too far rostral, such that the OCB was left intact. In each of these 4 cases, slow suppression was unaffected relative to the 'intact' condition. All OCB 'hit' and 'miss' cases were verified histologically by AChE stains on brainstem sections (see *Methods*); an example of a successful lesion is shown in Figure 32.

II.C.5.d Olivocochlear lesion during contralateral noise

The lesion experiments have shown the involvement of the OC bundle in onset and delayed suppression. To distinguish between peripheral and central origins of the delayed buildup and recovery of the suppressive effects, we conducted two additional experiments where we sectioned the OCB *during* the contralateral noise, when suppression had reached its greatest magnitude.

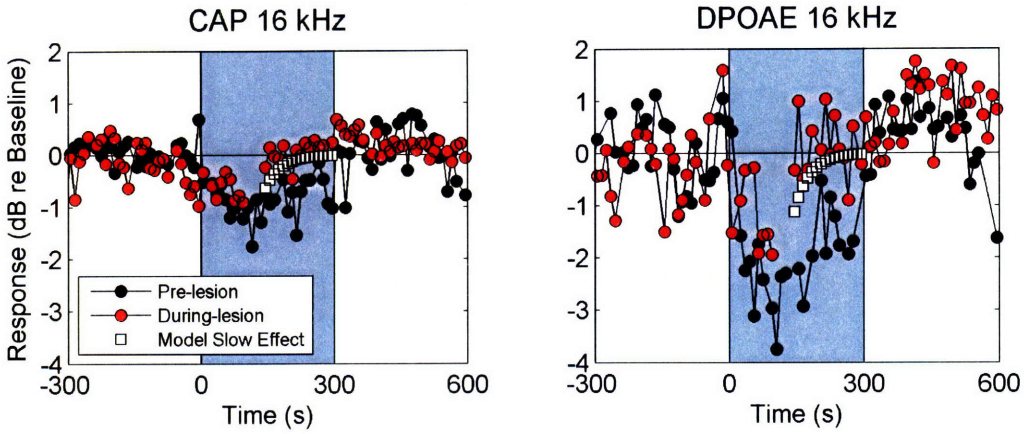

Figure 31. CAP (left) and DPOAE (right) responses at 16 kHz with an intact (black, mean of 4 trials) and lesioned (red, mean of 4 trials) OCB; to improve signal-to-noise ratio, all ipsilateral CAP and DPOAE stimuli were set to the same frequency and level, effectively acquiring 4x as much data as is normal for 1 trial. The lesion was performed while the contralateral noise was on, when suppression had reached its largest magnitude at about 120 s (the experimenter was in the chamber during 105-135 s, hence data is omitted in this time window; data from EL145). We overlaid a model MOC slow effect return to baseline also, for t>135 s. For this, we assumed that CAP was at -1.3 dB at 120 s (for DPOAE AT -2.3 dB), and at that point decayed to baseline with an exponential time constant of 35 s (as given by Sridhar et al. 1995).

We first performed the experiment with an intact OCB to ascertain whether suppression in these animals was within normal range, after which the lesion trial was run. Both experiments yielded identical results: one of these is shown in Figure 31. CAP and DPOAE responses at 16 kHz in the intact condition (black) and during the lesion (red) are matched up to 105 s; at that point, the experimenter entered the chamber and placed the lesion (around 120 s); until t=135 s, the experimenter was in the chamber so data is not shown. After cutting the OCB, responses appear at baseline at all following samples, rather than gradually recovering, as in the intact condition after noise offset (black). This result is not consistent with what would be expected of the MOC "slow effect", as this decays relatively slowly after an OCB lesion (Sridhar et al. 1995). This more gradual return is shown Figure 31 (white) by a model response assuming an exponential time constant of 35 s (as given by Sridhar et al.), assuming a CAP suppression of 1.2 dB (2.3 dB for DPOAE) at the time of the lesion (120 s). The first few visible samples of the model response (at 145 – 165 s) are all below baseline and do not fit the data (red) well. Thus, it appears that onset and delayed suppression are mediated by changing responses within the MOC fibers, rather than a peripheral effect.

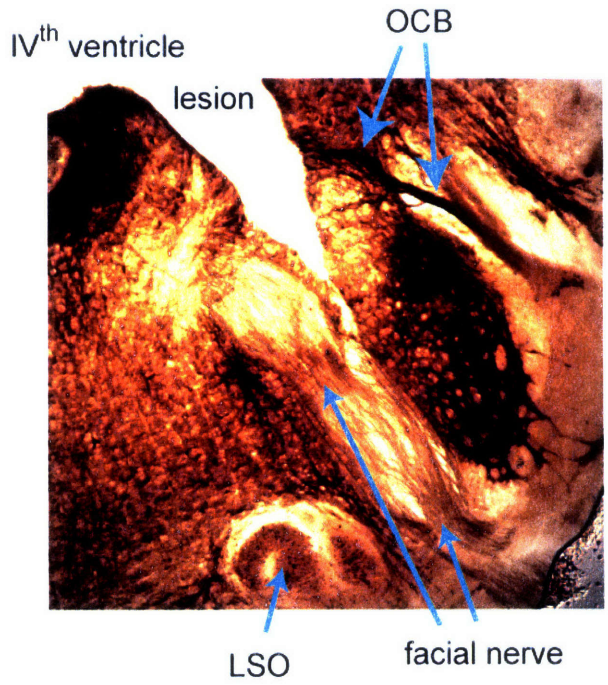

Figure 32. AChE-stained brainstem section (right half) shows complete transaction of the ipsilateral OCB (indicated). The facial nerve is spared. Also indicated are the IVth ventricle (top) and LSO (bottom). Compare to a wider field of view from an intact brainstem, as in Figure 7.

II.D Discussion

II.D.1 Summary of findings

We demonstrated robust suppression of round window (RW) noise, CAP, and DPOAE, in response to sustained (5 min) contralateral broadband noise of approximately 75 dB SPL in anesthetized guinea pig (typical responses in Figure 9 and Figure 10). The suppression has two phases: an onset phase, acting within the first 10 s after contralateral noise onset, and a delayed phase, which builds up gradually and generally reaches a maximum at 2-3 minutes. Although delayed suppression shows considerable inter-animal variability, pooling data across 21 animals yields mean delayed suppression magnitude of 0.7 and 0.8 dB for CAP and DPOAE (1.1 and 0.5 dB when expressed as equivalent attenuation) and no marked frequency dependence up to 22 kHz; mean late suppression of RW noise is 0.5 dB. In these respects, it is similar to the onset suppression component; the latter appears in all respects consistent with the MOC fast effect: its frequency distribution (Figure 13), its stimulus level dependence (Figure 16), and its sensitivity to gentamicin (Figure 27). Although the MOC fast effect builds up on a timescale of 100 ms and is thus too fast to resolve on the timescale of our measurements (~10 s), other possible mechanisms for the onset suppression were ruled out (see below). Depending on exactly how long after contralateral noise onset measurements were taken (order of measurement was: RW noise, CAP, DPOAE), the onset component may reflect partial contribution of continuing (late) suppression. It is therefore possible that our estimates of onset suppression are overestimates of MOC fast effect, and that the delayed suppression component is concomitantly slightly underestimated.

II.D.2 Late suppression is mediated by a central modulation of the medial olivocochlear system

Contralateral noise can affect ipsilateral cochlear responses through different mechanism and various neural pathways. To be confident that the suppression effects we studied were of olivocochlear origin, these other possibilities should be assessed first.

II.D.2.a Non-olivocochlear effects

Acoustic crosstalk is the direct transmission of acoustic energy via air, bone, or the experimental apparatus from the contralateral acoustic system to the ipsilateral cochlea. We directly assessed the potential contribution of crosstalk in several experiments, in which we lesioned the contralateral cochlea after establishing baseline suppression characteristics. The lesions were made by penetrating the contralateral cochlea through the round window with a fine metal probe and cracking the bony capsule. This effectively eliminated all measurable responses from the contralateral ear, yet should not affect the various acoustics paths from the contralateral acoustic assembly to the ipsilateral cochlea. Such lesions always completely abolished suppression (example in Figure 11), both early and late components, indicating that acoustic crosstalk could not be responsible for the observed suppression. Rather, suppression must be mediated by a neural pathway that originates in the contralateral cochlea.

The middle ear muscle (MEM) reflex acts to contract middle ear muscles bilaterally in response to loud sounds in either (or both) ears. The muscle contractions increase the impedance of the middle ear (Borg 1972), decreasing sound transmission into the cochlea, and suppressing cochlear evoked responses (Borg 1968). Fortunately, in guinea pig, the MEM reflex appears to

be weak even in awake animals (Avan et al. 1992), and should be even weaker during anesthesia. However, its potential contribution to our data should be carefully evaluated. The only aspect of our baseline suppression data which appears to be directly incompatible with the MEM reflex is the suppression of RW noise, as it is a measure of spontaneous cochlear activity, and should not be affected by middle ear transmission characteristics. However, it cannot be ruled out that RW noise contains some contribution from low-level ambient noise in the recording chamber (possibly generated by the animal), and if so, would partially reflect sound-driven cochlear activity, which could be sensitive to middle ear transmission.

However, a more careful examination of suppression characteristics as well as the outcome of additional experiments seems to rule out an important role for the MEM reflex in the suppression we observed. The change in middle-ear impedance caused by the MEM reflex is primarily an increase in stiffness (Borg 1972), which therefore primarily attenuates low-frequency sounds (Borg 1968). Yet, neither onset nor delayed components of suppression magnitude of CAP and DPOAE showed such a low-frequency bias (Figure 13). After converting suppression magnitude to equivalent attenuation, as would be appropriate for a mechanism that simply attenuates sounds entering the cochlea, displays no frequency such dependence either (Figure 15). In experiments where baseline suppression measurements were followed by systemic gentamicin injections, all components of the suppression were abolished (Figure 27 and Figure 28), although gentamicin has no known effects on the MEM reflex. Finally, systemic injection of curare (a non-depolarizing muscle relaxant) at a dose of 3 mg/kg – several times higher than used for paralysis in electrical stimulation experiments (Groff 2003; Sridhar et al. 1995), see also Figure 6 – did not abolish suppression (Figure 26). Indirect evidence showing no activation of the MEM reflex was obtained by measuring DPOAE primary levels, which increase measurably during MEM contractions, and are frequently used as a MEM reflex assay (Guinan 2006). Although we did observe such changes occur at *random* times (corresponding to spontaneous MEM contractions), there were no such *systematic* changes in primary levels during contralateral noise. Taken together, the available data provides strong evidence against a role for the MEM reflex in onset or delayed suppression.

II.D.2.b Onset and delayed suppression are mediated by the olivocochlear system

Having ruled out acoustic crosstalk and the MEM reflex as causes of the suppression, the olivocochlear (OC) system is the most likely candidate to account for both early and late suppression. As the OC system is already known to mediate the MOC fast effect, with which our early component suppression data is wholly consistent, we further focus on the late suppression component. Beside the OC system, the peripheral sympathetic innervation of the cochlea could conceivably play a role as well. This innervation derives from the stellate ganglion (SG) as well as the superior cervical ganglion (SCG); the former forms the perivascular component, while the latter terminates on afferent neurons in the spiral ganglion and together these do appear to be able to modulate cochlear responses (Gallego and Geijo 1987). Because late suppression was evident in DPOAE data, its origin must lie at or before the level of outer hair cells – ruling out an exclusive role for the SCG sympathetics and rather pointing towards the perivascular component from the SG. If this component is able to modulate endolymphatic potential (EP) by altering cochlear metabolism/blood flow, sound amplification would be reduced and all cochlear responses would be suppressed: the effect of reductions in EP on cochlear neural responses has been well documented (Sewell 1984). We have, however, two key lines of evidence that sympathetic innervation is not the source of early or late suppression.

The first evidence is the delayed *enhancement* in cochlear microphonic (CM) that was observed in one experiment where it was measured in response to low-frequency, high-level tone pips (Figure 12). Such enhancement is always seen in conjunction with MOC activation, and is believed to result from the increasing transduction current through the outer hair cells as a result of the decrease in their membrane resistance (Gifford and Guinan 1987; Mountain et al. 1980). That this CM enhancement was seen on a slow timescale, along with a slow suppression of CAP and DPOAE, is strong evidence in favor of an MOC origin. It is not consistent with delayed suppression being caused by a reduction of EP alone, as caused by the sympathetic innvervation only, because this would not alter outer hair cell membrane resistance and therefore result in a CM suppression. The magnitude of the CM enhancement relative to CAP equivalent attenuation was within the expected range, based on data obtained with shock-evoked MOC activation in cats (Gifford and Guinan 1987).

The second, and most direct, evidence in favor of the MOC vs. sympathetic origin of delayed suppression is from the brainstem lesions. We performed a total of 9 lesion experiments targeting the OCB. These lesions were placed on the ipsilateral side of the brainstem at the level of the IVth ventricle; cuts were made in a rostro-caudal direction, in a plane oriented dorso-medially to ventro-laterally. The depths of the lesions were from 50 to 90% of the depth of the brainstem at that location. All lesions were inspected histologically with an acetylcholinesterase (AChE) stain to mark the cholinergic MOC and LOC cells and axons; 5 of 9 lateral lesions sectioned the entire OC innervation to the ipsilateral ear, while the remaining 4 lesions missed the OC bundle (OCB), as they were placed too far rostrally. In all cases where the OCB was successfully lesioned, onset and delayed suppression was abolished (e.g., Figure 30); in all cases where the OCB was missed, onset and delayed suppression were unaffected (data not shown). This selectivity in abolishing suppression conditional on successful lesions to the OCB is strong evidence in favor of the OC origin of onset and delayed components of the suppression. A potential caveat is that our lesions, besides cutting the OC axons, may also have damaged adrenergic locus ceruleus (LC) cells or pathways. The LC lies rostral with respect to the OCB, and given its widespread innervation to the rest of the brain, some trauma to the sympathetic system as a result of our cuts might occur. However, trauma to LC cells or axons is more likely for lesions that miss the OC by cutting too rostral, as was the case for all of our missed cuts. Given that we did not find any changes in suppression in such missed cases, but only in cases where the OCB was cut, we have strong evidence that our brainstem lesions did not interfere with sympathetic circuitry in the brain.

II.D.2.c Role of medial vs. lateral olivocochlear systems

The available evidence as presented above strongly suggests that the OC system is solely responsible for onset and delayed suppression. Because the OC system is composed of a medial (MOC) and lateral (LOC) component, the observed suppression may be mediated by either or both of these two subsystems. The LOC axons synapse exclusively in the inner hair cell area (Liberman 1980; Maison et al. 2003b), and are not thought to affect the function of the outer hair cells. As such, delayed suppression of DPOAE (and delayed enhancement of CM) must be mediated by the MOC system; at the level of the inner hair cell area, downstream from the OHCs, this causes delayed suppression of CAP responses. When expressed as equivalent attenuation, delayed suppression has a greater effect on CAP than on DPOAE (Figure 15, Table 2), which is consistent with sound-evoked MOC fast suppression in cat (Puria et al. 1996). The relatively larger effects on CAP vs. DPOAE in both species could reflect LOC effects during contralateral noise, although by itself this is not compelling evidence.

Suppression of RW noise (a measure of auditory nerve spontaneous activity, Dolan et al. 1990) is analogous to suppression of auditory nerve spontaneous rates that occur during shock-evoked MOC activation (Guinan and Gifford 1988a). Although at first sight reduced cochlear gain would not be expected the affect spontaneous activity, the presumed mechanism is that MOC activity reduces endocochlear potential (EP) (Mountain et al. 1980), thereby diminishing the driving force for K^+ into inner hair cells, ultimately leading to hyperpolarization and a reduction of synaptic activity; the effect of EP on spontaneous rate has been shown by direct measurement (Sewell 1984). Spontaneous rates are typically only reduced by a few percent (Guinan and Gifford 1988a), which is smaller than the mean total RW noise suppression we found (approximately 0.7 dB in total, i.e. approximately 8%), but the auditory nerve experiments used shock-evoked MOC activity and would therefore not include delayed components but only reflect onset suppression, which was 0.19 dB (~2%) on average in our experiments, consistent with the auditory nerve data. There is no auditory nerve data during prolonged (several minutes) sound stimulation with which to compare our RW noise delayed suppression magnitude.

The relationship between spontaneous rate and EP was shown to be linear when using log spontaneous rate (Sewell 1984); the proportionality factor being -0.02 log rate per mV, on average, for high-spontaneous rate fibers (these fibers should dominate gross potentials and therefore contribute most to RW noise). Expressing RW noise as 20 log(rate/R_0), where R_0 is an arbitrary reference rate, this factor translates into RW noise suppression of about 0.4 dB per mV reduction in EP. Electrical stimulation of ipsilateral MOC neurons (innervating the cochlea via the uncrossed OCB) during 100 ms leads to reductions in EP of about 1 mV (Gifford and Guinan 1987); these same neurons are also stimulated in our experiments during contralateral noise, such that our onset suppression of RW noise (~0.2 dB) is consistent with MOC effects on EP if we assume that sound-induced MOC response rate is lower than electrical shock rate used by Gifford and Guinan (200 s^{-1}). Assuming that a 1 mV reduction in EP accounts for onset suppression of RW noise, then a 3.5 mV reduction is required to account for total RW noise suppression (~0.7 dB). Such a large change in EP reduction (from 1 to 3.5 mV) appears surprising, so that delayed RW noise suppression mediated *solely* by the MOC system is hard to explain. Instead, some contribution of the LOC system to delayed suppression could provide a plausible alternative hypothesis for the relatively large delayed RW noise effects. However, we have no direct evidence for involvement of the LOC system.

Systemic gentamicin is a known blocker of the MOC reflex (Yoshida et al. 1999), presumably by interfering with the $\alpha9/\alpha10$ nicotinic acetylcholine receptor on OHCs; the fact that gentamcin (at 150 mg/kg) reduced onset and delayed suppression further points towards a main role for the MOC system. Although suppression was not always completely abolished (Figure 28), unpublished data from shock-evoked DPOAE suppression from this laboratory (S.F. Maison, personal communication) shows a mean reduction of MOC-induced suppression of about 50%, such that it is not straightforward to interpret this finding with respect to MOC vs. LOC contributions. Nonetheless, our data indicate a main role of the MOC system in both onset and delayed suppression effects. On the other hand, some role for the LOC system cannot be completely excluded. It is possible that the neural responses to contralateral noise include a small suppression or enhancement due to the LOC contribution; however, given that the relative sizes of neural vs. DPOAE effects are roughly as expected, any such LOC effects would presumably be small. The best evidence for involvement of the LOC system is the relatively large delayed RW noise suppression, which is poorly accounted for by MOC effects on EP alone.

The MOC innervation of the ispilateral ear consists of a crossed and uncrossed component, which have cell bodies on the contra- and ipsilateral half of the brainstem, respectively (Schwartz 1992). Because MOC cells are driven by contralateral sound, we expect that ipsilateral suppression by contralateral sound involves the uncrossed component of the MOC system. A contribution of the crossed component would imply that it is activated by the probe tones used in monitoring the CAP and DPOAE responses; this appears less likely, because the tones are brief (5 ms for CAP and 40 ms for DPOAE primaries) and thus poor elicitors of MOC activity. However, it is possible that repeated short tone bursts in combination with facilitation by the contralateral noise, may evoke strong enough MOC responses in the crossed fibers to induce suppression. To test this hypothesis we created a midline cut (interrupting the crossed, but not the uncrossed, MOC fibers; verified histologically, not shown) in one experiment with clear delayed suppression. The late suppression persisted despite the lesion, indicating that the crossed fibers do not play a major role in the suppressive effects. Rather, the contralateral noise drives MOC cells on the ipsilateral side of the brainstem, which send their uncrossed axons into the ipsilateral cochlea. This reflex pathway has been well established already (Guinan 2006), but the fact that persistent sound stimulation leads to increasing suppression had not been firmly established.

II.D.2.d Central vs. peripheral origin of the delayed component of suppression

Delayed suppression via the MOC system may occur as a result of an increased response rate of MOC neurons or by a peripheral mechanism. Central modulation of MOC response rate has been well documented as mediated by sounds presented to the non-preferred ear; this is referred to as facilitation (Brown et al. 1998a; Liberman 1988b). Such facilitation does not only enhance response rate, but also decreases MOC thresholds on- and off-CF, and these effects are measurable for several minutes after the facilitating stimulus has stopped (Liberman 1988b). If the delayed suppression in our data is due to central modulation of MOC responses, it would imply that these cells can be modulated not only by inputs from the non-preferred ear, but also from the preferred ear alone, if such stimulation acts sufficiently long.

Peripheral enhancement of MOC suppression has been documented in electrical stimulation paradigms (Sridhar et al. 1995); continued shocks evoke several dB of suppression in addition to the MOC fast effect, building up over 1-2 minutes. This is thought to involve slow recruitment of distant SK2 channels in outer hair cell membranes by release and diffusion of internal calcium stores, and has been called the "MOC slow effect". To distinguish between central and peripheral sites of action for delayed suppression in our data, we lesioned the OCB to the ipsilateral ear half-way through the contralateral noise epoch, when delayed suppression had built up completely, in two animals. As indicated in Figure 31, ipsilateral responses returned to baseline immediately after the lesion, while prior data from the same animal displayed slow return at that point. A fast recovery is not consistent with a peripheral site of action, which would yield a slow return to baseline (as in Sridhar et al. 1995), but rather suggests that the late suppression is due to an enhanced response rate of the MOC neurons. Overlaying a model MOC slow effect return to baseline at the time of the lesion (white squares in Figure 31) shows that indeed a longer recovery would be expected for the MOC slow effect. The immediate return to baseline can be observed in some intact animals also, e.g. as in Figure 9, where recovery after contralateral noise appears to consists almost exclusively of an offset ("immediate") component, which is never observed with the MOC slow effect.

The results of the "during-noise" OCB lesion point towards the central origin of the delayed suppression component. There are also other aspects of the data that are more compatible with a central modulation of the MOC system than with the peripheral MOC slow effect. The frequency dependence of delayed suppression is modest, although there is a minimum at mid-frequencies (where onset suppression has a maximum). In contrast, the MOC slow effect has a high-frequency bias (Sridhar et al. 1995), as illustrated in Figure 33 (left; data below 8 kHz were not reported, but presumably slow effects remain small in that range). When adding sound-evoked onset and delayed suppression, the resulting magnitude is essentially constant across the frequency range we measured (Figure 33, right). This compares favorably with the near-constant cochlear innervation density of MOC terminals at these frequencies in guinea pig, as estimated from bouton areas of acetylcholinesterase-stained (AChE) terminals (Brown 1987; converting place to frequency using the guinea pig cochlear map from Tsuji and Liberman 1997). The same procedure applied to shock-evoked MOC fast and slow effects does not remove the tendency for total suppression magnitude to decline at high frequencies (Figure 33, right). This discrepancy for the shock-evoked case may not be problematic because the physiological mechanisms of the MOC slow effect are due to processes occurring *within* the outer hair cells that may not depend only on the strength of the MOC-OHC synapse, and in that case would not be revealed with AChE staining. On the other hand, both onset and delayed sound-evoked effects are determined by the response rate of MOC fibers, and should be consistent with synaptic innervation patterns.

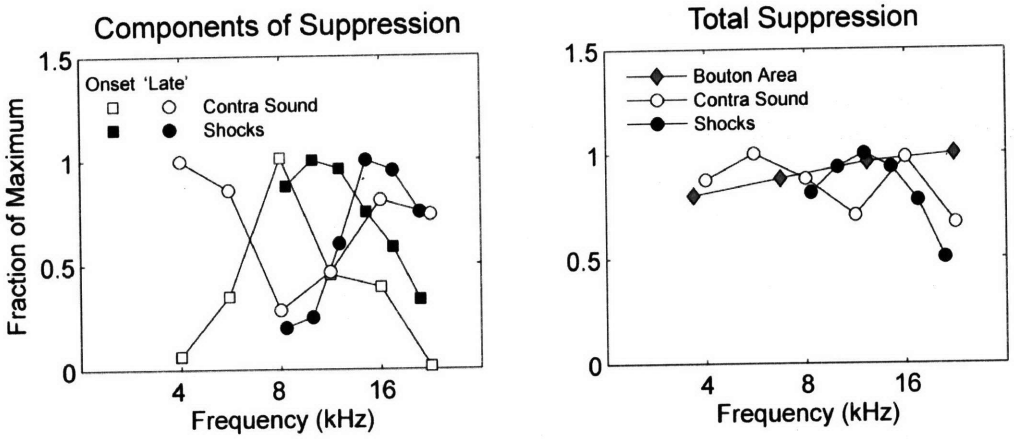

Figure 33. Comparison of onset and 'delayed' suppression for contra sound- vs. onset and 'slow' shock-evoked MOC activity (left) reveals differences in frequency dependence ('late' refers to either 'delayed' or 'slow'). Sound-evoked delayed suppression is present at all frequencies, while shock-evoked slow effects have a high-frequency bias. Onset suppression magnitude peaks at mid frequencies in both cases. Adding onset and 'late' suppression yields total suppression (right), which is compared to MOC efferent innervation density (assessed via terminal bouton area). Sound-evoked total suppression magnitude follows the innervation density reasonably well, while shock-evoked total suppression magnitude declines raidly at high frequencies. All data are represented as fractions relative to their own maximum. Sound-evoked data from Figure 15; shock-evoked data and bouton area as function of cochlear place from prior work (Brown 1987; Sridhar et al. 1995). Cochlear place was converted to frequency using the guinea pig cochlear map (Tsuji and Liberman 1997).

Another feature of MOC late suppression that is more consistent with a central origin is the negative correlation of MOC onset suppression (corresponding to the MOC fast effect) and MOC delayed suppression (Figure 22 and Figure 23). This negative correlation is even visible in the pooled data when binned into frequency bands (Figure 15, Figure 33): frequencies with

strong onset suppression (mid-frequencies) have smaller delayed suppression, and vice versa (low- and high frequencies). If delayed suppression was the result of a peripheral accumulative effect, one would most likely expect a positive correlation with onset suppression: a larger initial input to the outer hair cells should yield a larger accumulative effect. Such a correspondence was indeed found for the MOC slow effect (shown in Fig. 8 in Sridhar et al. 1995); however, we found exactly the opposite. Prior experiments involving facilitation of MOC neurons found that facilitation was strongest (weakest) for cells that had weaker (stronger) responses to the preferred stimulus alone (Brown et al. 1998b; Liberman 1988b). Apparently, the inverse correlation between the onset response and response enhancement (whether by facilitation or sustained monaural stimulation) is an intrinsic property of MOC cells. It suggests that the responses of these cells can be modulated, but not beyond a particular maximum rate.

The physiological mechanism responsible for response enhancement of MOC neurons due to sustained monaural stimulation is not known, and neither is the mechanism responsible for binaural facilitation. There are several possibilities, including changes in synaptic input or modulation of the cell's internal state. There is anatomical evidence for noradrenergic input to the superior olive (and cochlear nucleus) from the locus coeruleus in rat and guinea pig (Horvath et al. 2003; Kromer and Moore 1980; Woods and Azeredo 1999), and iontophoresis of noradrenaline leads to inward currents in a majority of identified MOC cells *in vitro* (Wang and Robertson 1997) and suppression (via the MSO) or enhancement (via the LSO) of CAP *in vivo* (Mulders and Robertson 2005). Additionally, cochlear nucleus neural responses can be modulated by application of noradrenaline (Ebert 1996) or electrical stimulation of the locus coeruleus (Chikamori et al. 1980); if this includes neurons within the MOC reflex pathway, this would provide another route through which responses of MOC cells can be modulated. Although there is no direct evidence that locus coeruleus neurons are responsive to sound, they receive inputs from widespread regions of the central nervous system (Cedarbaum and Aghajanian 1978), so that some indirect auditory component may well exist. The putative impact of locus coeruleus neurons on peripheral auditory processing does not seem outside the scope of the locus coeruleus system as a regulator of behavioral state and modulator of sensory information processing (Berridge and Waterhouse 2003; Devilbliss et al. 2006; Kössl and Vater 1989). Alternatively, certain cell types in the auditory pathway have been shown to alter their response properties during prolonged stimulation via 2nd-messenger systems, e.g. through phosphorylation of membrane channels (Song et al. 2005) or changes in expression of surface receptors (Chen et al. 2007); these or other mechanisms could conceivably also alter response properties of MOC neurons during sustained acoustic stimulation without the need to invoke the noradrenergic inputs. Given that 2nd-messenger systems can have large effects on cellular physiology and are used throughout the central nervous system, such 'instrinsic' mechanisms for MOC response modulation may be the most likely candidates.

II.D.3 Comparison to prior studies

Our experiments were designed understand the mechanism(s) behind sound-evoked slow effects, as originally described by Lima da Costa et al. (1997a). They measured suppression of RW noise in awake guinea pigs in response to long-term contralateral noise, and found fast and "slow" suppression, which persisted up to 2 hours without adapting. Their fast suppression was sensitive to low doses of gentamicin (150 mg/kg), but the "slow" component was not affected by this dose, and required 250 mg/kg to be abolished. They ascribed their "slow" suppression to the MOC slow effect (Sridhar et al. 1995); however, it is possible that it was the same MOC delayed

suppression that we found, and showed to be mainly of central MOC origin, through a delayed enhancement of MOC response rate. In the remainder, we will refer to their fast and "slow" suppression in the terms we used, i.e. onset and delayed suppression.

The conclusion regarding the origin of the delayed suppression observed by Lima da Costa et al. was based primarily on circumstantial evidence: that the time constant of their effect was similar to the MOC slow effect, and of approximately equal size. They discounted the LOC system on grounds that this nucleus projects nearly exclusively to the ipsilateral cochlea, but because there is no evidence that LOC cells do not respond to contralateral sound such a discounting is unwarranted. However, by measuring inner hair cell/neural potentials and also outer-hair cell based responses (DPOAE, CM) we were able to provide solid evidence for the involvement of the MOC system in the delayed modulation of suppression. Our data does not rule out a contribution of the LOC system, but if present, is probably minor compared to that of the MOC system. Besides measuring additional ipsilateral metrics, we also added experiments involving curare to rule out middle ear muscle effects, and brainstem lesions as positive controls for the involvement of the OC system.

Overall our results on suppression of RW noise compare reasonably well with those of Lima da Costa et al. in the sense that we both report onset and delayed suppression, with comparable time constants. However, we found suppression magnitudes (mean over animals) of about 0.2, 0.5, and 0.7 dB for onset, delayed, and total suppression components, while Lima da Costa et al. found about 3, 1.5, and 5.5 dB, respectively. One important difference was that Lima da Costa et al. used awake guinea pigs, which presumably would lead to larger MOC suppression and may prevent adaptation; it is thought that while Fentanyl does not affect MOC response rate, pentobarbital (Nembutal) depresses MOC activity in a dose-dependent manner, up to about 50% for dosage typically used for guinea pigs (Boyev et al. 2002). Thus, anesthetic state may explain the differences in suppression magnitude between Lima da Costa et al. and our data, although it is not meaningful to attempt a precise calculation of the effects of anesthesia in our paradigm.

Delayed suppression in our experiments tended to adapt after reaching a maximum in 2-3 minutes (typical examples in Figure 30), although not in all animals, and in some cases delayed suppression continued to increase for the full 5 minute of contralateral noise. Mean adaptation was roughly 1/3 of delayed suppression magnitude both for CAP and DPOAE (Figure 24). The late suppression in Lima da Costa et al. did not adapt, even for contralateral noise durations of up to 2 hours. It is unclear how this difference in adaptation might occur; perhaps as a result of anesthesia. The MOC fast effect does not adapt in anesthetized guinea pig (Brown 2001), so it appears adaptation reflects a weakening of the delayed effect, which is consistent with the aforementioned mathematical correlation between adaptation and delayed suppression.

Gentamicin is a known blocker of the MOC reflex (Yoshida et al. 1999), and we found both onset and delayed suppression to be abolished 2 hours after an injection of systemic gentamicin at 150 mg/kg (Figure 27 and Figure 28). However, for Lima da Costa et al. this dose only abolished onset suppression, while delayed suppression required 250 mg/kg. It is possible that strain differences (we used albino, whereas Lima da Costa et al. used pigmented guinea pigs) lead to differential sensitivity to gentamicin, or that our animals required a smaller dose because of the difference in anesthetic state. We did not use different doses of gentamicin, so we do not know whether our MOC onset and delayed effects could be dissociated like in Lima da Costa et al. It is possible that the delayed effect requires a higher dose because the MOC-OHC synapse has to be blocked more completely, as delayed suppression reflects a higher response rate of the MOC neurons.

II.D.4 Functional implications of delayed suppression

By studying peripheral effects of the MOC system during persistent sound stimulation, we found increased suppression relative to the MOC fast effect. The mean magnitude of delayed suppression seems to be at least as large as onset suppression, both for CAP and DPOAE (Figure 13 and Table 1). When expressed as equivalent attenuation, delayed suppression for CAP is about twice as large as onset suppression, approx. 1 vs. 0.5 dB, and about similar for DPOAE, about 0.5 dB (Figure 15 and Table 2). Although we did find a tendency for delayed suppression to adapt over time, this may be a result of anesthesia, as adaptation does not seem to occur in awake guinea pigs (Lima da Costa et al. 1997a), although in that case only RW noise was measured.

II.D.4.a Application to natural conditions

Although the magnitude of delayed suppression as measured in our experiments appears rather modest, the effects could be considerably larger in naturalistic conditions. First, our animals were anesthetized, which depresses MOC activity; for barbiturate anesthesia (Nembutal), MOC-induced fast suppression of DPOAE is reduced by about 50% relative to unanesthetized controls (Boyev et al. 2002). Also, evoking the MOC reflex using contralateral sound activates only 1/3 of the total MOC innervation to the ipsilateral ear (Guinan 1996); the remaining 2/3 consists of the ipsilateral MOC reflex, which would be activated in naturalistic conditions considering that ambient noise will usually be of approximately the same level in both ears. If we fully account for these two factors, effective attenuations could be 6x larger, i.e. nearly 10 dB total equivalent attenuation for CAP (about 1/2 – 2/3 of which would be due to delayed suppression), although without a direct measurement in these conditions this figure must be interpreted with caution. Further complications of binaural stimulation would be that all of the participating MOC neurons will be facilitated (e.g., Liberman 1988b), further increasing their response rate and increasing cochlear suppression; on the other hand, continual background noise in the ipsilateral ear will cause adaptation at the inner hair cell-neural synapse (Fuchs 1996), which depresses CAP responses, but can be 'unmasked' to some extent by the MOC system (Dolan and Nuttal 1988).Eestimating the magnitude of late suppression in awake animals with binaural noise stimulation is too complex to attempt a meaningful computation and requires direct experimental data. What does seem clear is that suppression in these circumstances will be larger, and quite possibly substantially larger, than measured with our paradigm.

II.D.4.b Implications for protection against acoustic injury

Among the various putative functional roles of the MOC system, protection against acoustic overexposure, anti-masking, and dynamic range extension are those most likely to be augmented by sound-induced delayed suppression. As we found that the size of delayed suppression, expressed in terms of equivalent attenuation, is at least as large, or larger, than onset suppression (Figure 15 and Table 2), its impact on cochlear physiology must be considered to be substantial. The role of the MOC system in protection against acoustic injury is well established, both for temporary as well as permanent trauma (Kujawa and Liberman 1997; Rajan 1991; Reiter and Liberman 1995; Zheng et al. 1997). At sufficiently high levels of the traumatizing stimulus, any further increase results in supra-linear increases in threshold shift, from 2 to 9 dB/dB in mice, depending on strain (Yoshida et al. 2000); in guinea pig the growth of PTS with noise level is more difficult to evaluate because inbred strains are not available so that between-animal variability is larger (e.g., Maison and Liberman 2000). Although it is commonly assumed that

MOC effects are most potent at low stimulus levels, this is based on the level dependence of suppression magnitude, which we also found (Figure 13). However, most (if not all) of this decrease in suppression can be explained by the reduction in slope of the I/O function with increasing level (both for CAP and DPOAE, cf. Figure 8 or Figure 14); when expressed as equivalent attenuation, MOC effects are found the be large at mid- and high stimulus levels also (Figure 15); this has been pointed out before (Gifford and Guinan 1987; Guinan and Stankovic 1996). Thus, when considering protective mechanisms, it may more meaningful to consider the effective reduction in input (equivalent attenuation) than reduction in output (suppression magnitude), although this depends on the mechanisms responsible for acoustic trauma, which are not well understood. However, if the input level shift is the correct metric, the MOC system should be considered to be effective in protecting against acoustic overexposure at high levels, and the fact that traumatic exposures are usually of long duration (>2-3 minutes) means that delayed suppression will be fully activated during such exposures (assuming there is no adaptation in awake animals). Characterizing total MOC reflex strength (onset and delayed components) may improve estimates of susceptibility to noise-induced injury relative to using MOC fast suppression only as in Maison and Liberman (2000).

It is not entirely clear whether our data resolve the discrepancy between the established role of the MOC system in reducing noise-induced injury at low and high frequencies (Kujawa and Liberman 1997; Zheng et al. 1997) and the findings that this protection is most likely based on the MOC slow effect (Reiter and Liberman 1995), which is effective at high frequencies only (Sridhar et al. 1995). Our data provide compelling evidence that the gradually increasing cochlear suppression induced by sustained contralateral noise is due to a gradually increasing MOC response rate, which can thus be seen as a gradual strengthening of the MOC fast effect. Additionally, MOC spontaneous rate would be increased also, explaining the gradual recovery of cochlear responses after noise offset. By itself, this increase in MOC fast effect should not increase resistance to acoustic injury, as was found in a study with overexpression of SK2 channels in transgenic mice (Maison et al. 2007a). On the other hand, overexpression of SK2 channels enhances the fast effect because of increased outward K^+ currents across the outer hair cell membrane, *not* because of a greater MOC input; whereas our delayed suppression *is* due to an increased MOC input. If protection results from downstream effects of MOC synaptic input to the outer hair cells (cf. Maison et al. 2007a; Yoshida et al. 2001), MOC delayed suppression might still be able to afford increased protection, perhaps via activation of the MOC slow effect or other downstream phenomena in the outer hair cells. The slow effect scales with MOC response rate (Sridhar et al. 1995), so it is possible that as a result of MOC late suppression, the MOC slow effect is evoked (or enhanced).

II.D.4.c Implications for anti-masking, dynamic range adjustment, and measurements in humans

The MOC system has been shown to increase the response to transient stimuli presented in a background noise, both in terms of response rate of single auditory nerve fibers, as well as CAP responses (Dolan and Nuttal 1988; Kawase et al. 1993; Kawase and Liberman 1993). This effect is thought to arise via a reduction of adaptation at the inner hair cell-neural synapse (Liberman and Guinan 1998). MOC delayed suppression during prolonged masking noise should be considered an effective addition to the fast effect in this role as anti-masking mechanism.

Dynamic range adjustments due to MOC late suppression, combined with the MOC fast effect, could yield a large shift in cochlear I/O functions, and would be effective at low and high

stimulus levels. This may be particularly useful for low-threshold, high-spontaneous rate (SR) auditory nerve fibers, which have relatively small dynamic ranges, on the order of 30 dB (Kiang 1965); high-threshold low-SR typically have much wider dynamic ranges, but would still benefit. Because MOC late suppression works on a slow timescale, it would act to slowly shift the operating point of neural response functions to a regime where they are more sensitive to changes in input level, thereby presumably improving intensity discrimination. Studies in the guinea pig midbrain have shown that principal cells in the inferior colliculus do shift their rate-level functions in response to the level statistics of the stimuli (Dean et al. 2005), and the basis for this ability would appear to commence in the cochlea through the action of the MOC reflex, aided by delayed MOC suppression.

The data presented indicates that sustained noise enhances the responses of MOC neurons and creates a "late suppression" component of cochlear responses in guinea pig; data presented elsewhere appears mostly consistent with our findings (Lima da Costa et al. 1997a). The size of the delayed suppression appears comparable or even larger than the fast suppression, so its functional implications may be of great importance. It would be interesting to investigate whether the effects seen here in the guinea pig also occur in humans. However, the experiments cannot be directly applied to humans due in part to the invasive nature of some of the measurements. Nonetheless, there may be several options that would allow non-invasive assessment of MOC late suppressions in humans. Although gross cochlear potentials (CAP, CM, RW noise) require opening of the middle ear space, otoacoustic emissions are completely non-invasive and are routinely measured in humans. Thus, it appears that this aspect of our paradigm can be directly applied to the human case. The only potential drawback is that DPOAEs are smaller in humans than in rodents, but other types of OAEs may offer suitable data – chiefly stimulus-frequency (SF) OAEs and transient-evoked (TE) OAEs. Both types are routinely measured in humans and can be used to assay MOC activity (Guinan 2006). SFOAEs may be more cumbersome, as they typically require measurement with and without suppressor tone to estimate the OAE component (Guinan 2006), and may not offer sufficient time resolution.

Non-invasive measurement of sound-evoked neural responses in human can be done with auditory brainstem responses (ABR), and can be used to detect efferent modulation of cochlear response (e.g., Sininger and Cone-Wesson 2006). However, compared to CAP, ABR amplitudes are much smaller: about 5 vs. 200-400 μV at high SPL in rodents. In humans, ABRs are measured with scalp electrodes, and are even smaller: Wave V is typically largest, on the order of 0.5 μV, and typically requires between 1000-2000 averages for sufficient signal-to-noise ratio (S.G. Kujawa, personal communication). This makes it unlikely that this is a feasible method to track changes in neural response with a sample time of about 10 s; a further complication is that Wave V is generated in the brainstem and may reflect more complex efferent influences than the CAP. Better results may be obtained by using electrocochleography, which uses a surface electrode closer to the auditory nerve, resulting in larger potentials; this approach has been shown to be able to measure contralateral-sound induced suppression of CAP in humans (Folsom and Owsley 1987).

Summary

We investigated peripheral olivocochlear effects of sustained contralateral broadband noise in anesthetized guinea pig. We found evidence of medial olivocochlear (MOC) effects on two timescales: the classic MOC 'fast effect', followed by a gradually increasing suppression, which we call MOC 'delayed suppression'. This suppression typically takes 2-3 minutes to build up, occurs at all frequencies of guinea pig hearing, and affects distortion product otoacoustic emissions (DPOAEs), compound action potentials (CAPs), and round window noise. In contrast to the MOC "slow effect", which has been reported for sustained shock-evoked MOC activity (Sridhar et al. 1995), MOC delayed suppression does not build up in the outer hair cells but probably reflects central modulation (enhancement) of MOC responsiveness and can be viewed as a gradual increase in the strength of the MOC fast effect. We found that, on average, the magnitude of the late suppression is comparable to that of the MOC fast effect and may have significant implications for the functional roles of the MOC system, such as protection against acoustic trauma, anti-masking, and dynamic range extension.

III Bilateral balancing of cochlear afferent output by the lateral olivocochlear system: Assessing changes in contralateral response after unilateral threshold shift

III.AIntroduction

The olivocochlear efferent system comprises two components, arising in the superior olivary complex and innervating cochlear sensory cells and neurons (for recent reviews, see Guinan 2006; Guinan 1996; Schwartz 1992). It has long been recognized that the medial (MOC) portion can reduce cochlear neural responses (Gifford and Guinan 1987; Wiederhold and Kiang 1970), and more recent insights identify cholinergic transmission to the electromotile outer hair cells as final effectors in this reflex pathway (reviewed in Lustig 2006; Santos-Sacchi 2003). The physiology and function of the lateral (LOC) portion has remained largely obscure, primarily because the LOC axons are thin and unmyelinated, preventing microelectrode recordings to elucidate their response properties and electrical stimulation to study their cochlear effects (Guinan 1996). However, indirect electrical stimulation via the inferior colliculus has shown that LOC neurons are able to enhance or depress compound action potentials (CAP) without affecting outer hair cell responses (Groff and Liberman 2003), consistent with the fact that LOC fibers terminate exclusively in the inner hair cell area (Liberman 1980; Maison et al. 2003a).

The LOC system (with cell bodies in the lateral superior olive, LSO) appears to contain a variety of neurotransmitters, some of which are classically considered inhibitory, such as γ-amino-butyric acid (GABA) and dopamine, and others excitatory, such as acetylcholine (ACh), and there is some evidence for the presence of various peptidergic and opioid neurotransmitters and/or -modulators also (Eybalin 1993). One of the proposed functions of the LOC system is protection of primary afferent neurons against acoustic injury, possibly through the ability of dopamine to reduce afferent discharge rates (d'Aldin et al. 1995; Darrow et al. 2007; Le Prell et al. 2003; Ruel et al. 2006).

Recently, a bilateral model for the LOC system has been proposed (Darrow et al. 2006a; for a more general point of view, see Illing et al. 2000). This model proposes that the LOC system continually monitors afferent discharge from both cochleas, and by integrating these with long time constants, is able to detect long-term differences in average output. By providing feedback to the ipsilateral cochlea, such long-term differences can be reduced, ensuring 'bilateral balance' of cochlear output, which would be important for binaural auditory processes such as sound localization and binaural signal detection. This model was based on findings in mice with unilateral LSO lesions which showed that (i) ipsilateral ABR amplitudes were higher than contralateral ABR amplitudes (implying that LSO feedback has a net negative sign) and (ii) the correspondence of ABR amplitudes between the two ears in these animals was very poor, while they were well matched in intact and sham controls. This model may represent a specific neurophysiological substrate of the behavioral plasticity observed in humans and other animals in sound localization tasks (Kacelnik et al. 2006; Van Wanrooij and Van Opstal 2005).

We aimed to test the bilateral balancing model of the LOC system with a different set of experiments. If the model is correct, then in animals with intact brainstem circuitry,

experimentally induced alterations to the afferent neural discharge of one ear should be matched contralaterally, without affecting contralateral thresholds or outer hair cell function. Accordingly, we used various cohorts of mice separated into treatment and control groups, and measured bilateral ABR and DPOAE input/output (I/O) functions about ten times during 1-2 months. About halfway through this period, we created a reduction in afferent neural discharge on one side, and observed the contralateral responses for the remainder of the experimental duration, and compared those to baseline values. Reductions in ipsilateral neural discharge, varying from mild to severe, were created through threshold shifts, using either high-level sound exposures or lesions creating conductive impairments.

III.BMethods

III.B.1 Animals and experimental manipulations

Four different cohorts of mice were tested; each cohort consisted of a treatment and control group. Controls went through the exact same protocol as treatment animals (i.e., same measurements taken on the same days), except for not receiving the treatment. For each cohort, bilateral ABR and DPOAE I/O functions were measured across a wide frequency and level range. These measurements were obtained 3-4 times over a period of about 2 weeks, constituting the baseline data for that cohort. At that point the treatment group received the unilateral manipulation. Immediately afterwards, and subsequently at approximately logarithmically spaced intervals, bilateral ABR and DPOAE I/O functions were measured as before, 5-6 times until 3-4 weeks post-treatment.

The manipulations for the treatment groups were designed to induce unilateral sensorineural hearing loss in two cohorts (inducing temporary and permanent threshold shift in one cohort each) or a conductive hearing loss in another cohort (tympanic membrane lesion). Another cohort was tested with a low-level non-traumatic stimulus that was used as low exposure level control. Full details regarding the exposures and measurement days for each cohort are given in the *Results* section.

Mice (*Mus musculus*, male and female, CBA/J or CBA/CaJ, Jackson Laboratories) entered the experimental protocol between 6 and 10 weeks of age. No surgery was required except for a small bilateral pinna slit to enable accurate positioning of the acoustic assembly at the ear canal. Animals were anesthetized during recordings using ketamine (100 mg/kg, i.p.) and xylazine (20 mg/kg, i.p). One booster of half the original dose was given halfway through the measurements (after about 45 minutes). In cases where animals were acoustically traumatized, they received a booster immediately after the exposure, followed by the standard recordings. Various cohorts of animals were tested, using different experimental manipulations, described below. Recordings were done in a table-top sound-insulated and electrically shielded chamber, which was heated to a constant 34° C.

III.B.2 Signal generation, acquisition, and stimuli

III.B.2.a Experimental system

All stimulus generation and signal acquisition was achieved digitally using custom software in Labview. D/A and A/D conversion was accomplished in a data acquisition (DAQ) board (National Instruments PCI-6052E) interfaced with a BNC terminal block (National Instruments BNC-2090). Output stimuli (sample rate 200 kHz) were fed through the DAQ, programmable attenuators (TDT-PA5), electrostatic speaker drivers (TDT ED-1) and electrostatic loudspeakers (TDT EC-1). Acoustic signals were recorded with a microphone, pre-amplified by 40 dB (Etymotics Research ER-10C), and fed into the DAQ (sample rate 200 kHz). The microphone was occasionally calibrated using a pistonphone (Bruel & Kjaer 4228) and a dedicated calibration microphone (Bruel & Kjaer 4132); the loudspeakers were calibrated every time they were inserted into an animal's ear canal. Gross potentials were bandpass filtered (300-3000 Hz) and pre-amplified 10,000x (Grass P55) and fed into the DAQ (sample rate 100 kHz). The same hardware was used for measuring both ears.

Acoustic overexposure made use of the same hardware system, except the loudspeakers were replaced by an electrodynamic tweeter (Realistic 40-1377, Radio Shack) capable of delivering up to approximately 130 dB SPL pure tones at 11 kHz (harmonic distortion approximately 40 dB down), driven by a power amplifier (Crown D-75) instead of the electrostatic speaker drivers.

III.B.2.bDPOAEs

DPOAE stimuli consisted of primaries f_1 and f_2; f_2 was set to 5.6, 8.0, 11.3, 16.0, 22.6, 32.0 and 45.6 kHz, and $f_2/f_1 = 1.22$. The f_2 level varied from 10 to 80 dB SPL in steps of 5 dB; the level of $f_1 = f_2 + 10$ dB. Both primaries were gated on and off synchronously and had a duration of 40 ms with no interruption between repetitions (effectively creating a continuous signal of 4 s). The magnitude of the cubic distortion component at $2f_1$-f_2 was computed from the average of 4 microphone spectra, while each spectrum used was the average of 25 waveforms. Sound delivery and pickup were combined in a miniature acoustic assembly that fit into the ear canal of the mouse. Each primary component was fed into separate electronics and loudspeaker to minimize intermodulation distortion in the system hardware. Distortion testing with a coupler indicated that system distortion was negligible up to nearly 80 dB SPL.

III.B.2.cABRs

ABR stimuli consisted of tone pips, measured at the same frequencies as the f_2 primaries in the DPOAE measurements. The stimulus level for I/O functions was varied from 5-25 (depending on frequency) to 80 dB SPL, initially in 5 dB steps, but increasing to 10 dB steps after the ABR amplitude reached a criterion level (0.75 μV peak-to-peak). Repetition rate of the tone pips was 40/s. The duration of the tone pips was 4 ms, with 0.4 ms raised-cosine ramps. Stimuli were presented in opposite-polarity pairs, such that cochlear microphonic could be removed from the ABR waveforms by averaging the responses of the pair. ABRs were averaged from 512 stimulus pairs (reduced to 254 after reaching the criterion level). ABR signals were recorded as the differential between transdermal electrodes placed at the vertex and bulla, using a ground near the tail (electrodes were inserted only during the experiments).

III.B.3Data analysis

III.B.3.aDPOAES

All data analysis was done offline in MatLab. DPOAE I/O functions were used to obtain DPOAE thresholds and suprathreshold response metrics. Threshold was computed as the f_2 level required to obtain a 0 dB SPL $2f_1$-f_2. This f_2 level was obtained by linear interpolation of the I/O function. Suprathreshold response level was extracted directly from the magnitude spectrum of the data.

III.B.3.bABRs

ABR I/O functions were also used to obtain ABR thresholds and suprathreshold response metrics. Threshold at each frequency was obtained by visual inspection of the stacked ABR waveforms (as recorded at successively increasing input levels at fixed frequency). The lowest input level at which any portion of the ABR waveform was discernable was regarded as threshold. Suprathreshold response amplitudes were obtained for the various portions of the ABR waveform. We analyzed the first five clearly identifiable waves of the ABR, and mark these 1 through 5, following conventions for mice (Burkard et al. 2001). The amplitude of each

wave was calculated as the peak-to-peak voltage, by subtracting the immediately following negativity from the wave's positivity (P1-N1 through P5-N5). Identification of the waves and extraction of the P1-5 and N1-5 amplitudes was achieved with semi-automated algorithms. To facilitate comparison with DPOAE, ABR amplitudes were converted to a dB scale expressed re 0.125 μV (the approximate noise floor of the averaged recordings).

The bilateral balancing model (Darrow et al. 2006a) specifies that cochlear afferent output, i.e. average response rates in the auditory nerve, should be matched between both cochleae, but it does not say anything regarding possible changes in brainstem physiology. Wave 1 of the ABR is generated exclusively by the auditory nerve, but later waves reflect activity in various nuclei and cell populations of the brainstem (Melcher et al. 1996; Melcher and Kiang 1996). Thus, with our paradigm we can also track changes in waves 2-5 over time to investigate any possible effects of unilateral changes in cochlear output on brainstem responses; we do so for one of the cohorts presented below.

III.B.3.c Response tracking over time

As we were interested in observing changes over time, both DPOAE and ABR data were plotted as a function of time (in days), separating frequencies into different panels. To facilitate comparison between ipsi- and contralateral responses (including those of controls), as well as ABR vs. DPOAE metrics, we show all data from an experiment in one single figure, e.g. as in Figure 35. The organization of these figures will be illustrated with reference to the examples shown in:

- Organization of axes: the horizontal axis indicates measurement days, where the trauma is set to day 0. Note that the measurement at day 0 was taken immediately *after* the trauma. This is indicated by the dashed vertical line, which is offset to -0.5 days for clarity. Response changes after trauma tend to occur rapidly initially but slower at longer time intervals. To better visualize such changes, the post-trauma time axis is *logarithmic*, while negative (baseline) days (up to and including day 0) are shown on a *linear* scale.
- The horizontal time axis has tick marks at the *exact* days when measurements were taken: due to the small size of the panels, not all days can be indicated with tick mark labels. To aid in the process of extracting the measurement days, the top portion of each figure contains a summary of measurement days during the baseline and post-trauma period, and also indicates the type of trauma induced on day 0, indicated by the dashed vertical line (which coincides in time with the dashed vertical line in the panels).
- ABR and DPOAE thresholds greater than 80 dB SPL and are encoded as either 80 dB SPL for ABR or 85 dB SPL for DPOAE data. We used 80 dB for ABR, because without a higher-level measurement it is difficult to tell whether 80 dB SPL is threshold or not (we use a qualitative visual criterion to determine threshold); however, for DPOAE we use a response level criterion, so that if threshold is not reached at 80 dB SPL, we can be certain that it is higher. To indicate such ceiling effects, upward triangles are placed at the appropriate day, and the accompanying number shows how many ears had supra-threshold ceilings. Indicated thresholds are thus lower-bound estimates of the true thresholds at those days.
- Response levels are indicated at a low (40 dB SPL) and high (70 dB SPL) stimulus level, indicated by a bright (high SPL) or dark (low SPL) shade of the base color (red, blue, or green).

- Noise floor is indicated by crosses in the response level panels. For ABR data, noise floor was estimated as the mean of the P1-N1 output level at the lowest two input levels (typically 2-4 ABR measurements were taken below threshold at any frequency), and the noise floor shown is the grand mean over all measurement days. For DPOAE data, noise floor is extracted as the mean spectral magnitude of 2 Fourier bins immediately above and below $2f_1$-f_2, and is reported as measured at each measurement day.

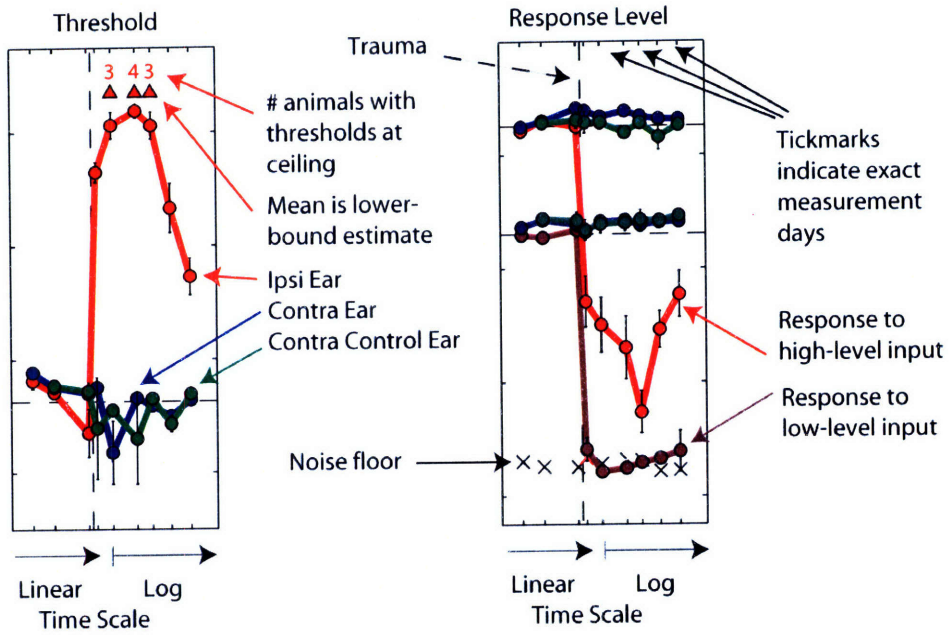

Figure 34. Illustration of DPOAE threshold (left) and response level (right) data as presented in Figure 35 and further (ABR data follow the same format). Each panel shows mean (± s.e.) data from ispilateral (red), contralateral (blue), and contralateral control (green) ears. Organization of panels explained in the text.

III.CResults

Four cohorts of mice were tested for contralateral effects in response to different ipsilateral manipulations. These manipulations consisted of exposures to loud sounds of varying level, producing moderate to minimal permanent threshold shifts, or alternatively a conductive hearing impairment induced by tympanic membrane perforation. One cohort of mice was exposed to low level sounds as a control.

For each of the cohorts presented below, we show ABR and DPOAE thresholds and suprathreshold responses at all 7 frequencies (5.6-45 kHz). DPOAE thresholds and response levels measured at 5.6 kHz are generally uninformative because they are typically at ceiling level or in the noise floor, respectively; at 8 kHz, this is slightly better (in contrast, ABR thresholds and response levels do not suffer from ceiling effects at any frequency). Response variability is generally smallest at the mid-frequencies (11, 16, 22.6 kHz) for both DPOAE and ABR. At 32 and 45.6 kHz, variability increases, likely in part because the small wavelengths at those frequencies (about 10 and 7 mm, respectively) makes calibration of sound pressure level at the eardrum more difficult than at lower frequencies.

III.C.1 Contralateral effects of ipsilateral noise-induced permanent threshold shift

Six CBA/CaJ mice (all female) entered the protocol at 6 weeks of age. Bilateral ABR and DPOAE measurements were taken over the course of about 11 weeks at 10 different days, divided into 3 baseline measurements and 7 post-exposure measurements (at days 0, 1, 2, 4, 8, 16, and 32). At day 0 animals received a pure tone exposure at 11 kHz, 118 dB SPL for 30 min in the right (ipsilateral) ear. A control group of six mice (CBA/J, all female) were measured similarly at a subset of the days the treatment group was measured (4 times over the 11 week period), but was not exposed. Four of the exposed animals sustained permanent threshold shifts (PTS), while the remaining two animals recovered. These two animals were added to the cohort that received a lower-level exposure (Section III.C.2) and will not further be considered in this section. We present an objective method for separating animals from one cohort into distinct subgroups in Appendix III.F.2.

The PTS of the exposed animals (peak of 40-50 dB shifts) led to ABR and DPOAE thresholds of 60 dB SPL or higher, as shown in the top two rows of Figure 35 for the ipsilateral (red) data. The amount of shift in ABR and DPOAE thresholds is approximately the same, which is commonly observed in noise-induced trauma (e.g., Maison et al. 2007a). An interesting feature of the threshold shifts is that at the lower frequencies threshold shift continue to increase over time; at 5.6 kHz, there is no initial threshold shift, but about 25 dB shift at day 4, which then decreases to about 15 dB (the increase at the last measurement is also reflected in the control data, and is probably not related to the exposure). This is only visible in the ABR data, as DPOAEs at 5.6 kHz are not measurable. We return to this issue in the *Discussion*. At mid and high frequencies, the immediate shift remains fairly stable until the final measurement day (32 days post-exposure).

Contralateral thresholds (blue) appear unaffected by the exposure, and are fairly stable over the entire experiment duration. Some changes do occur, e.g. improvements in threshold from day -20 to 0, perhaps a maturation phenomenon; this is also visible in the ipsilateral ears and those of controls (green). In some cases, contralateral thresholds appear to go through a minimum several

days post-exposure, especially for ABR, but this appears to be simply a continuation of what occurred prior to the exposure. The control group in the PTS cohort was not measured in the first few days after the exposure, so we do not know whether threshold of these controls also had a minimum during the same period. Nonetheless, the data show no sign of contralateral threshold changes due to the ipsilateral exposure.

Changes in ipsilateral suprathreshold ABR and DPOAE response levels over time are consistent with the threshold data. The bottom two rows of Figure 35 show ipsi- (shades of red) and contralateral (shades of blue) ABR P1-N1 and DPOAE levels, and contralateral controls (shades of green), for both low (40 dB SPL, dark shade) and high (70 dB SPL, bright shade) stimulus levels. There is a bilateral increase in response prior to the exposure at some frequencies, consistent with the simultaneous decrease in ABR and DPOAE thresholds. Ipsilateral response levels decrease greatly immediately after the exposure, and remain stable thereafter, except at the lowest frequencies, where responses decay slowly after day 0. The decrease is only about 20 dB for the ABR responses, whereas ABR threshold shifts of up to 40 dB occurred; this can be explained by the sub-linear growth of ABR responses with input level (cf. Figure 39 below). The decrease in DPOAE responses is as large as 40 dB, commensurate with the steeper I/O growth functions. Contralateral ABR responses go through a small maximum after the exposure, but as explained above with regard to contralateral thresholds, it is likely not an exposure-related effect. With that in mind, overall post-exposure contralateral responses, both ABR and DPOAE, seem consistent with control data across frequency and post-exposure time. Taken together, neither threshold nor response level data from the PTS cohort indicates marked contralateral effects of a unilateral PTS exposure.

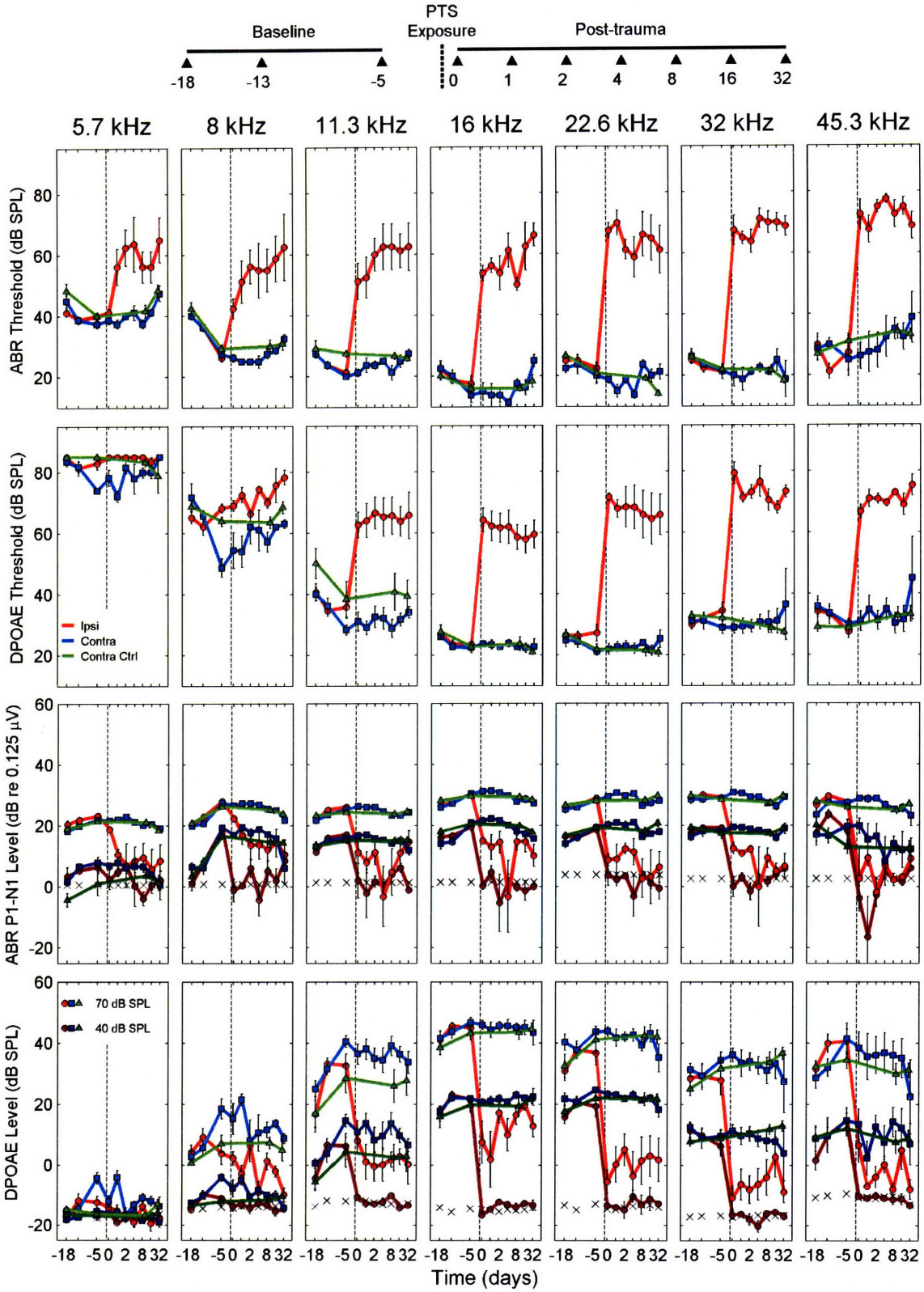

Figure 35. ABR and DPOAE thresholds (upper two rows) and suprathreshold response levels (bottom two rows) for ipsi (red, n=4), contra (blue, n=4), and contra control ears (green, n=6) of the PTS cohort.

III.C.2 Contralateral effects of ipsilateral noise-induced temporary threshold shift

Four CBA/CaJ (all male) entered the protocol at 7 weeks of age. Bilateral ABR and DPOAE measurements were taken over the course of 6 weeks at 9 different days, divided into 4 baseline measurements and 5 post-exposure measurements (at days 0, 2, 4, 8 and 16). At day 0 animals received a pure tone exposure at 11 kHz, 115 dB SPL for 30 min in the right ear. Two animals (both female, CBA/J) from the PTS cohort were added to this TTS cohort because their post-exposure response recovery was very similar (they did not sustain a PTS). These additional animals were measured at all the post-exposure days the TTS cohort was measured, so the data was pooled, yielding a total of six animals for the exposed group in the TTS cohort (the age of the two additional animals at the exposure day was nearly 9 weeks, while the age of the other four animals was more nearly 11 weeks when exposed). Finally, a control group of four mice (CBA/CaJ, all male) were measured in similar fashion at the exact same days as the exposed animals, but were not exposed.

Figure 36 shows ABR and DPOAE thresholds (rows 1 and 2) for ipsilateral (exposed, red), contralateral (blue), and control contralateral (green) ears. Immediately after the exposure, a threshold shift of about 40 dB occurs for both ABR and DPOAE, at 16 kHz and higher (8 and 11.3 kHz show smaller shifts). These recover over the course of the following days, more slowly as frequency increases. Small thresholds shifts (5-10 dB) remain at most frequencies; at 45.6 kHz, thresholds did not appear to have stabilized yet at day 16. Contralateral thresholds do not change by more than a few dB immediately after the exposure (and thus probably unrelated to the exposure), and changes in the subsequent days appear unremarkable. At 22.6 and 32 kHz there is a weak trend for contralateral ABR thresholds to decrease after the exposure, but this can be seen in DPOAE thresholds at 22.6 kHz, too. In any case, mean changes are modest relative to standard errors, and also with respect to control data.

Suprathreshold responses for ABR and DPOAE are shown in rows 3 and 4 of Figure 36, for ipsilateral (exposed, shades of red), contralateral (shades of blue), and contralateral control (shades of green) ears, at low (40 dB SPL, dark shade) and high (70 dB SPL, bright shade) stimulus levels. Ipsilateral responses decrease strongly immediately after exposure (except at the lowest frequencies) – for the lower stimulus level, responses are mostly at the noise floor. ABR responses at the higher stimulus level generally return to (near) baseline levels at day 2, although recovery is slower at the highest frequencies. However, at the lower stimulus level, responses appear to stabilize slightly below baseline levels, consistent with the small PTS seen in the threshold data. This incomplete recovery of response levels appears in the DPOAE data also. Contralateral response levels are not affected immediately after the exposure (or at most by a few dB), nor is there a systematic drift in response in subsequent days, or a marked change with respect to control data. This is the case both for the mid frequencies, where ipsilateral responses recovered rapidly (by day 2) as well as at the higher frequencies, where responses remain depressed for several more days (and at the highest frequency have not yet recovered by day 16). Taken together, neither threshold nor response level data from the TTS cohort indicates marked contralateral effects of a unilateral TTS exposure

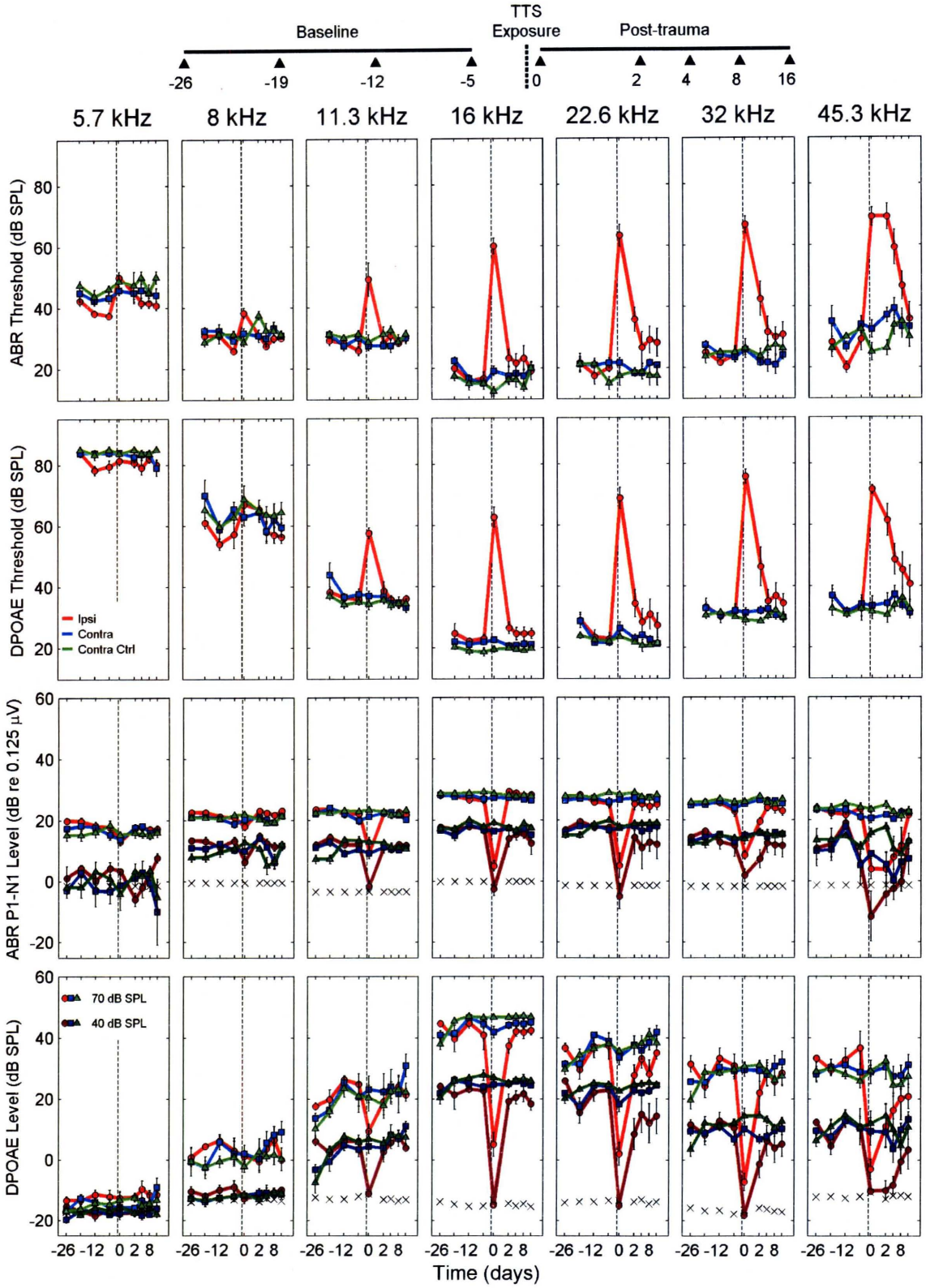

Figure 36. ABR and DPOAE thresholds (top two rows) and response levels (bottom two rows) for ipsi (red, n=6), contra (blue, n=6), and contra control (green, n=4) ears, obtained from the TTS cohort.

III.C.3 Ipsilateral effects of low-level exposures

Nine CBA/J (4 female, 5 male) entered the protocol at 9 weeks of age. Bilateral ABR and DPOAE measurements were taken over the course of about 2.5 weeks at 6 different days, divided into 2 baseline measurement and 4 post-exposure measurements (at days 0, 2, 4, and 8). At day 0 animals received a pure tone exposure at 11 kHz, for 30 min in the right ear at 70 (n=2), 96 (n=3), or 103 dB SPL (n=4). We report ipsilateral thresholds and response levels; contralateral data was generally stable, as was also found for the PTS and TTS exposures reported previously. These exposures were chosen to range from well-below to mildly traumatic levels to obtain an extensive record of cochlear effects of a wide range of exposures, with high time resolution. Two additional animals (both female) were not exposed and served as controls; they were measured at the same days.

Figure 37 shows ipsilateral ABR and DPOAE thresholds (rows 1 and 2) across frequency (columns 1-7) and over time (horizontal axis), for the 3 groups exposed at 70 (yellow), 96 (magenta), and 103 dB SPL (cyan), as well as unexposed controls (green). Thresholds of the 70 dB SPL group do not appear to differ in any systematic way from the control group. On the other hand, the 103 dB SPL group clearly sustained a moderate TTS, which was largest immediately after the exposure, peaking around 16 and 22.6 kHz, where the shift was about 40 dB for both ABR and DPOAE. Thresholds recovered by day 2, or at the latest day 4 at some frequencies. At the intermediate exposure level of 96 dB SPL, a small TTS of about 10 dB for both ABR and DPOAE is apparent at 16 kHz, which resolved by day 2.

The ipsilateral suprathreshold responses measured at 40 (dark shade) and 70 dB SPL (bright shade) stimulus level, shown in Figure 37 (rows 3 and 4), yield similar conclusions. The 70 dB SPL group does not differ meaningfully from controls at any of the data points. In contrast, the 103 dB SPL group shows clearly depressed response levels immediately after the exposure; reductions are greater for DPOAE than ABR, but this is consistent with the much steeper growth function of DPOAE vs. ABR I/O functions. As was the case for the 103 dB SPL group thresholds, response levels return to control values at 2 (or at most 4) days post-exposure. For the intermediate exposure level of 96 dB SPL, the most marked change is a small response depression in DPOAE at 16 kHz, while the ABR response at that frequency does not appear to be affected.

These data show that trauma resulting from pure-tone acoustic overexposure follows a repeatable and predictable pattern as a function of exposure level and post-exposure time. The data is also useful in comparing with contralateral data from the PTS and TTS exposures reported previously: the absence of post-exposure threshold or response level changes in those cases corresponds to the ipsilateral responses shown here with a 70 dB SPL exposure. Apparently, acoustic crosstalk attenuation is sufficient such that ipsilateral sound levels of 110-120 dB SPL are at least well below 96 dB SPL and perhaps around 70 dB SPL.

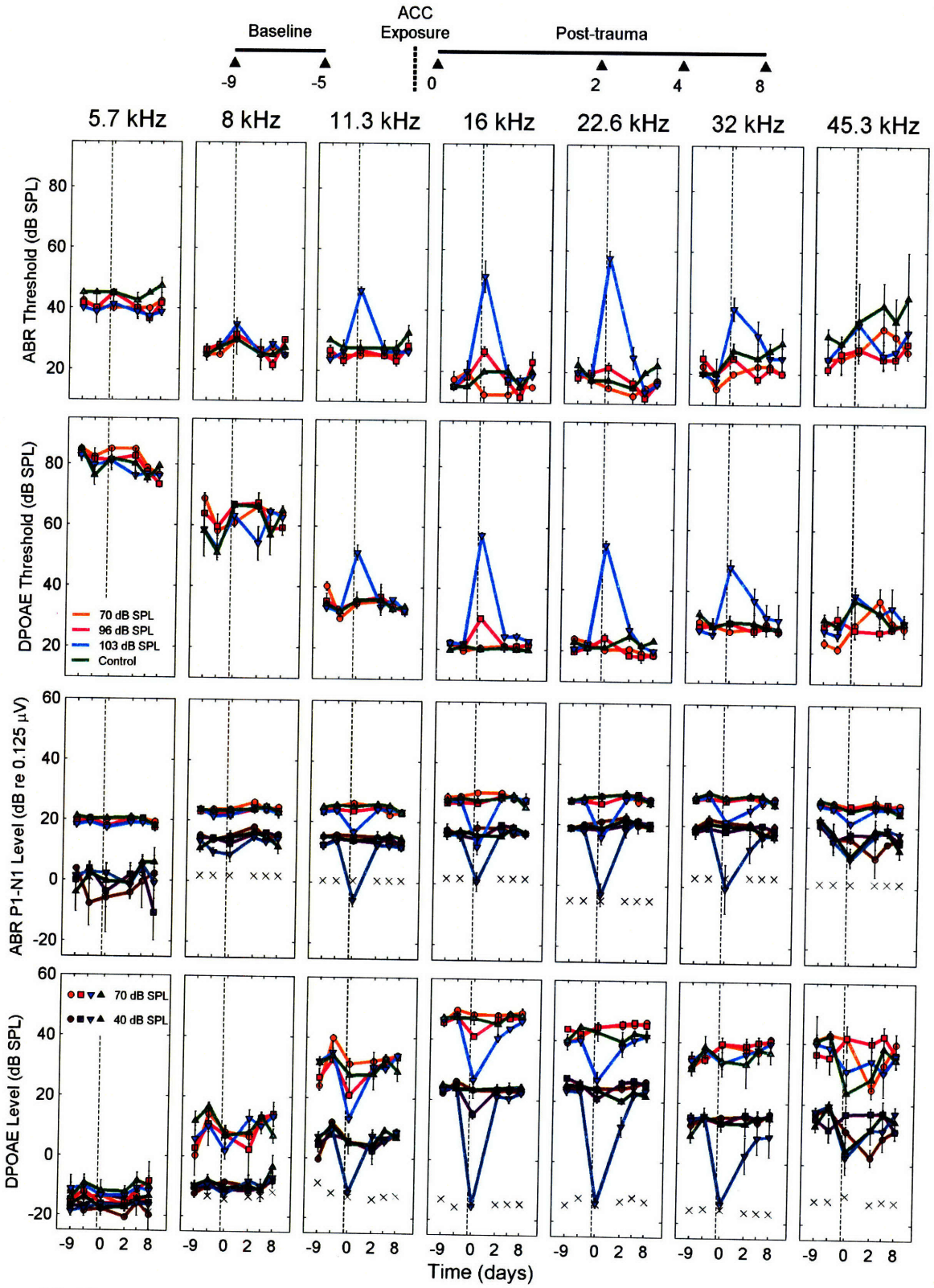

Figure 37. ABR and DPOAE thresholds and suprathreshold response levels for the ipsilateral ears of the ACC cohort; animals were exposed at various levels to probe potential effects of acoustic crossatlk.

III.C.4 Contralateral effects of ipsilateral conductive hearing loss

Four CBA/J mice (all male) entered the protocol at 10 weeks of age. Bilateral ABR and DPOAE measurements were taken over the course of 7 weeks at 9 different days, divided into 3 baseline measurements and 6 post-lesion experiments. At day 0, animals received a lesion to the right tympanic membrane (TM), by making a large perforation with a microknife. We attempted to remove as much of the TM as possible, i.e. the entire portion that was visible from the external ear canal. However, the anatomical configuration prevents easy access to the entire TM, and it is possible that we merely removed a portion the pars flaccida, leaving a substantial remainder. Bilateral ABR and DPOAE measurement were taken immediately after the TM lesion and at logarithmically spaced intervals thereafter (1, 3, 6, 14, and 34 days post-trauma). A control group of four mice (CBA/J, all male) were measured in similar fashion at the exact same days the lesion group was measured (with exception of the first baseline measurement, which was skipped for the controls), but did not receive a TM lesion.

The TM lesion initially caused a moderate amount of ABR threshold shift, as shown in the first row of Figure 38 (red). The shift increased from about 20 to 30 dB as frequency increased from 5.7 to 45.6 kHz, except for a smaller shift of only about 20 dB at 32.0 kHz. The ipsilateral DPOAE threshold shifts were larger (second row, red), about 40 dB, which is expected for a conductive hearing loss, because sound travels twice (forward and backward) through the impaired middle ear (cf. Margolis 2002). At most frequencies thresholds increased by an additional 5-15 dB in the following week. After about 1 week, thresholds decreased, in most cases to below immediately post-lesion values. The recovery appeared largest for the ABR thresholds (although DPOAE threshold recovery was clear also), where at low frequencies thresholds approached baseline values to within about 10-20 dB, while at the highest frequencies final threshold values were still strongly elevated. Contralateral thresholds (blue) show no systematic change immediately after the TM lesion, nor at later times, and remained at values within the range bracketed by control data.

ABR P1-N1 and DPOAE responses are shown in rows 3 and 4 of Figure 38, for ipsilateral (shades of red), contralateral (shades of blue), and contralateral control (shaded of green) ears, at lower (40 dB SPL, dark shade) and higher (70 dB SPL, bright shade) stimulus levels. Ipsilateral levels decrease immediately after the trauma, and in some cases the decrease continues in the first few days post-trauma, for both ABR and DPOAE. At the last few measurement days, responses tend to increase, commensurate with the improvement in thresholds observed before. Contralateral response levels are generally stable throughout the experimental series, and well matched with those from control ears, for both ABR and DPOAE. There are a few large and apparently unexplained changes in response, in particular for DPOAE at 11.3 kHz; we return to this issue later in the *Discussion*.

Post-mortem examination of several animals revealed that the lesioned TMs has healed to varying extents, in some cases apparently quite well (a crust overlaid the outward-facing portion of the TM, presumably being responsible for the threshold elevation that remained at 34 days); in one particularly well-dissected animal, the TM appeared completely normal with no signs of prior lesion (except for a crust overlahying the outer portion of the TM). Evidently, the extent of the lesion, although substantial, was insufficient to create a permanent TM perforation. Visual inspection of the dissected ear canal and bulla revealed that the TM appears to be attached in such a way that it is not entirely accessible from the external ear canal. Thus, it may not be possible to completely remove the TM by simple resection using our approach. It must be expected that most lesions made in this way will recover after 1-2 weeks.

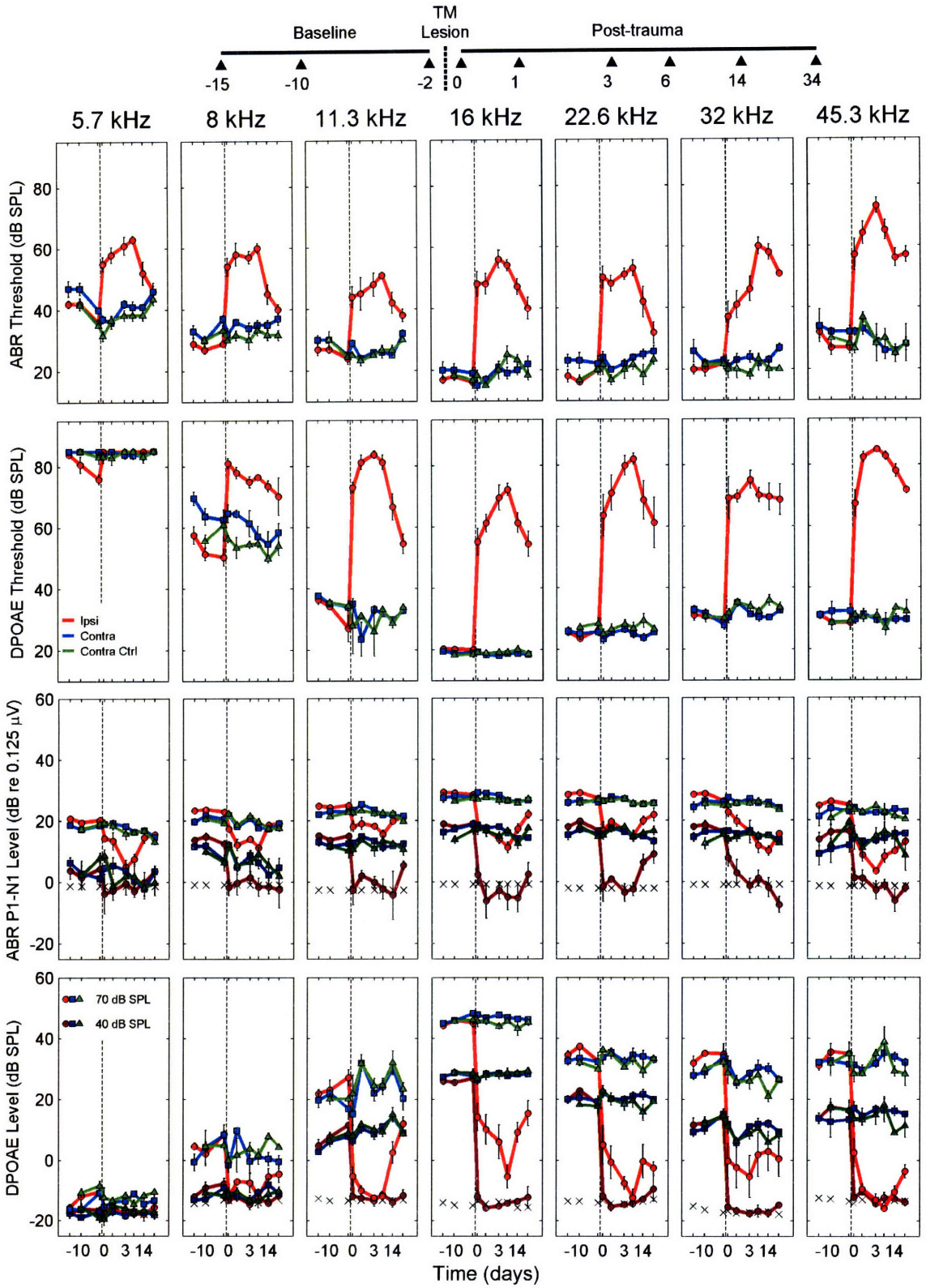

Figure 38. ABR and DPOAE thresholds (top two rows) and response levels (bottom two rows) for ipsi (red, n=5), contra (blue, n=5), and contra control (green, n=3) ears, obtained from the TM cohort.

III.C.5 Analysis of ABR waves 2-5

Whereas wave 1 reflects activity in the auditory nerve only, the other waves in the ABR are generated by various auditory nuclei in the brainstem (Melcher et al. 1996; Melcher and Kiang 1996). It is possible that a disrupted peripheral binaural input is adjusted in one or more of these nuclei, and may be revealed by tracking the amplitudes of these waves as we have done for wave 1 previously. Accordingly, we now present data on the amplitudes of waves 2-5 (computed as P2-N2, P3-N3, P4-N4, and P5-N5).

Figure 39 shows I/O growth functions for each of the ABR waves 1-5 (distinguished by shading) at all measurement frequencies, using data from the contralateral ears from the lesion group of the TM cohort, taken at the last measurement before the TM lesion was made. Growth functions for waves 2-5 are offset vertically in increments of 20 dB for clarity. Typically, the output range for any wave is about 20-25 dB over the measured input range, indicating that the ABR wave growth functions are strongly compressed. The growth functions are somewhat different for the various waves, and also depend on frequency.

The frequency dependence of the ABR wave amplitudes is shown in (using the same data as in Figure 39). The left panel shows wave output levels for 40 dB SPL tone pips, while the right panel shows wave output levels for 70 dB SPL tone pips. In general, error bars are small, indicating that intra-animal variability is modest. Furthermore, wave 1 is largest, at all frequencies, both at low and high input levels. Waves 2 and 4 are next largest and are comparable in magnitude, while waves 3 and 5 are relatively smaller. This is not entirely consistent with rank ordering of ABR wave amplitudes that has been found before for CBA mice (Burkard et al. 2001), but those ABRs were measured with click trains and potentially different recording configurations, which could lead to different waveforms. All five waves are largest at 16 kHz, decreasing towards higher, but especially lower, frequencies.

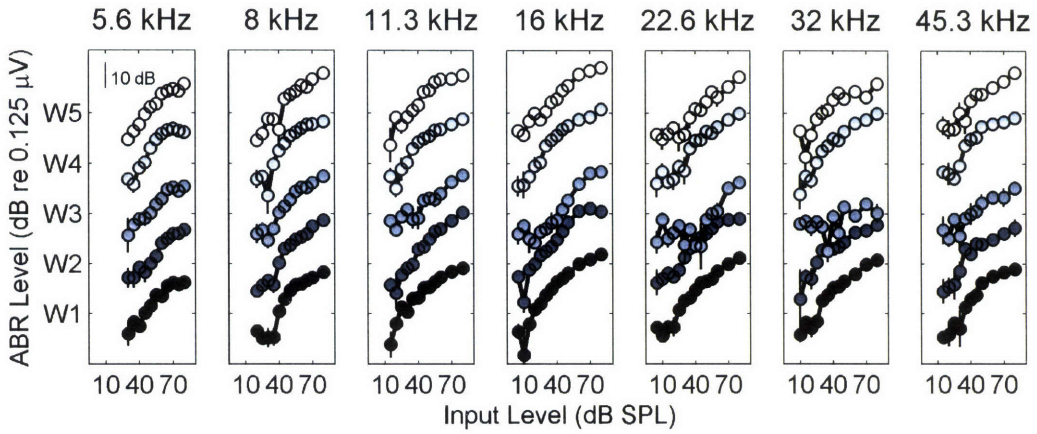

Figure 39. Mean (± s.e.) I/O growth functions for ABR waves 1-5 (indicated by W1-W5) from animals (n=5) in the lesion group of the conductive hearing loss cohort. Data is from the contralateral ear at the last measurement before the TM lesion. Waves 2-5 are offset vertically in increments of 20 dB (vertical scale as indicated by scale bar).

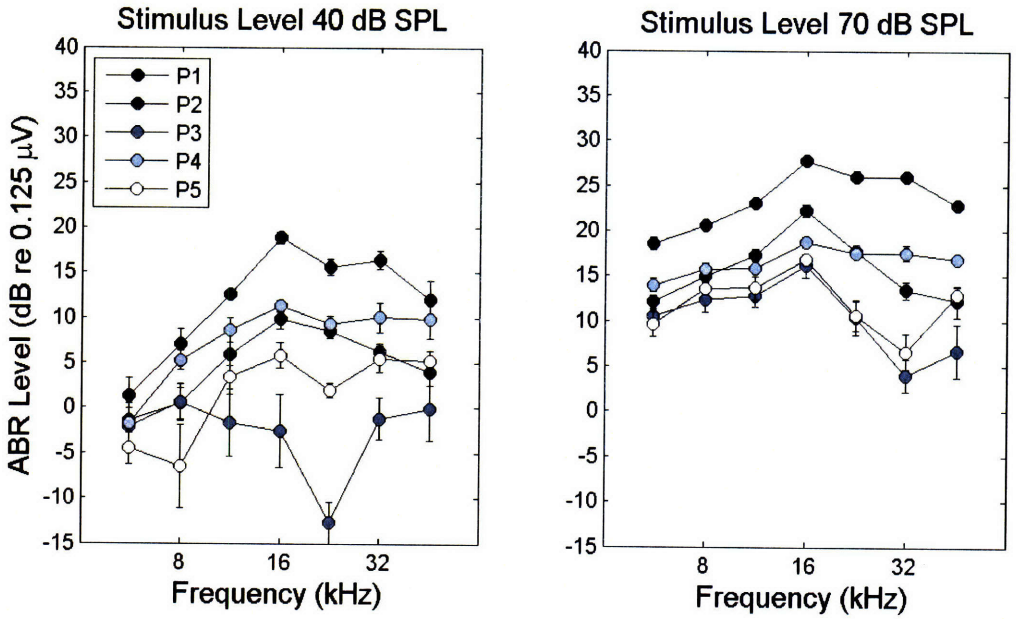

Figure 40. ABR waves 1-5 output mean (± s.e.) levels (dB re 0.125 μV) in response to either 40 dB SPL (left) or 70 dB SPL (right) tone pips, from animals (n=5) in the lesion group of the TM cohort. Data is from the contralateral ear at the last measurement before the TM lesion.

Response levels for waves 2-5 are presented sequentially in rows 1-4 of Figure 41; each rows contains ipsilateral (exposed, shades of red), contralateral (shades of blue), and control contralateral (shades of green) ears, measured at a low (40 dB SPL, dark shade) and high (70 dB SPL, bright shade) stimulus level. Ipsilateral responses show the same pattern for waves 2-5 as for wave 1 (Figure 38): an immediate post-lesion decrease, a further decrease in the first few days, followed by a later recovery. Contralateral response levels do not show a consistent trend across frequency for any of the waves 2-5, even though the ispilateral response patterns are quite consistent across frequency. Also, contralateral control data is within a few dB of the contralateral data at all data points. Although part of this dataset is very noisy and somewhat difficult to interpret, those parts that are measured with high precision do not give any evidence for contralateral changes induced by the TM lesion at day 0.

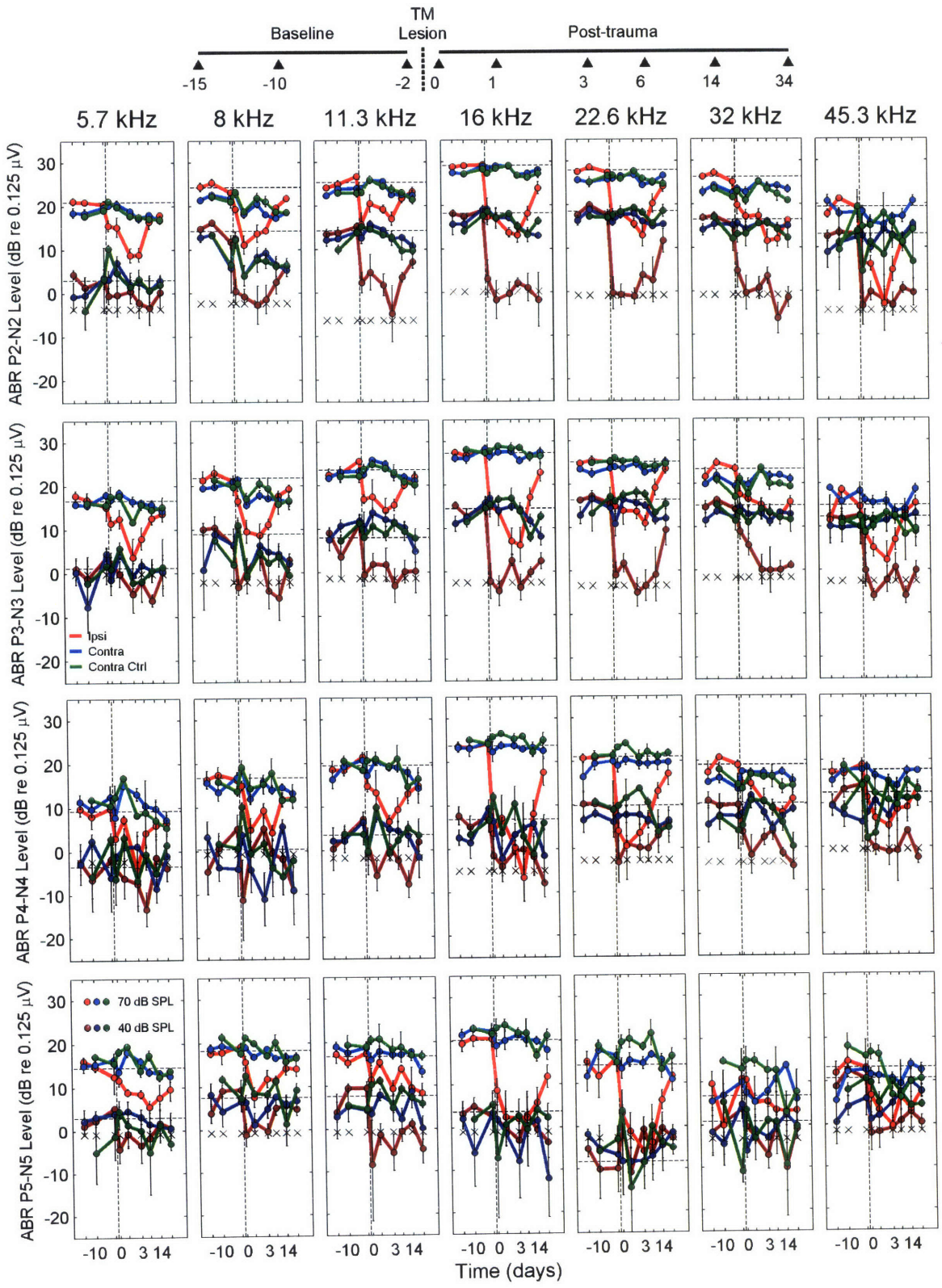

Figure 41. ABR response levels for waves 2-5 (rows 1-4, respectively) for ipsi (red, n=5), contra (blue, n=5), and contra control (green, n=3) ears, obtained from the TM cohort.

III.DDiscussion

We set out to directly test the LOC balancing model (Darrow et al. 2006a) in intact mice by creating unilateral changes in afferent output and observing contralateral ABRs for evidence of decreased amplitudes, as the model predicts. We conducted several series of experiments with separate cohorts of mice, creating unilateral reductions in afferent output in different ways. The overarching finding was that we did not obtain any clear-cut evidence for the expected contralateral neural changes. Below, we first discuss the appropriateness of using our methods for testing the LOC balancing model, and review the results of the various cohorts.

III.D.1 Criteria for evaluating response level data

In order for our experimental paradigm to be able to evaluate the LOC balancing hypothesis, we needed to be able to detect changes over time in contralateral ABR responses following an ipsilateral change. We also needed to exclude that such changes were caused by changes in cochlear amplification; although that would be of interest, the model predicts that ABR response modulation occurs at the inner hair cell/neural level, and is not a downstream effect caused by a change in outer hair cell response. Finally, we needed to verify that any contralateral changes were related to the ipsilateral manipulations, and not variations in chamber temperature, acoustic assembly, experimenter bias in processing ABR waveforms, or other unrelated causes. Thus, response level data needed to be examined at several levels.

1. Comparison of ABR/DPOAE response changes to control ABR/DPOAE changes.
2. Comparison of post-exposure/lesion responses to baseline responses.
3. Comparison of ABR response changes to DPOAE response changes.

We address these issues in turn.

III.D.1.a Use of control animals

The use of control animals is necessary because slow response changes in exposed/lesioned animals could be due to developmental or aging effects; although CBA mice do not suffer from early-onset hearing loss, as far as we know there is no publicly available data on bilateral ABR and DPOAE data measured repeatedly every few days for a period of 1-2 months, in relatively young CBA mice, and therefore we needed to collect this data. For example, contralateral data from the PTS cohort (Figure 35) appeared to show increasing threshold and declining response levels over time, but these were matched by control data. Without these controls, we may have interpreted the change as arising because of the exposure at day 0 and the subsequent ipsilateral hearing loss. Conversely, our data shows some evidence that ABR and DPOAE responses continue to mature in mice after 6 weeks of age (the effect is most clear in Figure 35); this was apparent in the control mice also. Because we measure the same mice many times over a relatively short period of time, repeated handling (or even repeated anesthesia) can also cause stress-induced changes that may affect auditory responses; for example, it has been shown that increased stress levels protect the ear against acoustic overexposure (Wang and Liberman 2002), and there may well be as yet unknown effects on regular ABR and DPOAE responses also. Therefore, we measured the control group mice at the exact same intervals as the exposure/lesion group mice, so that the only difference between these groups was the exposure (or TM lesion) itself. Finally, day-to-day variations in the experimental setup, e.g. temperature, slight changes in

the acoustic assembly or electronic hardware, conditions in the animal care facility, etc., cannot be completely avoided. In many cases seemingly random day-to-day variations in ABR/DPOAE data were exactly matched by control data (e.g., rows 3 and 4 of Figure 38 illustrate this point). These random variations of unknown origin can be subtracted out by analyzing the difference in ABR/DPOAE responses with respect to those of control animals.

The aforemention 'random' variations can, in some cases, be quite large, especially in the DPOAE. A particularly good example is the 11.3 kHz high-level DPOAE response, in the bottom row of Figure 38. The response level goes through a series of very large changes at consecutive measurements. We found that these abrupt changes are due to the characteristics of the DPOAE I/O function, as reproduced in Figure 42. Shown are mean DPOAE I/O functions from the contralateral ears of the lesioned animals (TM cohort) at a subset of the measurement frequencies. As is normal for DPOAE I/O functions, at higher stimulus levels a notch is sometimes present. This notch is particularly deep at 11.3 kHz, and the minimum occurs at 70 dB SPL, which happens to be the stimulus level that is used to track high-level DPOAE and ABR responses. Immediately (+1 hour, red) and 3 days (green) after the lesion, this notch is present, but at an intermediate measurement (+1 day, blue) it is not – leading to a large increase in DPOAE level. These changes correspond exactly to the abrupt changes in DPOAE response at 11.3 kHz in Figure 38, but only at the high stimulus level (the absence of a commensurate large change for the low-level response confirms it is not a global change in level). At 16 kHz, the notch is smaller, and has a minimum at 60 dB SPL, while at 22.6 kHz, the notch is very shallow; in both cases, measurement made at 70 dB SPL are not, or at least much less, sensitive to the notch.

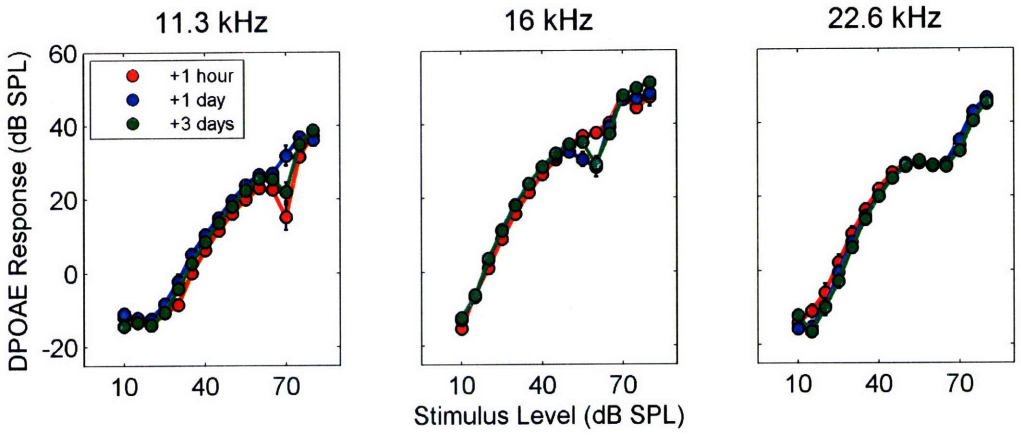

Figure 42. Mean (± s.e.) DPOAE I/O functions measured at three different times in the contralateral ears of the animals (n=5) with ipsilateral TM lesions; corresponds to time series data of Figure 38. At each of these three frequencies, the I/O function has a notch, which is deep at 11.3 kHz, modest at 16 kHz, and shallow at 22.6 kHz. Time series data in Figure 38 tracks the DPOAE response at 70 dB SPL; this is exactly in the notch at 11.3 kHz, but above the notch at other frequencies. This causes DPOAE levels at 70 dB SPL to be more variable at 11.3 kHz relative to the other two frequencies. Measurements are referenced relative to the TM perforation in the legend key.

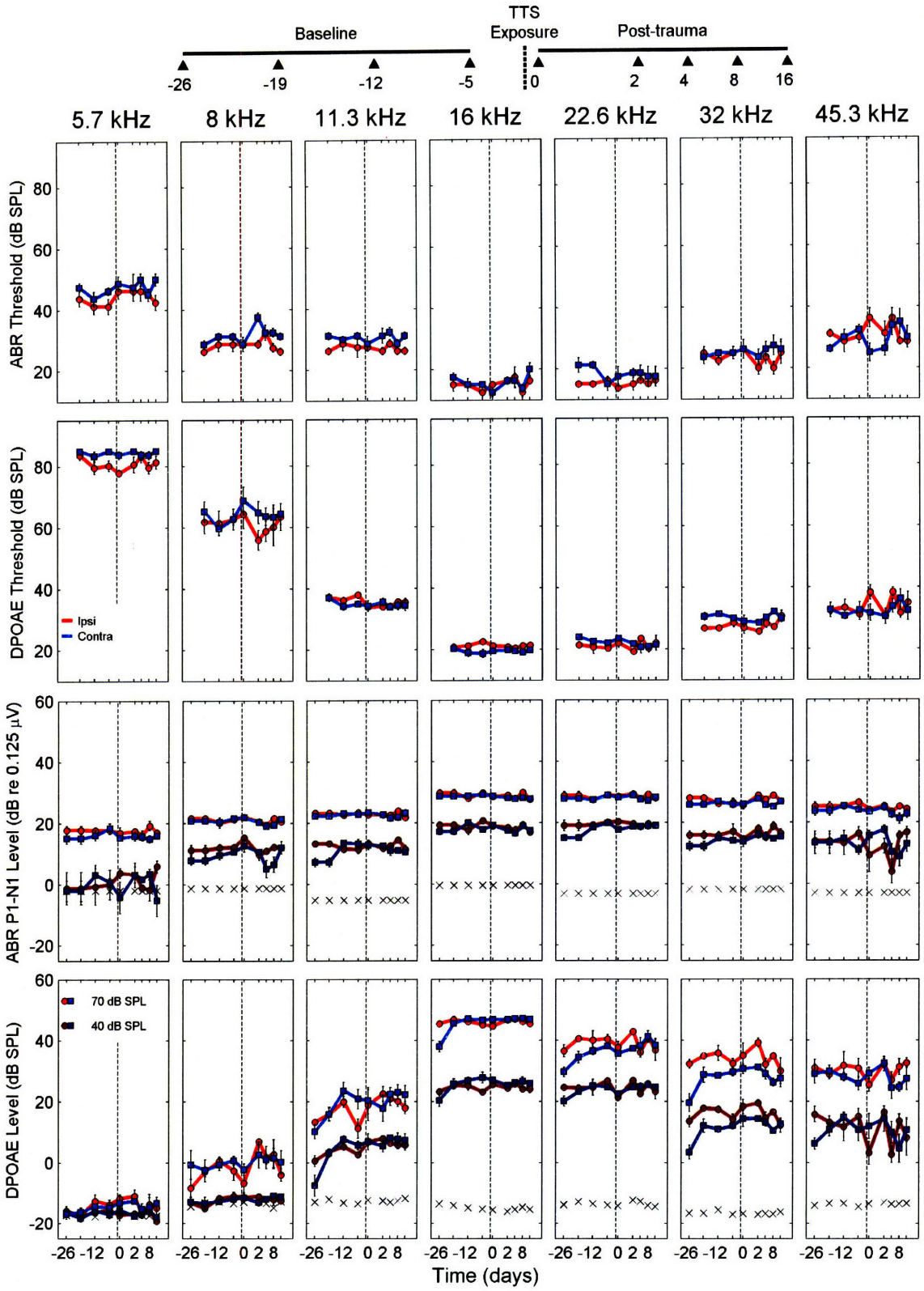

Figure 43. ABR and DPOAE thresholds (top two rows) and response levels (bottom two rows) for ipsi (red, n=4) and contra (blue, n=4) control ears only, obtained from the TTS cohort.

The reason for the change in the notch at 11.3 kHz is unclear; it could be a physiological change in all of the animals, or a change in some part of the equipment, perhaps causing a change in the primaries f_1 and f_2 (microphone and earphone response are both smooth around 16 kHz, though). DPOAEs are sensitive to the frequency ratio, but in particular the level ratio: changes of one dB in one primary (while holding the other constant) can lead to DPOAE response changes of tens of dB when operating near the notch (Kujawa and Liberman 2001; Maison and Liberman 2000).

Another use of control animals is to compare bilateral thresholds and response levels over time. As these animals undergo no manipulations, this data provides a good indication of how well ipsi- and contralateral data is matched over time. Using data obtained from the TTS cohort, it appears that the differences between ipsi- and contralateral thresholds and response level data, shown in Figure 43, are comparable to those between contralateral ears of exposed and control animals, shown in Figure 36. This confirms that the small differences between exposed and control animals that were seen are most likely due to inherent fluctuations in the animals' hearing rather than a systematic difference between exposed and control animals.

III.D.1.bComparison of post-exposure/lesion to baseline data

In the ideal case, baseline data (measured at 3-4 occasions prior to the exposure/lesion) is completely stable, such that post-exposure/lesion changes are easily recognizable. Although mean baseline data was generally quite precise (small error bars) and could be very consistent (e.g., Figure 38), some cases were less stable making it more difficult to assess response level changes later in the series. We unexpectedly found evidence for, what may be, maturation effects (decreasing thresholds, increasing response levels), especially at the low frequencies in mice that were between 6 and 10 weeks of age, see Figure 35. Similar but smaller effects are apparent in another study, but only 16 kHz data was reported (Kujawa and Liberman 2006).This complicated the analysis of post-exposure/lesion changes, because it is less clear what the baseline level is: mean of all baseline data, the last baseline measurement prior to day 0, or an extrapolation of changes seen in the baseline data? None of these methods is very satisfactory. After discovering this effect we attempted to use slightly older mice, although this adds the complication that between the ages of 8-16 weeks CBA mice transition from being susceptible to resistant against acoustic injury (Kujawa and Liberman 2006); using mice in this age range would presumably increase variability in post-exposure data. Overall, relying purely on baseline data to interpret changes in post-exposure/lesion responses appears unwise; rather, one should also rely on control animals.

III.D.1.cComparison of ABR and DPOAE response level changes

The balancing model predicts that contralateral DPOAE thresholds and suprathreshold response levels should not be affected, because the action of the LOC system is thought to exclusively involve the inner hair cell/neural component. However, DPOAE response level changes do occur over time when measuring cohorts of animals for up to 2 months, as can be seen in all figures of the *Results* section. Some of these changes may represent sources of variability that are related to the experimental system rather than underlying changes in the animals' hearing, but some changes may be of physiological origin. Because DPOAEs are generated by outer hair cells, 'upstream' of ABRs, any change in outer hair cell response will necessarily affect responses at the inner hair cell/neural level also, and thus be reflected in ABR

response levels. In those cases, it is useful to assess how much of the ABR change is caused by the DPOAE change vs. a change in afferent transmission alone.

However, we did not find any *systematic* contralateral changes in any of the cohorts, and no marked differences with respect to control data. Therefore, it was not necessary to assess ABR response changes in view of possible DPOAE changes. Nonetheless, potential follow-up studies should be well aware of the above if systematic and marked contralateral changes do occur and need to be quantitatively analyzed. Because ABR input/output (I/O) functions are much shallower than DPOAE I/O functions, changes in DPOAE can appear much larger than those in ABR, even if the equivalent shift in input level are in fact larger for ABR then for DPOAE. In those cases, meaningful comparisons between ABR and DPOAE changes will have to be done based on equivalent shifts in input level, and not on the change in response level. A change in output response can be converted to a shift in input level using methods described previously (Gifford and Guinan 1987).

III.D.2 Experimentally-induced ipsilateral changes

Here we review the nature of the ispilateral threshold and response level changes following loud sound exposures inducing permanent, temporary, or no threshold shifts, as well as following a tympanic membrane (TM) lesion, and their potential implications for proper testing of the LOC balancing model.

III.D.2.a Ipsilateral effects of sound-induced permanent threshold shift

Animals in the permanent threshold shift (PTS) cohort were exposed to a pure tone at 11 kHz at 118 dB SPL for 30 min (see Figure 35). The results were negative in the sense that there was no contralateral reduction in ABR response level to match the exposure-induced reduction at the ipsilateral ear, even though the ipsilateral responses were significantly reduced for a period of 1 month. However, the nature of the ipsilateral response changes in this cohort may have interfered with the 'normal' function of the putative LOC balancing circuit.

First, post-exposure ABR thresholds in the ipsilateral ear were 60 dB SPL or higher at all frequencies that we measured. Animals were kept in standard animal care facilities, which are not quiet, but do not contain many high-level sounds. This may imply that the exposed ear would have rarely received suprathreshold stimulation after the exposure, which means that a portion of the brainstem circuitry was not stimulated. If such sound stimulation is essential for the LOC balancing circuit to function, this may (partially) explain why we did not see a balancing effect in the PTS cohort. Alternatively, near-complete abolition of auditory nerve activity may in certain aspects resemble unilateral cochleotomy, which causes degeneration and specific cellular changes in brainstem nuclei, and similar processes have been shown to occur after severe PTS (Illing et al. 2000).

Second, ABR thresholds at frequencies of 11.3 kHz and lower tended to increase in days after the exposure. This is particularly marked at the lowest frequency (5.6 kHz), which showed no threshold shift at all immediately after the exposure. However, at day 1 about 15 dB threshold shift occurred, and at day 4 mean shifts peaked at about 25 dB, after which some recovery occurred (to about 15 dB shift). The parallel data from DPOAE metrics are difficult to evaluate because low-frequency DPOAEs are very small; the data at 8 kHz is generally consistent with slowly increasing thresholds. The underlying mechanisms for the slow low-frequency threshold shifts are not clear, although some sort of role for oxidative stress-induced apoptosis may be suspected (for a review of oxidative stress in hearing loss, see Henderson et al. 2006). Extensive

histopathological examination of cochlear tissues in noise-exposed (8-16 kHz, 2 hours) CBA mice (Wang et al. 2002b) indicate that intense exposures can result in widespread and permanent pathology of diverse cochlear tissues and structures, including strial shrinkage, mechanical deformation, ligament fibrocyte and outer hair cell loss, and stereocilia loss, collapse, or disarray. At the highest exposure levels, these pathologies can be observed over a wide range of the cochlear spiral, although they are generally more modest in the apex, such that delayed threshold elevations at the 5.6 kHz place are still not well explained; perhaps trauma-induced phenomena from nearby regions somehow spread to the apex also.

In any case, it appears safe to assume that the exposed cochleae were in a severely pathological state, both acutely and chronically, which may interfere with the normal function of the LOC balancing circuit: cellular-molecular and physiological changes in the auditory brainstem, including the superior olive, following cochlear manipulations have been reported (e.g., Illing 2001; Illing et al. 2000; Wang et al. 2002a). Even thought the exact consequences of such changes on the OC system cannot at present be interpreted, it seems clear that the PTS exposure does more than merely decrease cochlear afferent response rate, and may not be the best approach for evaluating the LOC balancing model.

III.D.2.bIpsilateral effects of sound-induced temporary threshold shift

In the temporary threshold shift (TTS) cohort animals were exposed to an 11 kHz pure tone at 115 dB SPL for 30 min (see Figure 36). The ipsilateral responses showed an immediate threshold shift of about 40 dB, which resolved to within 5-10 dB of baseline values at day 2; recovery took longer at the highest frequencies. Response levels showed a similar pattern of a large immediate reduction, followed by near complete recovery at day 2 (or slightly later at the higher frequencies). Response levels remained several dB below baseline values for ABR; the discrepancies were slightly larger for DPOAE. Given the near-complete recovery of hearing in the ipsilateral ear, this kind of exposure may have avoided the lack of acoustic stimulation of the ipsilateral ear post-trauma that we argued could have confounded the test of the balancing model in PTS cohort (due to ABR thresholds being in excess of 60 dB SPL for those animals). Still, contralateral response levels did not decrease to match those of the ipsilateral ears in the days after the exposure. At mid-frequencies, contralateral response levels (and thresholds), especially at the higher stimulus level, were quite stable and had little variance, such that a systematic downward shift should have been noticeable. Thus, the fact the contralateral responses did not balance with ipsilateral responses seems strong evidence against the LOC balancing model prediction.

Regarding noise-induced pathology as discussed with respect to the PTS cohort, it is uncertain to what extent this occurred in the exposed cochleae of the TTS cohort. Although the TTS exposure was only 3 dB lower than for the PTS cohort, noise exposures over a range of levels indicates that some cochlear tissues appear to have a critical point where chronic trauma transitions from modest to severe over a very small range of exposure levels (Wang et al. 2002b). The latter include hair cells (particularly outer hair cells, but also inner hair cell stereocilia) and limbus fibrocytes; such 'transition regions' are also apparent for acute trauma of the stria vascularis (acute swelling followed by chronic shrinkage), collapse of the space of Nuel, and reticular lamina rupture. It is possible that our PTS and TTS exposures straddled the transition region for any or several of these cochlear structures, possibly explaining the large difference in permanent threshold shift observed between the two cohorts.

For exposures at lower levels, as would occur at the contralateral ear of unilaterally exposed animals due to crosstalk, no TTS was observed (this was true also in the PTS cohort). This was consistent with findings from a control cohort that was exposed unilaterally at levels (70-103 dB SPL) in a range bracketing the level estimated to occur at the contralateral ears of the PTS/TTS cohorts (80-85 dB SPL). These findings are presented in detail in Appendix III.F.1.

III.D.2.c Ipsilateral effects of conductive hearing loss

For this cohort a different approach was used to induce afferent response reduction. This avoided any direct cochlear trauma by creating a conductive impairment by means of a tympanic membrane (TM) perforation (see Figure 38). A TM perforation decreases the pressure difference across the TM, resulting in reduced ossicular coupling to the cochlea and a conductive hearing loss, especially at low frequencies, the severity of which depends strongly on the size of the TM perforation (in rat, Bigelow et al. 1996; and in human, Mehta et al. 2006; Merchant and Rosowski 2003; Voss et al. 2001). Using the 20-30 dB threshold shifts, compared to air-bone gap data from humans (Mehta et al. 2006; Merchant and Rosowski 2003), it appears likely that no more than 50% of the TM was removed. A curious pattern in the frequency dependence of the thresholds shift in these animals was that it increased with frequency, opposite to the pattern normally observed, which may indicate a small amount of cochlear trauma.

Thresholds tended to increase over the course of the subsequent week (more at higher frequencies), perhaps due to accumulation of debris or crusts in the middle ear, after which they decreased (i.e. hearing recovered) in the final weeks of this cohort. We found that the late improvement was due to healing of the lesion in the TM. Still, for about one week modest ABR shifts of 20-30 dB existed, which should have been ample time for the LOC balancing circuit to function. This manipulation created a pure attenuation of incoming sounds, and should be eminently suitable for testing the LOC balancing model. Contralateral responses showed no marked changes after the TM lesion; although at some frequencies gentle downwards trends were visible, these were quite small and overall similar trends were observed in data from control animals. The conclusion must be that moderate attenuations in input sound level unilaterally cause no changes in threshold or response level in the contralateral ear.

III.D.3 Revisiting the LOC balancing model

The original LOC balancing model was based on the fact that the observations from ABR wave 1 could be explained completely by the loss of ipsilateral LOC neurons. However, the lesions employed affected more than just the LOC cells, which may have impacted the physiological effects. Also, the LOC balancing model does not make explicit predictions about contralateral thresholds, while in our experiments such as ours, it may be informative to analyze changes in thresholds also. Below we discuss possible implication of the LOC balancing model for contralateral thresholds, after reviewing the LSO lesions and their possible implications.

III.D.3.a Physio-anatomical basis for the LOC balancing model

The LOC balancing model was derived from neuroanatomical lesions and concomitant physiological response data (Darrow et al. 2006a). The lesions 'selectively' targeted the LSO on one side of the brainstem only by injection of a melittin (see also Le Prell et al. 2003), a membrane-active lytic peptide that is the principal toxic component of bee venom (for a review, see Raghuraman and Chattopadhyay 2007). In neural tissue, both cell bodies *and* axons are lesioned, which may be significant as the balancing model strictly only assumes the LOC cells,

their efferent projections to the cochlea, and the ipsilateral trapezoid body are lesioned. However, in addition, LSO principal cells would be affected, and although their efferent projections (to the inferior colliculus) do not appear to play a role in the feedback loop to the cochleae, there is a potential for unexpected consequences. Perhaps more important is the question of whether axons of passage, disrupted by the mellitin, altered some important aspect of the brainstem circuitry that was relevant in Darrow et al.'s experiments. For example, some of the LSO lesions encroached upon, and probably lesioned, the trapezoid body, which contains axons from the ipsilateral cochlear nucleus to the contralateral superior olivary complex (which contains the LSO). If true, those animals had no functionally intact LSO left: the ipsilateral one was lesioned completely, while the contralateral one was deprived a substantial portion of its normal input. Perhaps the LSO lesions also destroyed other axons of passage of some importance.

III.D.3.bThreshold changes in the LOC balancing model

In view of testing the bilateral balancing model, we are most interested in suprathreshold responses. However, our data sets contain detailed information about thresholds also, so it is interesting to consider how thresholds may be affected by a putative balancing circuit. The balancing model makes no explicit prediction about thresholds, and without knowing much about LOC physiology, it is hard to make predictions. If we assume LOC fibers titrate neural excitability up or down by a fixed percentage independent of rate, this would amount to a fixed upward or downward dB shift of the ABR I/O function (Darrow et al. 2006a; Groff and Liberman 2003; Le Prell et al. 2005; Le Prell et al. 2003; Maison et al. 2003b; Ruel et al. 2001). ABR thresholds are usually determined by visual inspection of waveforms, and such a threshold criterion may be relatively insensitive to modest changes in waveform amplitude. From this point of view, we would expect to see at most modest ABR threshold changes in response to LOC-induced contralateral effects.

However, the visual inspection method is chosen because of poor signal-to-noise ratios of low-level ABR measurements, and is artificial, considering that the high noise levels of the measurements do not reflect noisy activity from within the auditory pathway, but represent general brain activity (and myogenic noise also) that is uncorrelated with the auditory stimulus. Thus, this noise is not 'visible' to the auditory system, so we can theoretically consider how to define ABR threshold if there was no extrinsic noise. If a response level criterion would be used, as is usual for compound action potentials, LOC-induced threshold changes could in fact be quite large, because the threshold change is approximately given by $-\Delta L/r$, where ΔL is the I/O function output shift (up or down), and r is the slope of the ABR I/O function (in dB/dB). Our data indicates r is roughly 1 around threshold levels (see Figure 39), although near threshold the slope is difficult to estimate, so a safe estimate for the range of possible values is probably 0.5 – 1.5. In that case, the threshold change may be as large as $-0.7 \times \Delta L$ to $-2 \times \Delta L$. Adjusting for a modest 5 dB decrease in long-term afferent output at one cochlea, would, if matched at the contralateral side, lead to an ABR threshold *increase* in the range of 3.5 to 10 dB!

This realization raises the question whether the LOC bilateral balancing model make sense from a neuroethological point of view: certainly the benefits of fine-tuning cochlear long-term output bilaterally are lost if this results in large changes in sensitivity (which could be losses or gains, depending on the sign of the contralateral output change). The situation may not be as bad as it seems: true ABR slopes near threshold may be larger than we estimated from the noisy data, which, if true, would lead to smaller ABR threshold changes. CAP I/O functions (which may be better for characterizing auditory nerve responses) are steeper than ABR near threshold, which

would tend to limit the change in threshold due to a response level change. Finally, a fixed response criterion is hardly realistic from an information-theoretic point of view. There are various views on how low-level signals induce detectable changes in activity from background, i.e. what an appropriate definition of threshold is (Geisler et al. 1985; Meddis 2006) and it is possible that LOC-induced changes in neural rate have only modest effects on sensitivity to near-threshold sounds. Finally, behavioral thresholds may not be simply related to commonly used measures or physiological threshold. However, with the above in mind, it may be worth while revisiting the LOC balancing model in view of its effect on cochlear thresholds.

III.D.4 Bilateral balancing and the role of the LOC system

The original findings of (Darrow et al. 2006a) were consistent with their LOC balancing model; however, an independent test presented here disagrees with the model's prediction. An essential difference between these studies was the fact that the model was based on findings with one lesioned LSO (and the other LSO possibly deprived of a substantial portion of its input), while our test was with two intact LSOs.

One possibility is that bilateral balancing occurs at a different level, i.e. not at the auditory nerve: possibly within the LSO itself, in the principal cells that receive excitatory and inhibitory inputs from both cochlear nuclei (for reviews of SOC anatomy and physiology, see Irvine 1992; Schwartz 1992). However, other possibilities exist: response plasticity in the auditory cortex is well established (for recent reviews, see Dahmen and King 2007; Jääskeläinen et al. 2007), but has been reported in the brainstem also (Kandler and Gillespie 2005), and the SOC appears plastic in diverse ways in response to changes in cochlear output (Illing et al. 2000). There is little reason to *a priori* exclude any portion of the auditory system for contributing in some form to 'bilateral balancing'. What data we have from the brainstem seems to exclude a marked role for the main cellular generators of the ABR (Melcher et al. 1996; Melcher and Kiang 1996). Evidence from behavioral experiments with animals seems to indicate that some form of active behavior aids recovery of binaural processing after unilateral disruption (Bergan et al. 2005; Kacelnik et al. 2006), and that a functional primary auditory cortex with intact descending projections is critical to this capability (King et al. 2007). We have no behavioral data from our animals, so we do not know whether any of the cohorts would have shown improvements in binaural *perception* after the unilateral manipulations similar to those described in the cited works. Lacking this information, we cannot be certain whether the lack of a contralateral change in ABR might correlate with a lack of behavioral binaural performance, or whether physiological balancing occurs at a different level.

Our data provides strong evidence that bilateral balancing does not occur at the level of the auditory nerve; because the auditory nerve (and inner hair cells) is the only known target of the LOC system, its balancing role should thus be questionable. Instead, the lack of correspondence in bilateral ABR amplitudes in (Darrow et al. 2006a) may have been caused by the general disorderly state of the LOC innervation in both cochleae: the ipsilateral cochlea had degenerated TH-positive nerve terminals, while the contralateral cochlea, while intact, may have had a functionally impaired LOC innervation because of the trapezoid body lesions that could have interrupted inputs to the contralateral LOC. If true, an intact LOC system may serve some role in cochlear homeostasis that does not extend to an explicit balancing of bilateral long-term output from the auditory nerve.

III.E Summary

We investigated the LOC bilateral balancing model, which proposes that the LOC system acts to balance long-term average neural output from both cochleae, which would be important for binaural processing of sounds. For this, we tested various cohorts of mice by repeatedly measuring bilateral auditory brainstem responses (ABR) and distortion product otoacoustic emissions (DPOAE) growth functions across a wide range of frequencies and levels for a period of 1-2 months. About halfway through the period, a unilateral reduction in neural output was created, either by acoustic overexposure or conductive impairment. Although the LOC balancing model predicts that the unilateral reduction in neural output should be matched contralaterally, we found no evidence for short-term or long-term efferent-induced contralateral response changes in any of the cohorts. Neither did contralateral cochlear gain change (as measured by DPOAE), nor was there evidence of LOC-induced modulation (as measured by ABR changes in the absence of DPOAE changes). In view of these results, a revision of the LOC bilateral balancing model is called for.

III.F Appendices

III.F.1 Crosstalk

During a traumatic unilateral exposure, a portion of the sound will reach the contralateral ear, and because of high levels involved, this crosstalk component could be fairly high. It is possible that this crosstalk directly affects contralateral cochlear responses, which would confound the interpretation of experimental data investigating efferent effects arising as a result of the ipsilateral cochlear changes. Such effects might be threshold increases, in case of trauma, or threshold *decreases*, if the crosstalk acts as a 'conditioning' stimulus. Such effects on cochlear thresholds, as well as increases in suprathreshold responses, have been reported in guinea pig (Kujawa and Liberman 2006), although in that protocol the conditioning stimulus was an octave band of noise for 6 hours daily over a period of 10 days.

To investigate the direct effects of acoustic crosstalk on contralateral responses, we first measured the amount of crosstalk in mice at 11 kHz, and then unilaterally exposed another cohort with the sound level *expected to occur at the contralateral ear canal* of the cohorts that were traumatized in the main experiments. We then tracked bilateral ABR and DPOAE responses in this cohort to asses any exposure-related changes, and we included a group of control animals that were measured at all days but which did not receive an exposure. This group of animals will be referred to as the acoustic crosstalk control cohort.

III.F.1.a Estimation of acoustic crosstalk

The most straightforward method to measure crosstalk would be by placing a microphone in the one ear canal and directly recording the sound pressure level with the acoustic system in the contralateral ear. However, this may obstruct the normal passage of sound, given the small size of the mouse ear canal, leading to incorrect estimates. Also, this method may not be sensitive to bone-conducted sound or sound transmitted via the experimental assembly. Thus, we measured cochlear responses in the contralateral ear via cochlear microphonic (CM), which leaves the ear canal open, and should be sensitive to any of the possible sound transmission pathways; access to the round window is obtained via a dorsal approach. The opened bulla may affect our estimates, but is unavoidable.

CM is measured by an electrode on the round window using otherwise similar approaches and the same hardware as described for ABR in *Methods*; the only critical difference is that the CM waveform is obtained by subtracting electrode signals from opposite-polarity tone pips (ABR waveforms use the averaged electrode signals). The amplitude of the CM at the stimulus frequency was computed by Fourier transform of the resulting signal and extracting the stimulus frequency component. Amplitude was then converted to a dB scale (arbitrary reference).

Crosstalk was measured at 11 kHz (the frequency used for acoustic overexposure) by recording CM input/output (I/O) growth functions unilaterally. First, the I/O function was measured with the acoustic system in the ipsilateral ear (the ear with the round window electrode), followed by the same measurement with the acoustic system in the contralateral ear. The latter I/O function will be shifted towards higher sound levels: the amount of shift is the estimate for crosstalk attenuation. Figure 44 shows both I/O functions, and indicates a shift of 33 dB. A potential artifact to the CM measurement can result from electromagnetic radiation from the experimental apparatus being picked up by the round window electrode, or CM generated in the contralateral ear; the strength of these interference effects from the equipment

was estimated by clamping the sound delivery tubes mechanically and repeating the measurement with the sound system in the ipsilateral ear. This showed that equipment interference was at least 45 dB lower than the ipsilateral CM signal component; however, interference from contralateral CM cannot easily be measured. Therefore, the 33 dB shift should be regarded as a lower bound estimate for crosstalk attenuation, as it may reflect contralateral CM instead.

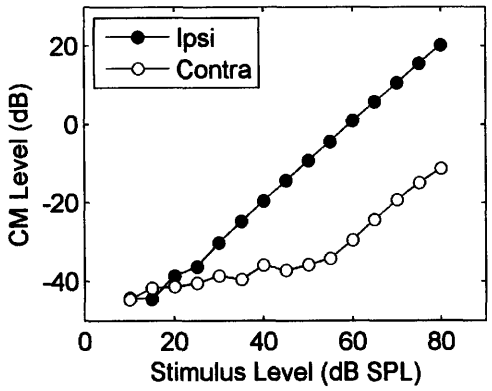

Figure 44. CM I/O functions in response to 11 kHz tone pips, measured with the acoustic system ipsilateral (filled symbols) and contralateral (open symbols). The latter I/O function is shifted rightward by 33 dB, providing an estimate of acoustic crosstalk attenuation at 11 kHz. Data from EL76.

III.F.2 Clustering of animals using DPOAE thresholds

In the PTS cohort (overexposure at 118 dB SPL), exposed animals had different degrees of recovery after the exposure at day 0, varying from essentially none to substantial threshold recovery. A hierarchical clustering algorithm (implemented in MATLAB) was used to analyze whether distinct subgroups in the data could be recognized. If true, subgroups should be analyzed separately. Although the subgroups of the 6 exposed animals in the PTS cohort were fairly obvious, this method should also be useful in other contexts, which is why we briefly describe it here.

The clustering method uses the ipsilateral DPOAE thresholds to assess pair-wise dissimilarity between animals, using a Euclidean distance metric between all pairs of animals (data from each ear was a 7-dimensional vector containing the DPOAE thresholds across frequency). Then, starting with each ear as its own cluster, the dissimilarities were used to iteratively build up a linkage tree by joining two clusters at each step, so as to minimize the increase of within-cluster sum-of-squares (measured with respect to the new cluster median vector); this is also known as Ward's linkage (for a review, see Aldenderfer and Blashfield 1984). When the linkage tree is complete (ending with all data in one group), a decision has to be made regarding how many clusters to form (because our clustering method is hierarchical, it is possible to choose any number of clusters). We used the percentage-of-variance explained in DPOAE and ABR threshold data to determine the appropriate number of clusters.

Accordingly, the cluster analysis indicated that subdividing the 6 exposed animals into two clusters explained about 65% of the overall variance in the DPOAE threshold data (59% when using the same clusters for the ABR thresholds); further increase in number of clusters did not raise variance explained by a useful amount. Of the resulting clusters, one consisted of 2 animals that recovered significantly from the initial trauma, whereas the other cluster of 4 animals

sustained a permanent thresholds shift, as shown in Figure 45. This clustering was consistent at most of the post-trauma measurements. For subsequent analysis in the PTS cohort, the 2 animals that recovered were not further considered, but were included in the TTS cohort.

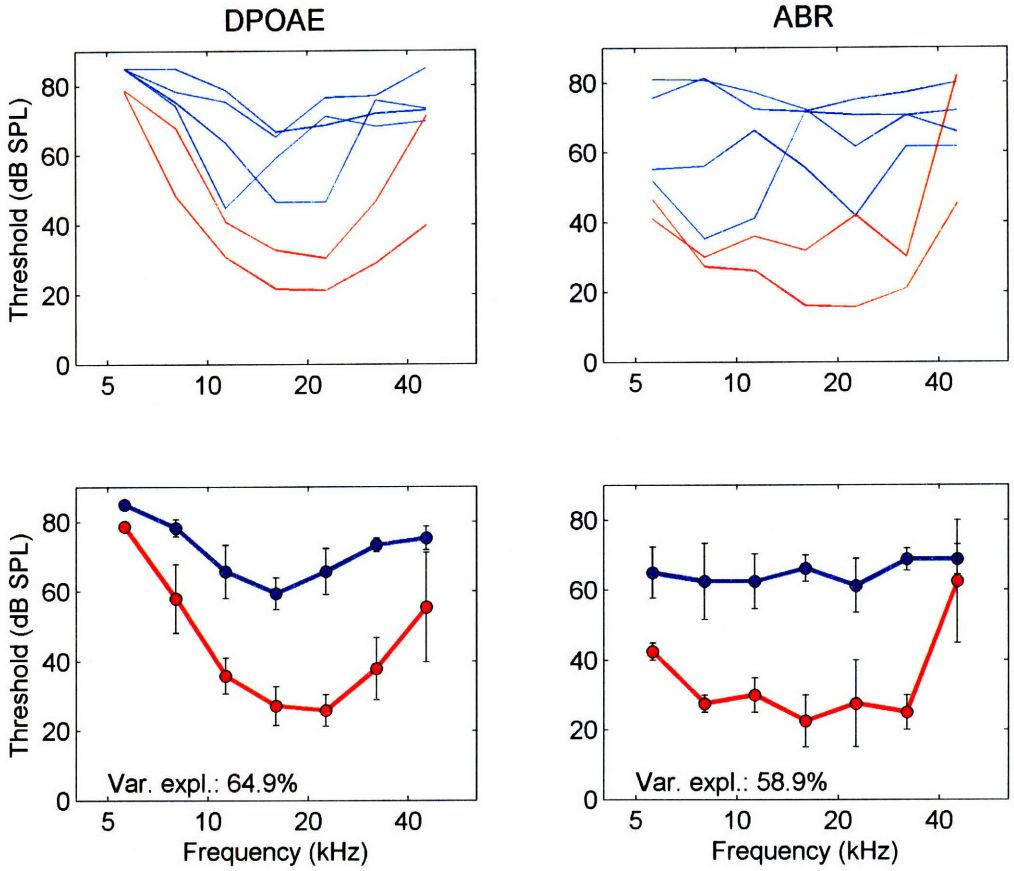

Figure 45. DPOAE (left) and ABR (right) threshold data from the PTS cohort (exposed animals) at post-trauma day 32. Individual thresholds (top) are input to a clustering algorithm which yields two natural clusters (blue vs. red) in the data. Averaging (bottom) the thresholds per cluster rather than for all ears together explains the overall variance by about 60% for both DPOAE and ABR thresholds.

IV Acknowledgments

In working through my PhD years at the Eaton-Peabody Laboratory, I've had help in many ways from many people, without which the end result would have been much worse, and the process far less enjoyable. I'd like to start thanking my supervisor, Charlie Liberman, for his guidance and support while I was in his lab. It has been a privilege to learn from and work alongside such an outstanding researcher who has made so many lasting contributions to hearing science. Mostly, I appreciate the time he made available to me, being receptive to my suggestions for changes in the experiments or directions of my projects, and allowing me a great deal of freedom while always ensuring I stayed on track; offering the right advice at the right moments, including troubleshooting the equipment or the animals. He encouraged the students (or at least seemed to) have fun at all times, as long as we were productive and serious about our work: this was a great environment to work in. The NIDCD provided financial support.

I also want to thank my thesis committee members: John Guinan, Chris Brown, and Doug Vetter. They invested their time in guiding my research at our committee meetings, and were always available to discuss any ideas or questions I had, or pointing out papers that I hadn't heard about. This same group also formed my 'proposal advisory committee' and oral qualifying exam committee, seeing me through the PhD almost from start to end. Beside my committee members, I also enjoyed and am grateful for the interactions and advice I received on multiple occasions from other faculty members, in particular Joe Adams, John Rosowski, Chris Shera, and Sharon Kujawa. Sharon was very generous in letting me use her table-top recording chamber for the mouse experiments, in some cases daily without interruption for several weeks.

Technical support from the EPL engineers Ishmael Stefanov, Chris Scarpino, and Frank Cardarelli was invaluable in keeping the equipment and software sane, and designed and built new ones if necessary. Haobing Wang and Brad Buran designed the software for the ABR peak analysis, which saved me the effort and speeded my analysis of that data. Connie Miller kept the lab afloat and stocked all the supplies without which none of this work could have been done, and Leslie Dodds taught me the guinea pig surgery. Dianna Sands deserves special mention for tirelessly working through loads of paperwork that go along with running a lab; she knew the answer to every question I had, as long as it wasn't technical, and could always be relied upon to brighten up any morning, no matter how early.

I enjoyed getting to know and work with the students (and residents) at EPL, and those in my SHBT class, and even more so for sharing good times outside of the lab, ranging from oysters after work to backpacking in the White Mountains. My labmates made the long hours enjoyable: Keith, Brad, Adam, Mina, Nicola, Sam, Harrison, Ann, Meritxell, and Stéphane; Sudeep taught me many ENT secrets. My classmates, even if in other labs, were always nearby on shbt2004@mit.edu. Naomi, Ann, Adam, and Ronit surprised and delighted me with an olivocochlear cake after my defense.

Finally, I want to thank Jeannie, who patiently supported me through the long years of graduate school, earning our bread and butter while I was playing with mice and guinea pigs. Without this support I wouldn't have been able to complete the PhD, and I dedicate this thesis work to her.

V List of references

Aldenderfer MS, and Blashfield RK. *Cluster Analysis*. Sage University, 1984.

Avan P, Loth D, Menguy C, and Teyssou M. Hypothetical roles of middle ear muscles in the guinea pig. *Hear Res* 59: 59-69, 1992.

Backus BC, and Guinan JJ. Time-course of the human medial olivocochlear reflex. *J Acoust Soc Am* 119: 2889-2904, 2006.

Bergan JF, Ro P, Ro D, and Knudsen EI. Hunting Increases Adaptive Auditory Map Plasticity in Adult Barn Owls. *J Neurosci* 25: 9816-9820, 2005.

Berridge CW, and Waterhouse BD. The locus coeruleus-noradrenergic system: modulation of behavioral state and state-dependent cognitive processes. *Brain Res Rev* 42: 33-84, 2003.

Bigelow DC, Swanson PB, and Saunders JC. The effect of tympanic membrane perforation size on umbo velocity in the rat. *Laryngoscope* 106: 71-76, 1996.

Blauert J. *Spatial Hearing: The psychophysics of human sound localization*. London, UK: MIT Press, 1997.

Borg E. On the Change in the Acoustic Impedance of the Ear as A Measure of Middle ear Muscle Reflex Activity. *Acta Oto-Laryngologica* 74: 163-171, 1972.

Borg E. A Quantitative Study of the Effect of the Acoustic Stapedius Reflex on Sound transmission Through the Middle Ear of Man. *Acta Oto-Laryngologica* 66: 461-472, 1968.

Boyev KP, Liberman MC, and Brown MC. Effects of anesthesia on efferent-mediated adaptation of the DPOAE. *J Assoc Res Otolaryngol* 3: 362-373, 2002.

Brown MC. Morphology and response properties of single olivocochlear fibers in the guinea pig. *Hear Res* 40: 93-109, 1989.

Brown MC. Morphology of labeled efferent fibers in the guinea pig cochlea. *J Comp Neurol* 260: 605-618, 1987.

Brown MC. Response adaptation of medial olivocochlear neurons is minimal. *J Neurophysiol* 86: 2381-2392, 2001.

Brown MC, Kujawa SG, and Duca ML. Single Olivocochlear Neurons in the Guinea Pig. I. Binaural Facilitation of Responses to High-Level Noise. *J Neurophysiol* 79: 3077-3087, 1998a.

Brown MC, Kujawa SG, and Liberman MC. Single Olivocochlear Neurons in the Guinea Pig. II. Response Plasticity Due to Noise Conditioning. *J Neurophysiol* 79: 3088-3097, 1998b.

Brown MC, and Nuttal AL. Efferent control of cochlear inner hair cell responses in the guinea-pig. *J Physiol* 354: 625-646, 1983.

Brown MC, Nuttall AL, and Masta RI. Intracellular recordings from cochlear inner hair cells: effects of stimulation of the crossed olivocochlear efferents. *Science* 222: 69-72, 1983.

Brown MC, Venecia RK, and Guinan JJ. Responses of medial olivocochlear neurons. *Exp Brain Res* 153: 491-498, 2003.

Burkard R, Durand B, Secor R, and McFadden SL. Auditory brainstem responses in CBA mice and in mice with deletion of the RAB3A gene. In: *Handbook of mouse auditory research From behavior to molecular biology*, edited by Willot JF. Boca Raton, FL: CRC Press, 2001.

Cedarbaum JM, and Aghajanian GK. Afferent projections to the rat Locus Cereleus as determined by a retrograde tracing technique. *J Comp Neurol* 178: 1-16, 1978.

Chen Z, Kujawa SG, and Sewell WF. Auditory sensitivity regulation via rapid changes in expression of surface AMPA receptors. *Nat Neurosci* 10: 1238-1240, 2007.

Chikamori Y, Sasa M, Fujimoto S, Takaori S, and Matsuoka I. Locus Ceruleus-induced inhibition of dorsal cochlear nucleus neurons in comparison with lateral vestibular nucleus neurons. *Brain Res* 194: 53-63, 1980.
Cooper NP, and Guinan JJ. Separate mechanical processes underlie fast and slow effects of medial olivocochlear efferent activity. *J Physiol* 548: 307-312, 2003.
d'Aldin C, Puel J-L, Leducq R, Crambes O, Eybalin M, and Pujol R. Effects of a dopaminergic agonist in the guinea pig cochlea. *Hear Res* 90: 202-211, 1995.
Dahmen JC, and King AJ. Learning to hear: plasticity of auditory cortical processing. *Curr Opin Neurobiol* 17: 456-464, 2007.
Darrow KN, Maison SF, and Liberman MC. Cochlear efferent feedback balances interaural sensitivity. *Nat Neurosci* 9: 1474-1476, 2006a.
Darrow KN, Maison SF, and Liberman MC. Selective Removal of Lateral Olivocochlear Efferents Increases Vulnerability to Acute Acoustic Injury. *J Neurophysiol* 97: 1775-1785, 2007.
Darrow KN, Simons EJ, Dodds L, and Liberman MC. Dopaminergic innervation of the mouse inner ear: Evidence for a separate cytochemical group of cochlear efferent fibers. *J Comp Neurol* 498: 403-414, 2006b.
De Venecia RK, Liberman MC, J. Guinan JJ, Jr, and Brown MC. Medial olivocochlear reflex interneurons are located in the posteroventral cochlear nucleus: A kainic acid lesion study in guinea pigs. *J Comp Neurol* 487: 345-360, 2005.
Dean I, Harper NS, and McAlpine D. Neural population coding of sound level adapts to stimulus statistics. *Nat Neurosci* 8: 1684-1689, 2005.
Delano PH, Elgueda D, Hamame CM, and Robles L. Selective Attention to Visual Stimuli Reduces Cochlear Sensitivity in Chinchillas. *J Neurosci* 27: 4146-4153, 2007.
Devilbliss DM, Page ME, and Waterhouse BD. Locus Ceruleus regulates sensory encoding by neurons and networks in waking animals. *J Neurosci* 26: 9860-9872, 2006.
Dolan DF, and Nuttal AL. Masked cochlear whole-nerve response intensity functions altered by electrical stimulation of the crossed olivocochlear bundle. *J Acoust Soc Am* 83: 1081-1952, 1988.
Dolan DF, Nuttal AL, and Avinash G. Asynchronous neural activity recorded from the round window. *J Acoust Soc Am* 87: 2621-2627, 1990.
Ebert U. Noradrenalin enhances the activity of cochlear nucleus neurons in the rat. *Eur J Neurosci* 8: 1306-1314, 1996.
Eybalin M. Neurotransmitters and neuromodulators of the mammalian cochlea. *Physiol Rev* 73: 309-373, 1993.
Fex J, Altschuler RA, Kachar B, Wenthold RJ, and Zempel JM. GABA visualized by immunocytochemistry in the guinea pig cochlea in axons and endings of efferent neurons. *Brain Res* 366: 106-117, 1986.
Folsom RC, and Owsley RM. N1 action potential in humans. Influence of simultaneous contralateral stimulation. *Acta Oto-Laryngologica* 103: 262-265, 1987.
Fuchs PA. Synaptic transmission at vertebrate hair cells. *Curr Opin Neurobiol* 6: 514-519, 1996.
Gallego R, and Geijo E. Chronic block of the cervical trunk increases synaptic efficacy in the superior and stellate ganglia of the guinea-pig. *J Physiol* 382: 449-462, 1987.
Geisler CD, Deng L, and Greenbert SR. Thresholds for primary auditory fibers using statistically defined criteria. *J Acoust Soc Am* 77: 1102-1109, 1985.
Gifford ML, and Guinan JJ. Effects of electrical stimulation of medial olivocochlear neurons on ipsilateral and contralateral cochlear responses. *Hear Res* 29: 179-194, 1987.

Groff JA. Modulation of cochlear afferent response by the lateral olivocochlear system: Activation via electrical stimulation of the inferior colliculus (doctoral dissertation). In: *Harvard-MIT Division of Health Sciences and Technology*. Cambridge, MA: Massachusetts Institute of Technology, 2003.

Groff JA, and Liberman MC. Modulation of Cochlear Afferent Response by the Lateral Olivocochlear System: Activation Via Electrical Stimulation of the Inferior Colliculus. *J Neurophysiol* 90: 3178-3200, 2003.

Guinan JJ, and Gifford ML. Effects of electrical stimulation of efferent olivocochlear neurons on cat auditory-nerve fibers. II. Spontaneous rate. *Hear Res* 33: 115-128, 1988a.

Guinan JJ, and Gifford ML. Effects of electrical stimulation of efferent olivocochlear neurons on cat auditory-nerve fibers: I. Rate-level functions. *Hear Res* 33: 97-114, 1988b.

Guinan JJ, Guinan SS, and Norris BE. Single auditory units in the superior olivary complex I: Responses to sounds and classifications based on physiological properties. *Intern J Neurosci* 4: 101-120, 1972a.

Guinan JJ, Jr. Olivocochlear efferents: anatomy, physiology, function, and the measurement of efferent effects in humans. *Ear & Hearing* 27: 589-607, 2006.

Guinan JJ, Jr. Physiology of olivocochlear efferents. In: *The cochlea*, edited by Dallos P, Popper AN, and Fay RR. New York, NY: Springer-Verlag, 1996.

Guinan JJ, Norris BE, and Guinan SS. Single auditory units in the superior olivary complex II: Locations of unit categories and tonotopic organization. *Intern J Neurosci* 4: 147-166, 1972b.

Guinan JJ, and Stankovic KM. Medial efferent inhibition produces the largest equivalent attenuations at moderate to high sound levels in cat auditory-nerve fibers. *J Acoust Soc Am* 100: 1680-1690, 1996.

Guinan JJ, Warr WB, and Norris BE. Differential projections from the lateral vs. medial zones of the superior olivary complex. *J Comp Neurol* 226: 21-27, 1983.

He DZZ, Zheng J, Kalinec F, Kakehata S, and Santos-Sacchi J. Tuning in to the Amazing Outer Hair Cell: Membrane Wizardry with a Twist and Shout. *J Membr Biol* 209: 119-134, 2006.

Henderson D, Bielefeld EC, Harris KC, and Hu B-H. The role of oxidative stress in noise-induced hearing loss. *Ear & Hearing* 27: 1-19, 2006.

Horvath M, Ribari G, Repassy G, Toth IE, Boldogkoi Z, and Palkovits M. Intracochlear injection of pseudorabies virus labels descending auditory and monoaminergic projections to olivocochlear cells in guinea pig. *Eur J Neurosci* 18: 1439-1447, 2003.

Illing RB. Activity-Dependent Plasticity in the Adult Auditory Brainstem. *Audiol Neurotol* 6: 319-345, 2001.

Illing RB, Kraus KS, and Michler SA. Plasticity of the superior olivary complex. *Micr Res Techn* 51: 364-381, 2000.

Irvine DRF. Physiology of the auditory brainstem. In: *The mammalian auditory pathway: Neurophysiology*, edited by Popper AN, and Fay RR. New York, NY: Springer-Verlag, 1992.

Jääskeläinen IP, Ahveninen J, Belliveau JW, Raij T, and Sams M. Short-term plasticity in auditory cognition. *TINS* 30: 653-661, 2007.

Jones N, Fex J, and Altschuler RA. Tyrosine hydroxylase immunoreactivity identifies possible catecholaminergic fibers in the organ of Corti. *Hear Res* 30: 33-38, 1987.

Kacelnik O, Nodal FR, Parsons CH, and King AJ. Training-Induced Plasticity of Auditory Localization in Adult Mammals. *PLoS Biol* 4: e71, 2006.

Kandler K, and Gillespie DC. Developmental refinement of inhibitory sound-localization circuits. *TINS* 28: 290-296, 2005.

Kawase T, Delgutte B, and Liberman MC. Antimasking effects of the olivocochlear reflex. II. Enhancement of auditory-nerve response to masked tones. *J Neurophysiol* 70: 2533-2549, 1993.
Kawase T, and Liberman MC. Antimasking effects of the olivocochlear reflex. I. Enhancement of compound action potentials to masked tones. *J Neurophysiol* 70: 2519-2532, 1993.
Kendall MG. A new measure of rank correlation. *Biometrika* 30: 81-93, 1938.
Kiang NYS. *Discharge patterns of single fibers in the cat's auditory nerve*. Cambridge, MA: MIT Research Lab of Electronics, 1965.
Kim DO, Dorn PA, Neely ST, and Gorga MP. Adaptation of distortion product otoacoustic emission in humans. *J Assoc Res Otolaryngol* 2: 31-41, 2001.
King AJ, Bajo VM, Bizley JK, Campbell RAA, Nodal FR, Schulz AL, and Schnupp JWH. Physiological and behavioral studies of spatial coding in the auditory cortex. *Hear Res* 229: 106-115, 2007.
Kirk CE, and Smith DW. Protection from Acoustic Trauma Is Not a Primary Function of the Medial Olivocochlear Efferent System. *J Assoc Res Otolaryngol* 4: 445-465, 2003.
Kössl M, and Vater M. Noradrenaline enhances temporal auditory contrast and neuronal timing precision in the cochlear nucleus of the mustached bat. *J Neurosci* 9: 4169-4178, 1989.
Kromer LF, and Moore RY. Norepinephrine innervation of the cochlear nuclei by Locus Ceruleus neurons in the rat. *Anat Embryol* 158: 227-244, 1980.
Kujawa SG, and Liberman MC. Acceleration of Age-Related Hearing Loss by Early Noise Exposure: Evidence of a Misspent Youth. *J Neurosci* 26: 2115-2123, 2006.
Kujawa SG, and Liberman MC. Conditioning-Related Protection From Acoustic Injury: Effects of Chronic Deefferentation and Sham Surgery. *J Neurophysiol* 78: 3095-3106, 1997.
Kujawa SG, and Liberman MC. Effects of Olivocochlear Feedback on Distortion Product Otoacoustic Emissions in Guinea Pig. *J Assoc Res Otolaryngol* 2: 268-278, 2001.
Larsen E, and Liberman MC. Contralateral sound evokes slow suppression of ipsilateral cochlear responses (abstract #133). In: *31st Midwinter Res Meeting*. Phoenix, AZ: Assoc Res Otolaryngol, 2008.
Le Prell CG, Halsey K, Hughes LF, Dolan DF, and Bledsoe SC. Disruption of lateral olivocochlear neurons via a dopaminergic neurotoxin depresses sound-evoked auditory nerve activity. *J Assoc Res Otolaryngol* 6: 48-62, 2005.
Le Prell CG, Shore SE, Hughes LF, and Bledsoe SC. Disruption of lateral efferent pathways: Functional changes in auditory evoked responses. *J Assoc Res Otolaryngol* 4: 276-290, 2003.
Liberman MC. Effects of chronic cochlear de-efferentation on auditory-nerve response. *Hear Res* 49: 209-223, 1990.
Liberman MC. Efferent synapses in the inner hair cell area of the cat cochlea: an electron microscopic study of serial sections. *Hear Res* 3: 189-204, 1980.
Liberman MC. Physiology of cochlear efferent and afferent neurons: direct comparisons in the same animal. *Hear Res* 34: 179-191, 1988a.
Liberman MC. Rapid assessment of sound-evoked olivocochlear feedback: suppression of compound action potentials by contralateral sound. *Hear Res* 38: 47-56, 1989.
Liberman MC. Response properties of cochlear efferent neurons: monaural vs. binaural stimulation and the effects of noise. *J Neurophysiol* 60: 1779-1798, 1988b.
Liberman MC, and Brown MC. Physiology and anatomy of single olivocochlear neurons in the cat. *Hear Res* 24: 17-36, 1986.
Liberman MC, and Guinan JJ. Feedback control of the auditory periphery: anti-masking effects of middle ear muscles vs. olivocochlear efferents. *J Comm Disord* 31: 471-483, 1998.

Liberman MC, O'Grady DF, Dodds LW, Mcgee J, and Walsh EJ. Afferent innervation of outer and inner hair cells is normal in neonatally de-efferented cats. *J Comp Neurol* 423: 132-139, 2000.

Liberman MC, Puria S, and Guinan JJ. The ipsilaterally evoked olivocochlear reflex causes rapid adaptation of the $2f_1$-f_2 distortion product otoacoustic emission. *J Acoust Soc Am* 99: 3572-3584, 1996.

Lima da Costa D, Chibois A, Erre J-P, Blanchet C, Charlet de Sauvage R, and Aran J-M. Fast, Slow, and Steady-State Effects of Contralateral Acoustic Activation of the Medial Olivocochlear Efferent System in Awake Guinea Pigs: Action of Gentamicin. *J Neurophysiol* 78: 1826-1836, 1997a.

Lima da Costa D, Erre J-P, Charlet de Sauvage R, Popelar J, and Aran JM. Bioelectrical cochlear noise and its contralateral suppression: relation to background activity of the eighth nerve and effects of sedation and anesthesia. *Exp Brain Res* 116: 259-269, 1997b.

Lustig LR. Nicotinic acetylcholine receptor structure and function in the efferent auditory system. *Anat Rec A Discov Mol Cell Evol Biol* 288: 424-434, 2006.

Maison SF, Adams JC, and Liberman MC. Olivocochlear innervation in the mouse: Immunocytochemical maps, crossed versus uncrossed contributions, and transmitter colocalization. *J Comp Neurol* 455: 406-416, 2003a.

Maison SF, Emeson RB, Adams JC, Luebke AE, and Liberman MC. Loss of αCGRP Reduces Sound-Evoked Activity in the Cochlear Nerve. *J Neurophysiol* 90: 2941-2949, 2003b.

Maison SF, and Liberman MC. Predicting Vulnerability to Acoustic Injury with a Noninvasive Assay of Olivocochlear Reflex Strength. *J Neurosci* 20: 4701-4707, 2000.

Maison SF, Luebke AE, Liberman MC, and Zuo J. Efferent Protection from Acoustic Injury Is Mediated via α9 Nicotinic Acetylcholine Receptors on Outer Hair Cells. *J Neurosci* 22: 10838-10846, 2002.

Maison SF, Parker LL, Young L, Adelman JP, Zuo J, and Liberman MC. Overexpression of SK2 Channels Enhances Efferent Suppression of Cochlear Responses Without Enhancing Noise Resistance. *J Neurophysiol* 97: 2930-2936, 2007a.

Maison SF, Rosahl TW, Homanics GE, and Liberman MC. Functional Role of GABAergic Innervation of the Cochlea: Phenotypic Analysis of Mice Lacking $GABA_A$ Receptor Subunits α1, α2, α5, α6, β2, β3, or δ. *J Neurosci* 26: 10315-10326, 2006.

Maison SF, Vetter DE, and Liberman MC. A Novel Effect of Cochlear Efferents: In Vivo Response Enhancement Does Not Require α9 Cholinergic Receptors. *J Neurophysiol* 97: 3269-3278, 2007b.

Margolis RH. Influence of middle ear disease on otoacoustic emissions. In: *Otoacoustic emissions: Clinical application*, edited by Robinette MS, and Glattke TJThieme, 2002, p. 190-212.

Meddis R. Auditory-nerve first-spike latency and auditory absolute threshold: A computer model. *J Acoust Soc Am* 119: 406-417, 2006.

Mehta RP, Rosowski JJ, Voss SE, O'Neil E, and Merchant SN. Determinants of hearing loss in perforations of the tympanic membrane. *Otol Neurotol* 27: 136-143, 2006.

Melcher JR, Guinan JJ, Knudson IM, and Kiang NYS. Generators of the brainstem auditory evoked potential in cat. II. Correlating lesion sites with waveform changes. *Hear Res* 93: 28-51, 1996.

Melcher JR, and Kiang NYS. Generators of the brainstem auditory evoked potential in cat. III. Identified cell populations. *Hear Res* 93: 52-71, 1996.

Merchant SN, and Rosowski JJ. Auditory Physiology (Middle-Ear Mechanics). In: *Surgery of the Ear*, edited by Gulya AJ, and Glasscock ME. Hamilton, ON: BC Decker, 2003.
Mountain DC, Geisler CD, and Hubbard AE. Stimulation of efferents alters the cochlear microphonic and the sound-induced resistance changes measured in scala media of the guinea-pig. *Hear Res* 3: 231-240, 1980.
Mulders WHAM, and Robertson D. Gentamicin abolishes all cochlear effects of electrical stimulation of the inferior colliculus. *Exp Brain Res* 174: 35-44, 2006.
Mulders WHAM, and Robertson D. Noradrenergic modulation of brainstem nuclei alters cochlear neural output. *Hear Res* 204: 147-155, 2005.
Murugasu E, and Russell IJ. The effect of efferent stimulation on basilar membrane displacement in the basal turn of the guinea pig cochlea. *J Neurosci* 16: 325-332, 1996.
Oppenheim AV, and Willsky AS. *Signals & systems*. Upper Saddle River, NJ: Prentice Hall, 1997.
Pujol R, Carlier E, and Devigne C. Different patterns of cochlear innervation during the development of the kitten. *J Comp Neurol* 177: 529-535, 1978.
Puria S, Guinan JJ, Jr., and Liberman MC. Olivocochlear reflex assays: Effects of contralateral sound on compound action potentials versus ear-canal distortion products. *J Acoust Soc Am* 99: 500-507, 1996.
Raghuraman H, and Chattopadhyay A. Melittin: A membrane-active peptide with diverse functions. *Biosci Rep* 27: 189-223, 2007.
Rajan R. *Protective function of the efferent pathways to the mammalian cochlea: A review*. St. Louis, MO: Mosby Year Book, 1991.
Reiter ER, and Liberman MC. Efferent-mediated protection from acoustic overexposure: relation to slow effects of olivocochlear stimulation. *J Neurophysiol* 73: 506-514, 1995.
Ruel J, Nouvian R, d'Aldin C, Pujol R, Eybalin M, and Puel J-L. Dopamine inhibition of auditory nerve activity in the adult mammalian cochlea. *Eur J Neurosci* 14: 977-986, 2001.
Ruel J, Wang J, Dememes D, Gobaille S, Puel J-L, and Rebillard G. Dopamine transporter is essential for the maintenance of spontaneous activity of auditory nerve neurones and their responsiveness to sound stimulation. *J Neurochem* 97: 190-200, 2006.
Santos-Sacchi J. New tunes from Corti's organ: the outer hair cell boogie rules. *Curr Opin Neurobiol* 13: 459-468, 2003.
Schwartz IR. The superior olivary complex and lateral lemniscal nuclei. In: *The mammalian auditory pathway: Neuroanatomy*, edited by Webster DB, Popper AN, and Fay RR. New York, NY: Springer-Verlag, 1992.
Sewell WF. The relation between the endocochlear potential and spontaneous activity in the auditory nerve fibres of the cat. *J Physiol* 347: 685-696, 1984.
Sininger YS, and Cone-Wesson B. Lateral asymmetry in the ABR of neonates: Evidence and mechanisms. *Hear Res* 212: 203-211, 2006.
Song P, Yang Y, Barnes-Davies M, Bhattacharjee A, Hamann M, Forsythe ID, Oliver DL, and Kaczmarek LK. Acoustic environment determines phosphorylation state of the Kv3.1 potassium channel in auditory neurons. *Nat Neurosci* 8: 1335-1342, 2005.
Sridhar TS, Brown MC, and Sewell WF. Unique Postsynaptic Signaling at the Hair Cell Efferent Synapse Permits Calcium to Evoke Changes on Two Time Scales. *J Neurosci* 17: 428-437, 1997.
Sridhar TS, Liberman MC, Brown MC, and Sewell WF. A novel cholinergic "slow effect" of efferent stimulation on cochlear potentials in the guinea pig. *J Neurosci* 15: 3667-3678, 1995.

Tsuji J, and Liberman MC. Intracellular labeling of auditory nerve fibers in the guinea pig: Central and peripheral projections. *J Comp Neurol* 381: 188-202, 1997.
Van Wanrooij MM, and Van Opstal AJ. Relearning Sound Localization with a New Ear. *J Neurosci* 25: 5413-5424, 2005.
Vetter DE, Li C, Zhao L, Contarino A, Liberman MC, Smith GW, Marchuk Y, Koob GF, Heinemann SF, Vale W, and Lee K-F. Urocortin-deficient mice show hearing impairment and increased anxiety-like behavior. *Nat Genet* 31: 363-369, 2002.
Voss SE, Rosowski JJ, Merchant SN, and Peake WT. Middle-ear function with tympanic-membrane perforations. I. Measurement and mechanisms. *J Acoust Soc Am* 110: 1432-1444, 2001.
Walsh EJ, McGee J, McFadden SL, and Liberman MC. Long-Term Effects of Sectioning the Olivocochlear Bundle in Neonatal Cats. *J Neurosci* 18: 3859-3869, 1998.
Wang J, Ding D, and Salvi RJ. Functional reorganization in chinchilla inferior colliculus associated with chronic and acute cochlear damage. *Hear Res* 168: 238-249, 2002a.
Wang X, and Robertson D. Two Types of Actions of Norepinephrine on Identified Auditory Efferent Neurons in Rat Brain Stem Slices. *J Neurophysiol* 78: 1800-1810, 1997.
Wang Y, Hirose K, and Liberman MC. Dynamics of noise-induced cellular injury and repair in the mouse cochlea. *J Assoc Res Otolaryngol* 03: 248-268, 2002b.
Wang Y, and Liberman MC. Restraint stress and protection from acoustic injury in mice. *Hear Res* 165: 96-102, 2002.
Warren EH, and Liberman MC. Effects of contralateral sound on auditory-nerve responses. I. Contributions of cochlear efferents. *Hear Res* 37: 89-104, 1989a.
Warren EH, and Liberman MC. Effects of contralateral sound on auditory-nerve responses. II. Dependence on stimulus variables. *Hear Res* 37: 105-121, 1989b.
Wiederhold ML, and Kiang NYS. Effects of electrical stimulation of the crossed olivocochlear bundle on single auditory nerve fibers in the cat. *J Acoust Soc Am* 48: 950-965, 1970.
Wiederhold ML, and Peake WT. Efferent inhibition of auditory-nerve responses: dependence on acoustic-stimulus parameters. *J Acoust Soc Am* 40: 1427-1430, 1966.
Winslow RL, and Sachs MB. Single-tone intensity discrimination based on auditory-nerve rate responses in backgrounds of quiet, noise, and with stimulation of the crossed olivocochlear bundle. *Hear Res* 35: 165-189, 1988.
Woods CI, and Azeredo WJ. Noradrenergic and serotonergic projections to the superior olive: Potential for modulation of olivocochlear neurons. *Brain Res* 836: 9-18, 1999.
Yamamoto Y, Matsubara A, Ishii K, Makinae K, Sasaki A, and Shinkawa H. Localization of γ-Aminobutyric Acid A Receptor Subunits in the Rat Spiral Ganglion and Organ of Corti. *Acta Oto-Laryngologica* 122: 709 - 714, 2002.
Yoshida N, Hequembourg SJ, Atencio CA, Rosowski JJ, and Liberman MC. Acoustic injury in mice: 129/SvEv is exceptionally resistant to noise-induced hearing loss. *Hear Res* 141: 97-106, 2000.
Yoshida N, Liberman MC, Brown MC, and Sewell WF. Fast, But Not Slow, Effects of Olivocochlear Activation Are Resistant to Apamin. *J Neurophysiol* 85: 84-88, 2001.
Yoshida N, Liberman MC, Brown MC, and Sewell WF. Gentamicin Blocks Both Fast and Slow Effects of Olivocochlear Activation in Anesthetized Guinea Pigs. *J Neurophysiol* 82: 3168-3174, 1999.
Zheng X-Y, Henderson D, Hu B-H, Ding D-L, and McFadden SL. The influence of the cochlear efferent system on chronic acoustic trauma. *Hear Res* 107: 147-159, 1997.